Retrospective Theses and Dissertations

Iowa State University Capstones, Theses and Dissertations

1983

Electric field distribution through multilayer environment in the vicinity of high voltage transmission lines

Bashir Mohamed Jomaa
Iowa State University

Recommended Citation

8316323

Jomaa, Bashir Mohamed

ELECTRIC FIELD DISTRIBUTION THROUGH MULTILAYER
ENVIRONMENT IN THE VICINITY OF HIGH VOLTAGE TRANSMISSION
LINES

Iowa State University   PH.D.   1983

University
Microfilms
International 300 N. Zeeb Road, Ann Arbor, MI 48106

PLEASE NOTE:

In all cases this material has been filmed in the best possible way from the available copy.
Problems encountered with this document have been identified here with a check mark __√__ .

1.   Glossy photographs or pages _____

2.   Colored illustrations, paper or print _____

3.   Photographs with dark background _____

4.   Illustrations are poor copy _____

5.   Pages with black marks, not original copy _____

6.   Print shows through as there is text on both sides of page _____

7.   Indistinct, broken or small print on several pages _____

8.   Print exceeds margin requirements _____

9.   Tightly bound copy with print lost in spine _____

10. Computer printout pages with indistinct print __√__

11. Page(s) _____ lacking when material received, and not available from school or author.

12. Page(s) _____ seem to be missing in numbering only as text follows.

13. Two pages numbered _____. Text follows.

14. Curling and wrinkled pages _____

15. Other_____

Electric field distribution through

multilayer environment in the

vicinity of high voltage transmission lines

by

Bashir Mohamed Jomaa

A Dissertation Submitted to the

Graduate Faculty in Partial Fulfillment of the

Requirements for the Degree of

DOCTOR OF PHILOSOPHY

Department: Electrical Engineering
Major: Electrical Engineering (Electric Power)

Approved:

Signature was redacted for privacy.

In Charge of Major Work

Signature was redacted for privacy.

For the Major Department

Signature was redacted for privacy.

For the Graduate College

Iowa State University
Ames, Iowa

1983

TABLE OF CONTENTS

I. INTRODUCTION

A. Transmission Line Environment

The study of electric and magnetic fields generated by an a.c. overhead transmission line has recently become a subject of major importance. Because of the expansion of EHV systems and the prospect of UHV transmission, serious questions have been raised regarding the potential health and environmental effects associated with the resultant higher levels of electric field intensity. The presence of the electric fields and the associated magnetic fields also create a number of related phenomena which include small arc discharges, air ions, low level acoustical noise, radio noise and TV interference. Typically, all of these phenomena are confined to the immediate vicinity (within a few hundred feet) of the power lines. Therefore, it becomes increasingly important to describe accurately the field interaction with objects and living things in close proximity to the transmission line right of way.

B. Review of Environmental Impact

1. Electromagnetic field coupling with objects

The overhead high voltage transmission line exhibits three primary electromagnetic field components near the ground: a predominantly vertical electric field, a

horizontal electric field, and a time-varying magnetic field. The fields from the high voltage lines are complex functions of the geometry of the power lines [11, 22], that is of conductor size, conductor spacing and height above ground. Prediction of induced currents and voltages for vehicles and other objects are determined under the assumption that these objects have negligible effect on the source of the electrostatic field and the surface charge on the conductors. The procedure used to compute the charging currents in objects close to ground are explained in more detail by Deno and Zaffanella [8] and by Deno [7]. In the following section, the mechanism by which the electric field is coupled into living objects such as humans or animals will be discussed.

2. Electromagnetic field coupling to animals

Electric field can produce two effects:

1. Induce external fields on the surface of the object much larger than the free field.

2. Induce currents and voltages in varying distribution throughout the object.

Therefore, when an animal walks beneath a transmission line, the electric charges on the line create force fields which cause opposite charges to accumulate on the animal's skin surface nearest the source. As a.c. power flows in the line, the charges on the wire change polarity, and this

causes a polarity change of the charges on the skin of the animal. The change of polarity causes charges to flow within the subject animals and this gives rise to a.c. current flow on the animal skin.

3. Electromagnetic field coupling to humans

The electric and magnetic fields induce surface charges onto humans. These surface charges on a typical biped create a localized perturbed electric field intensity close to the skin on the head which have values in excess of ten times that for the unperturbed field [7, 8]. In the case of the biped, the maximum body currents induced by the electric field from a transmission line is much greater than the body current or body current density induced by the magnetic field. The reason for that is the disparity in magnitude between the electric field (kV/m) compared to the magnetic field (tens of milligauss).

The distribution of the internal body current density varies occurs along the body of the biped and the maximum value in the lower legs, where a typical value is in the order of 15 mA/ kV/m [30]. This current flow can cause a voltage to be developed between the person standing on insulating material (such as rubber soles) and grounded conducting objects [8, 11]. If the individual reaches out to touch the grounded objects, a series of small arcs will form at his finger tips and current will flow into the

grounded objects. These internal current densities are responsible for the ability of humans to detect the presence of currents by a tingling sensation. If this current density is substantially increased, paralysis of various muscles may occur.

The calculation and measurements of the electric and magnetic fields are extremely affected by the presence of objects and humans as indicated above. Of great importance, is the environment coupling that exists between the transmission line conductors and the objects or living things. This space, be it air or media, will play a very significant role in the determination of all electric field effects close to ground. All the studies that are available in the literature have focused on the assumption that the coupling medium is free space. This assumption, however, is not accurate since the medium under the line and through the ground is actually composed of various dielectric layers. Therefore, the problem becomes a multilayer case rather than a single layer case.

The multilayer dielectric in the air may represent different environmental conditions that might occur at the same time or separately. These environmental conditions may represent clouds, fog, rain, snow or dust. Cement works, chemical factories, power stations (using coal) and industrial areas contribute greatly to air pollution which

changes the dielectric permittivity of the air and, thus, the value of the electric field. High winds create considerable problems in desert areas, where particles of dirt and grit are spread through the air. High winds also carry snow, fog, and dirt and thus change the environmental dielectric constant.

The multilayer dielectric may also exist through the ground. The ground may have different levels of structure such as sand, rock or agricultural land. The agricultural land may be covered with vegetation. The effect of moisture content, salt and chemical content in the soil must also be taken into consideration. Each of the above mentioned conditions will have different field distribution due to the different values of the dielectric constants. Most high voltage transmission lines cross agricultural land where vegetation such as corn or soybeans grows under the lines. This vegetation will then create a medium that has a different characteristic than free space. The field distribution will be different than free space. Since people, animals and farm machinary do very often exist in such regions, there is a need to examine the impact of the agricultural crops under the transmission line on the magnitude of the electric field close to or a few meters above ground. The determination of the electric field distribution inside the vegetation medium is a very

important parameter for studying field effects. This field distribution is also necessary to determine some other field effect related factors such as currents or voltages to objects that may exist in such regions.

C. Purpose of the Thesis

1. Introduction

This investigation is focused on the study of the electric field distribution through a multilayer environment in the vicinity of a high voltage transmission line. In this study, the multilayers environment considered are:

a) The air under the transmission line.

b) The vegetation above the ground.

c) The ground, be it a perfect conductor
    or a lossy dielectric.

The principal objectives of the research leading to this dissertation were:

a) Multilayer environment problem.

b) Modeling of the vegetation, particularly corn
    fields.

c) Testing the developed models and comparing
    the numerical results with measured data taken
    inside a corn field under a 345 kV transmission
    line.

2. Method of solution

A general solution of Laplace's Equation for the potential in the case of n different resistivity layers has been proposed by Stefensco and Schlumberger as cited in Ianovici and Morf [18]. It is difficult, however, to use this approach in practice, even for a limited number of layers. This is because the solution is presented in terms of Hankel integrals and the numerical calculations of such integrals require a rather elaborate computer technique.

In this work, the method of images for calculating the field due to the point charge and the line charge in the presence of multilayer dielectric is used. This technique is then applied to solve for the field distribution in the case of vegetation medium underneath the high voltage transmission line.

The multilayer dielectric solution will be divided into three cases:

1. Three dielectric media.
2. Four dielectric media.
3. Five dielectric media.

The problem will be solved first for the point charge source cases and the solution for the line charge source will follow.

In the case of three dielectric media, two methods are used: the image method followed by boundary value problem

solution of Poisson's equations using the separation of
variable technique. Both solutions are in terms of infinite
series and are equal.

In the case of more than three media, the solution of
Poisson's equation is found to be not attractive as
mentioned above and the method of images is preferable.

A computer algorithm is developed for the four
dielectric case to generate the images similar to Takashima
and Ishibashi algorithm [36]. The developed algorithm has
been verified by comparison to published data [36], and an
exact results' correspondence is obtained. This algorithm
is then extended to the five dielectric media case.

The above developed algorithms for the three, the four
and the five dielectric case are then modified for the line
charge case. Superposition is used to account for the
three-phase transmission line case.

3. Modeling the environment under the transmission line

In this study, the air medium will be represented by a
single layer of dielectric constant equal to that of free
space. This medium in which the transmission line is
located will be called either medium I or region I. The
ground will be represented by a single layer of infinite
depth along the plane perpendicular to the transmission
line. The dielectric constant of the ground will be chosen
to be infinite to represent the perfect conductor case. Due

to the lack of information concerning the dielectric constant of the vegetation, and since there are no available data in the literature for such cases, the following assumptions will be used.

The media are "isotropic" which means the behavior of all media is the same regardless of the direction of the field vectors. If the field relations depend on field direction, the medium is "anistropic." The media are linear, that is to say, the relations between the physical quantities in question do not depend on their magnitudes. To simplify the analysis for the vegetation medium, the following assumption will be added: flat ground, uniform height of the vegetation, uniform distribution of leaves and uniform distribution of water content.

Therefore, the following mathematical model for the vegetation is proposed: the vegetation medium will be divided into layers of infinite extent in a plane perpendicular to the transmission line. Each layer is assumed to have its own unique dielectric constant. These dielectric constants for the layers are an unknown parameters. To determine the permittivity of each layer, a computer simulation technique using the developed algorithm will be used. An arbitrary value of permittivities combination are then used. Based on these values, the electric field distribution will be computed. The

dielectric constant values which give an electric field distribution that fit close to the measured field are then assumed to be the correct ones.

This simulation technique is similar to these that have been used in the application of the electromagnetic sounding toward the interpretation of the field data in order to identify the geoelectrical parameters in the ground. Interpretation means that the measured field data will be matched to the best fitting curves, which are obtained by numerical evaluation [6, 28].

D. Thesis Outline

A summary of the thesis outline is as follows. Chapter II is concerned with a brief historical background of the application of the image method in the two media case. A few cases are reported to the multilayer dielectric case. All the necessary equations for the two media case are stated here. Some interesting features about the two media solution are also stated in this chapter.

Chapter III deals with the solution of the field problem due to a point charge in the three dielectric case. Two methods are presented in this chapter. The first method is the extension of the two media solution of Chapter II, to cover the three media case using the image technique. A detailed explanation of the images generation with their

positions in all three media are presented. A collection of all the images with their location for each medium is summarized. A closed form solution for each medium has been found by induction.

The second method is to write a set of partial differential equations for each medium using the separation of variable technique subjected to the following boundary conditions: the potential, the tangential component of the electric field and the normal component of the electric flux density must be continuous at the dielectric boundaries.

A closed form solution for the three media has been found in terms of infinite integrals. These integrals can be written in an infinite series form similar to the terms obtained by the first method. The proof is written in Appendix A.

In Chapter IV, the four and the five dielectric media are analyzed. The image method is used in both cases. The four dielectric media model is analyzed first. A new approach is developed to solve this problem using a digital computer technique to generate the images [36]. This technique is found to be very easy to apply. The computer algorithm developed is outlined here where the images and their position will be generated in advance in a subprogram. The computer algorithm is then tested for arbitrary values of the source charge and the dielectric constants, and the

boundary conditions are shown to be satisfied to a reasonable accuracy. Extension of this algorithm to cover the five dielectric media case is then developed. This five dielectric algorithm is the most general algorithm, because this algorithm can be used as four, three or even two dielectric media case, by letting some of the permittivities to be equal. The accuracy of the algorithm is shown by the numerical examples given at the end of the chapter.

Chapter V deals with the electric field distribution through multilayer vegetation underneath EHV transmission lines. A brief review of the EHV transmission line function is presented. The computation of the line charges to represent the three-phase conductors are discussed. A single line charge per conductor is used. This approximate representation is then tested for the two media case (special case of the multilayer dielectric), to calculate the electric field at ground and at a few meters above ground. Results similar to those published by Cowan [5] are obtained. The application of the three, four, and five dielectric models are then used.

In the three dielectric case, the vegetation is modeled as one single layer. This is the simplest representation. In the four and the five dielectric cases, the vegetation is modeled as two and three layers respectively. A computer simulation is then applied to all three cases with different

values of dielectric constants. From these output graphs of the electric field distribution, it is found that the five dielectric model is the most reasonable model to represent the vegetation underneath the EHV transmission line.

Chapter VI includes a summary and conclusions reached as well as suggestions and comments concerning future research.

Chapter VII contains most of the pertinent references related to the subject of the image method.

Appendices A and B are outlined at the end of the work. Appendix A contains the derivation of the proof of the infinite integral obtained in Chapter III to be written as an infinite series form. Appendix B deals with the case of solving the field problem for the complex media case where conductivity is present.

Finally, a brief description of the computer programs used are outlined in Appendix C.

II. THE IMAGE METHOD

A. Historical Background

The method of images was first introduced by Lord
Kelvin [20]. In 1848, he showed that the field of an
electric charge in front of a conducting sheet could be
correctly represented as the field of the charge alone plus
the field of its mirror image in the conducting sheet. He
used the term "image" in order to point out the close
similarity between the electrical and the optical images.
In optics, an image is defined as a point or system of
points which, if it existed, would emit the system of rays
that are actually due to reflected light from a mirror or
lens.

The initial electrostatic work by Kelvin was signifi-
cantly expanded by Maxwell [23]. Maxwell was mainly
concerned with problems of spherical electrodes. He
examined combinations of spheres and planes which, in the
presence of electric charges, give a finite number of
images. He then applied the method of images to calculate
the potential and the electrical or magnetic field
distribution around electrostatic charges or electrical
currents in the presence of conductors, dielectric or
magnetic materials.

Searle [31] successfully applied the method of images to magnetic problems of finite permeability. Hammond [16] has treated the problem of the electric field given by a linear charge in the presence of a dielectric. He then examined the case of linear and circular currents in the proximity of a ferromagnetic material. Hague [15] applied the image method to the case of linear currents in the gap of an electrical machine. Up to the year 1967, the method of images has been used essentially in the case of two different media.

In 1968, Silvester [33] extended the image method to combination of dielectrics of the type air-dielectric-air to study the properties of microstrip transmission lines. Giao and Sarma [14] and Dawalibi and Mukhedkar [6] applied the image method to the case of air and two different resistivity materials which models substation ground situations. These cases are, in fact, particular cases of three different media structure.

In 1977, calculation of the potential distribution around a point charge in the presence of three dielectric media using the image technique was examined by Ianovici and Morf [18]. The solution was found in terms of infinite series for all three media. A year later, computation of the electric field distribution due to a point charge and

spherical conductor in the presence of three dielectric media on top of a grounded plane was performed by Takashima and Ishibashi [36]. They used a digital computer algorithm for the image generation. One of the features which makes this method very attractive for field computations is the fact that it does not need any special techniques for treatment of the boundary, and the field strength can be calculated directly.

This research will be mainly devoted to the solution for the electric field distribution due to a point charge in multilayer dielectric. Application of these models to the three-phase case will be developed later. Three methods of solution will be used for the three dielectric media case. It will be shown that the final results of all methods are the same. This contradicts the statement made by Ianovici and Morf [18], in which it was stated that "the image method can be used only if the condition h < d is satisfied." h is the position of the charge in medium I, and d is the thickness of medium II in the three dielectric media case. There are no closed form solutions to the cases of four and five dielectric media. The images will be generated using a digital computer algorithm similar to the one obtained by Takashima and Ishibashi [36] in the case of a four dielectric media. This research extends the four dielectric computer algorithm to cover the five dielectric media case.

The algorithm is then tested under some special cases such as four, three and even two dielectric regions; good results are obtained.

The following section contains a brief discussion of the basic equations from which the underlying concepts used in this·dissertation are obtained.

B. Basic Equations

Several equations that serve as background for this dissertation are now reviewed briefly.

1. Point image in a plane conductor

The method of images is useful when it is desired to find the field arising from point charges or line charges in the vicinity of conductors of certain simple shapes. The most simple case is that of a point charge near a grounded conducting plane, as in Fig. 2.1. Boundary conditions require that the potential along the plane be zero. The requirement is met if in place of the conducting plane an equal and opposite image charge is placed at x = -h. The potential at any point P is then given by

$$\Phi(x,y,z) = \frac{1}{4\pi\varepsilon} \left[\frac{Q}{R} - \frac{Q}{R^{\scriptscriptstyle\top}} \right] \tag{2.1}$$

where Q is the point charge in coulombs and ε is the dielectric constant of the medium, in Farads/m, where the charge is located.

R and R' are the separation vectors between the point of observation P, and charge Q and its image respectively.

$$R = \sqrt{(x-h)^2 + y^2 + z^2}, \quad R' = \sqrt{(x+h)^2 + y^2 + z^2}$$

(2.2)

Φ is the potential in volts.

This expression gives zero potential along the plane x = 0, so that Eq. 2.1 gives the potential for any point to the right of the plane, i.e., x > 0.

The expression does not apply for x < 0, because inside the conductor the potential must be 0 everywhere.
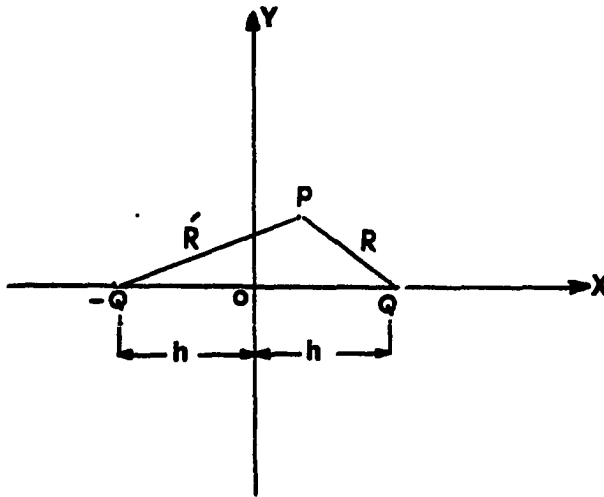
Fig. 2.1. Point charge image in a plane conductor

2. Line image in a plane conductor

If there is a line charge of strength q coulomb/meter (col/m) parallel to a conducting plane and distance h meter

from it, then the image will be (-q) at x = -h. The potential at any point x > 0 is then:

$$\Phi(x,y,z) = q/2\pi\epsilon \ln R/R' \tag{2.3}$$

where R and R' are defined in Eq. 2.2.

3. Point image in a plane dielectric

Smyth [34] and others [36, 38] provide a fairly simple solution to this type of boundary problem for the static field. In order to calculate the field of a point change Q, located in a semi-infinite medium I, a distance h meters from the plane interface of a semi-infinite medium II, as shown in Fig. 2.2. Where medium I has a dielectric constant ϵ_1, and medium II has a dielectric constant ϵ_2. The solution to this problem can be divided into two parts:

a) For all calculations related to medium I, retain the original charge Q at x = h, but replace medium II by a charge

$[(\epsilon_1-\epsilon_2)]/(\epsilon_1+\epsilon_2)]Q$

located at x = -h, the image of Q as shown in Fig. 2.2b.

b) For all calculations related to medium II, replace both medium I and Q by an equivalent charge

$[(2\epsilon_2/(\epsilon_1+\epsilon_2)]Q$

at x = h, as shown in Fig. 2.2c.
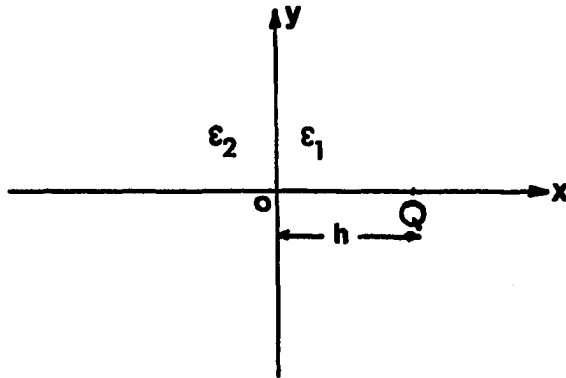
a) Original problem
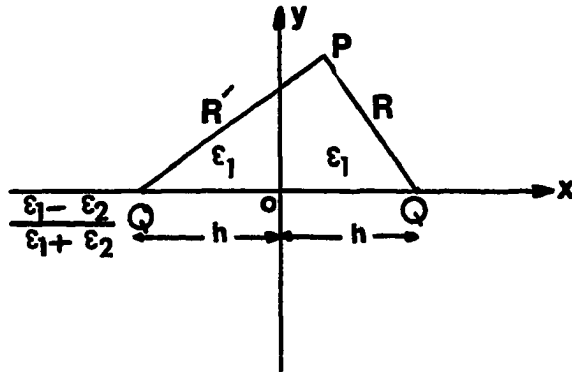
b) Charge array for medium I field calculation
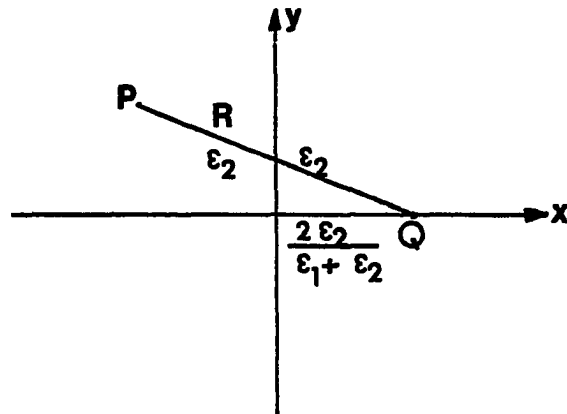
c) Charge array for medium II field calculation

Fig. 2.2. Point charge in a plane dielectric

Typical field plot of the partial field and the resultant fields matched at the interface are shown in Fig. 2.3. The true fields are shown as solid lines, while the apparent fields are shown as dotted lines in the construction.

There are several interesting features to notice about the solution of the two dielectric media case:

a) As ε_2 approaches ε_1 in value, the problem reduces to a simple point charge problem as it ought.

b) The image in medium II may be a positive or negative charge, depending upon the relative values of the permittivities.

c) The field in medium II is always radial.

d) For values of $\varepsilon_2 >> \varepsilon_1$ or as ε_2 approaches infinity, the image in medium II approach -Q in value and the field in medium II tends to 0, these relationships conform exactly to the case where medium II is a perfect conductor.

C. Summary

The review of prior research has provided a broad survey of the most current research related to the application of the image method in solving the electric field problem in the case of point and line charge. However, more research and development remains to be done in the
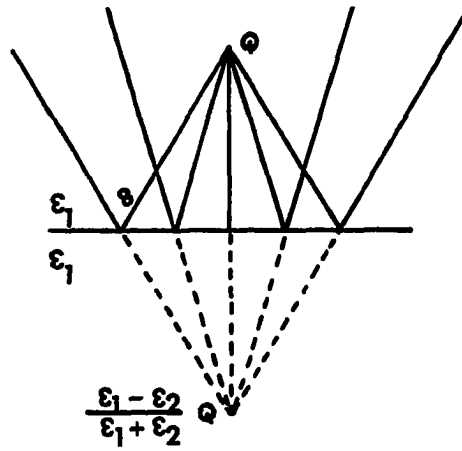
a) Construction of field in region I
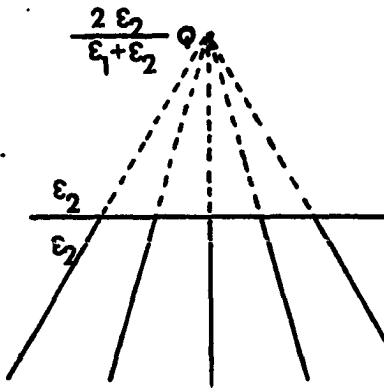
b) Construction of field in region II

Fig. 2.3. Electric field in the vicinity of a dielectric boundary

application of this method to the case of multilayer di-
electrics. Electrical machines, power transformers, under-
ground cables, ground structures and the environment near
the vicinity of EHV transmission lines contain three or more
dielectric layers. Therefore, the need to extend the two
media case solution to the multilayer dielectric case is a
must.

Chapter III discusses the application and the extension
of the image method to cover the three dielectric case. Two
methods of solution will be used. The first method is the
application of the image technique. The second method will
be the application of the boundary value problem solution.
The two solutions are found to be the same.

III. THE THREE DIELECTRIC MEDIA

A. Introduction

A review of the basic equations for the two media case has been presented in Chapter II. It was also pointed out that there exists a need for the development of a solution to the case of multilayer dielectrics. In this chapter, two methods of solution are discussed. The first method will be the application of the image technique using the basic equations introduced in Chapter II. The second method is the solution of Poisson's equation using the separation of variables technique. Both solutions are found to give the same result.

B. The Image Method

1. Principle of the method

Let the whole space be filled with dielectric media (ε_1 and ε_3) semi-infinite in the z direction and separated by a medium that has different permittivity (ε_2) with parallel separation faces as shown in Fig. 3.1. Medium II has a thickness (b) m and together with the semi-infinite medium I and medium III, is infinite in the x and the y directions.

The problem of a point charge in the presence of two dielectric media ε_1 and ε_2 was explained in Chapter II. The
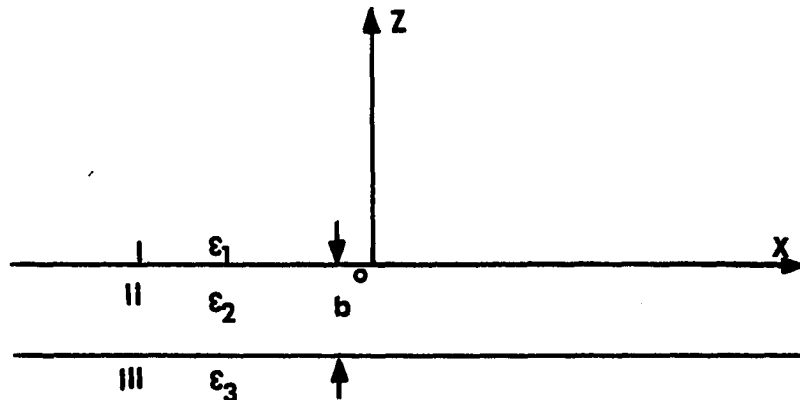
Fig. 3.1. Three dielectric media system

necessary equations for this case will be written here for convenience. Medium I charges are: Q and its image

$$\frac{\varepsilon_1 - \varepsilon_2}{\varepsilon_1 + \varepsilon_2} Q \tag{3.1}$$

Medium II charge is

$$\frac{2\varepsilon_2}{\varepsilon_1 + \varepsilon_2} Q \tag{3.2}$$

The location of these charges is shown in Fig. 3.2.

2. Solution procedure

Let a point charge Q coulombs lie at a point P (0,0,h) in medium I as shown in Fig. 3.3. In order to solve this problem, the following technique will be followed.
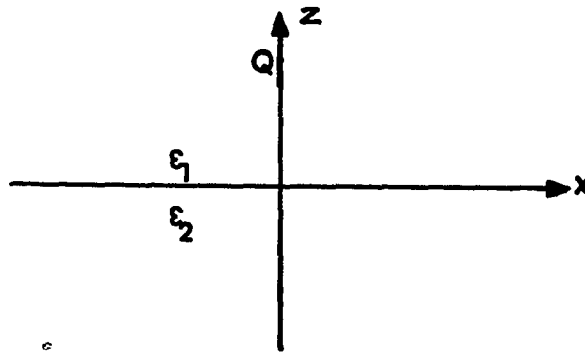
a) Original problem
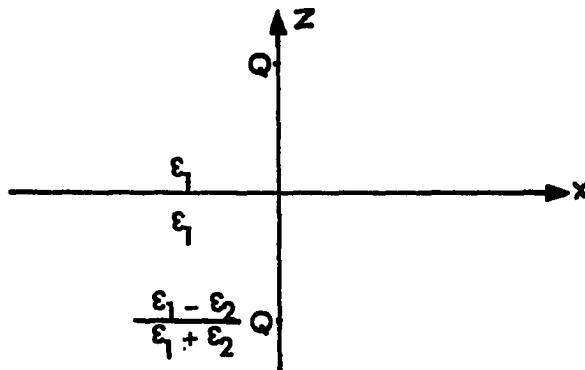
b) Model for determining the field in region I
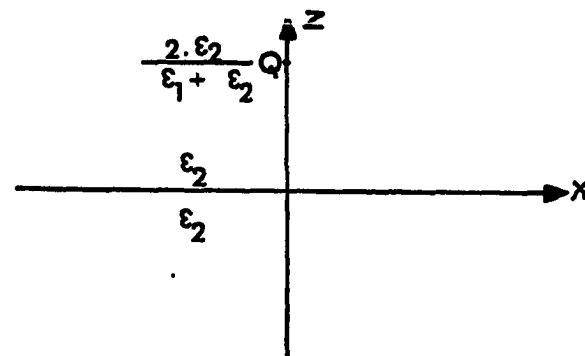
c) Model for determining the field in region II

Fig. 3.2. Point charge in two dielectric media

a) Since the source charge is in medium I, then the
    solution for the reflection and the equivalent
    images due to plane I interface will be done first.
    Solution.to this two media case was explained in
    detail in Chapter II.

b) Using the equivalent charge of medium II, which is
    determined from the previous step as a source, then
    another two images will be generated due to the
    plane II interface which separates medium II and
    medium III.

c) The previous step will create a new image in medium
    II due to dielectric II, dielectric III interface.
    Then we go back and determine the equivalent
    images due to plane I interface of this image.
    The cycle of images generation will then be re-
    peated.

d) The last step will be the collection of these
    images in the three regions.

Consider a point charge Q in three dielectric media as
shown in Fig. 3.3. Each medium is characterized with a di-
electric constant ε. Due to the presence of two separation
planes, an infinite number of reflections take place which
produce an infinity of images. In order to compute the
potential at any point of the space using the image method,
it is necessary to take into account the following
considerations.
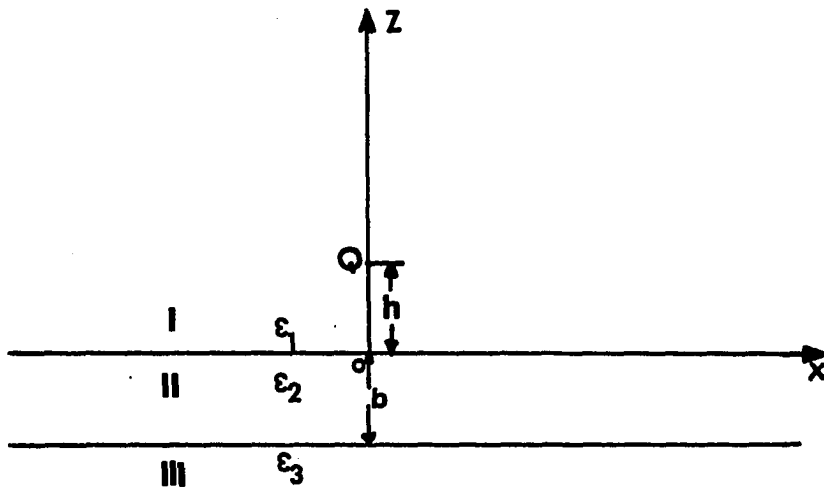
Fig. 3.3. Point charge in three dielectric media

a) The geometrical location of the images is a
    function only of the thickness of medium II and
    the position of the source charge h.

b) The total value of the potential in a point of the
    space is obtained by superimposing the effects due
    to the source charge and those of the infinity of
    images. To determine these images in the three
    dielectric case, the two media case models will be
    used.

c) In order to use the two media models in the three
    dielectric media case, one has to regard the
    plane with respect to which the reflection
    takes place as the unique plane of separation.
    It can be assumed then that space is occupied only
    by the two dielectrics separated by this plane

provided that the value of the charges placed in
the third dielectric are affected by a correction
which takes into account the suppressed dielectric.

In what follows, we shall expose in detail the deduction of the potential expressions in the three regions of the three dielectric media case.

It is very convenient for the development of formula of the three dielectric case to define relations between permittivities entering the equations for the image charges generation as follows:

$$\alpha_{mn} \triangleq \frac{\varepsilon_m - \varepsilon_n}{\varepsilon_m + \varepsilon_n} \qquad (3.3)$$

and call α_{mn} the reflection factor, while

$$\beta_{mn} \triangleq \frac{2\varepsilon_n}{\varepsilon_m + \varepsilon_n} \qquad (3.4)$$

is called the equivalence factor because it defines the equivalent charge.

Equation 3.4 can be written in terms of α_{mn}, using Eq. 3.3 as follows:

$$\beta_{mn} = 1 - \alpha_{mn} \qquad (3.5)$$

The double index used for this factor is necessary in the case of multilayer dielectrics. Double index will also be used for the images. The first index will denote the region number and the second index will carry the image number.

For example, $Q_{11}, Q_{12}, \ldots Q_{1n}$ imply the n images for region I. The same rule will be applied to all the region's charges. After these definitions, let us apply the above four steps as follows.

Consider that medium II fills the whole space occupied by dielectric II and dielectric III as shown in Fig. 3.4. Substituting Eqs. 3.3 and 3.4 into Eqs. 3.1 and 3.2, we obtain the following images:

$$Q_0 = \alpha_{12} \ Q \qquad\qquad (3.6)$$

$$Q_{21} = (1-\alpha_{12}) \ Q \qquad\qquad (3.7)$$

These are the first images in medium I and medium II respectively. The image charge Q_0 is located at $(-h)$ m and the image charge Q_{21} is located at $(+h)$ m, as shown in Fig. 3.4b and Fig. 3.4c, respectively. Notice that the model that is shown in Fig. 3.4b is only part of the complete model of region I. Q_{21} is the first image in region II. This charge will be the source for all the remaining images.

Introduce dielectric III to Fig. 3.4c as shown in Fig. 3.5a. Therefore, the reflection and the equivalent charges due to the interface of dielectrics II and III will be determined using Eqs. 3.1, 3.2 and relations 3.3 and 3.5, where m = 2 and n = 3. Then,

$$Q_{22} = \alpha_{23} \ Q_{21} \qquad\qquad (3.8)$$

and

$$Q_{31} = (1-\alpha_{23}) \ Q_{21} \qquad\qquad (3.9)$$
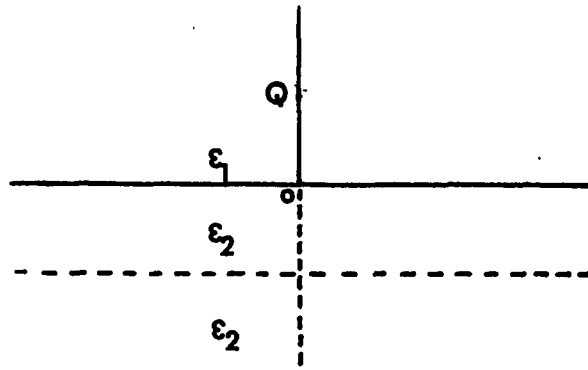
a)   Original problem
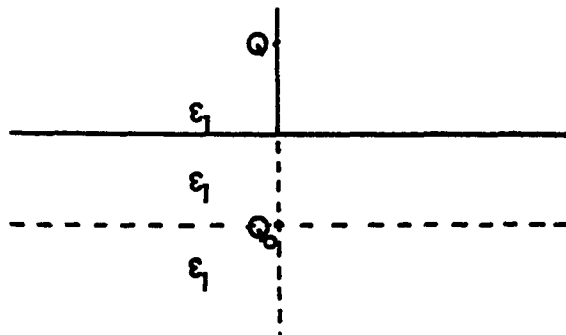
b)   Model for determining the field in region I
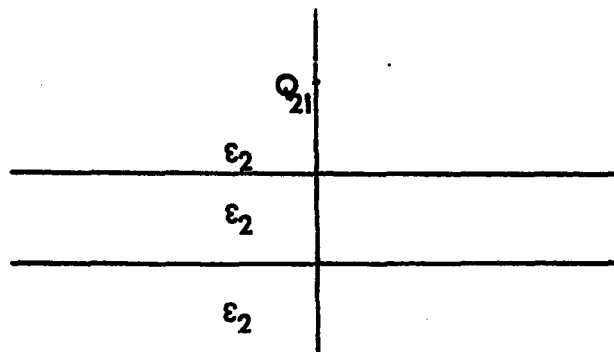
c)   Model for determining the field in region II

Fig. 3.4.   Model for determining the field in region I
and II (three dielectric media)

Substituting Eq. 3.7 into Eqs. 3.8 and 3.9, the above equations then become

$$Q_{22} = \alpha_{23} \, (1-\alpha_{12}) \, Q \qquad (3.8a)$$

and

$$Q_{31} = (1-\alpha_{23}) \, Q_{21} \qquad (3.9a)$$

where the position of these images are at $(-(h+2b))$ m and $(+(h))$ m respectively, as shown in Figs. 3.5b and 3.5c. Q_{22} is the second image in region II, and Q_{31} is the first image in region III.

The image charge Q_{22} will then create two new images due to dielectrics I and II interface. These images are determined by Eqs. 3.1-3.5, where $m = 2$ and $n = 1$. Therefore,

$$\begin{aligned} Q_{23} &= \alpha_{21} \, Q_{22} \\ &= -\alpha_{12} \, Q_{22} \end{aligned} \qquad (3.10)$$

and

$$Q_{11} = (1+\alpha_{12}) \, Q_{22} \qquad (3.11)$$

Substituting Eq. 3.8a into Eqs. 3.10 and 3.11 to get

$$Q_{23} = \alpha_{21} \, \alpha_{23} \, (1-\alpha_{12}) \, Q \qquad (3.10a)$$

and

$$Q_{11} = \alpha_{23} \, (1-\alpha^2_{12}) \, Q \qquad (3.11a)$$

where Q_{23} is the third image in region II, and Q_{11} is the first image in region I if Q_0 is excluded. The positions of these images are $(+(h+2b))$ m and $(-(h+2b))$ m respectively, as shown in Figs. 3.6b and 3.6c.
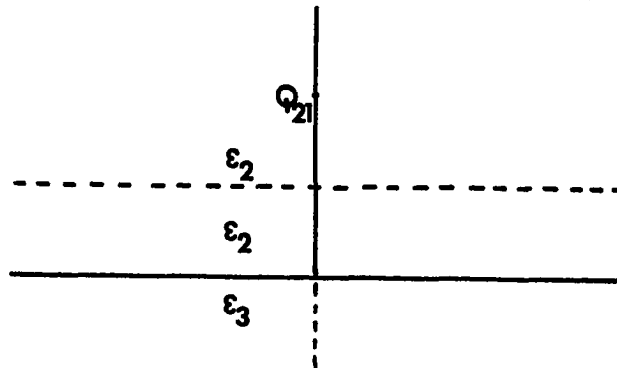
a) Position of first image in region II
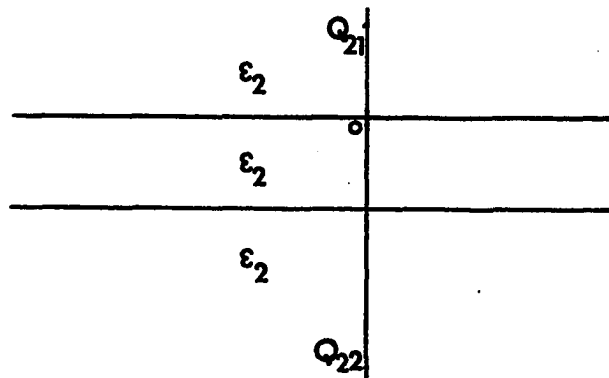
b) Positions of first and second images in region II
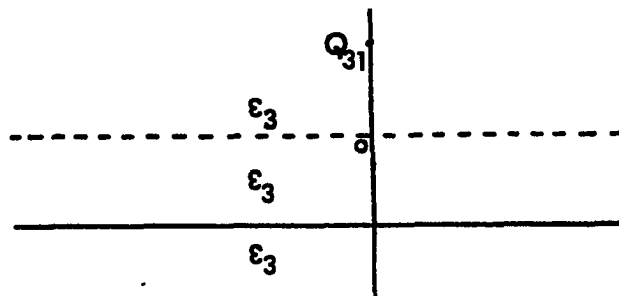
c) Position of first image in region III

Fig. 3.5. Model for determining the field in region II and
III
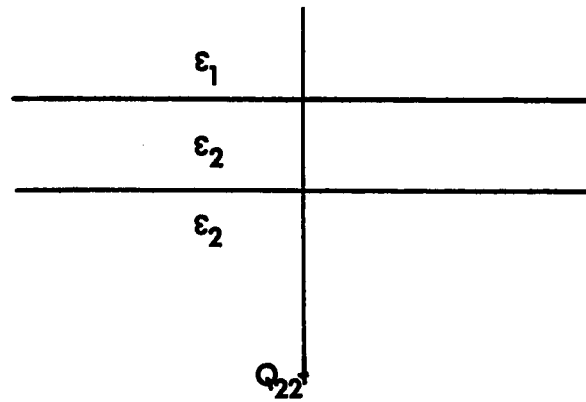
a) Position of second image in region II
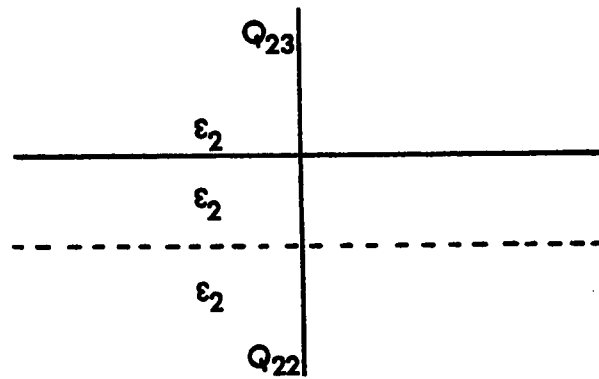
b) Positions of second and third images in region II
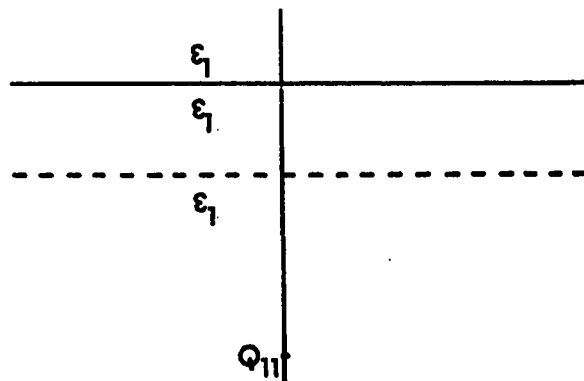
c) Position of first image in region I

Fig. 3.6. The second image location in region II, with
medium I introduced

This will now complete one cycle of image charges generation. The first cycle started with Q_{21} which is located at (h) m in region II. The second cycle will start with the image Q_{23}, located at (h+2b) m as shown in Fig. 3.6b. Thus, following the same procedure, the next images to be generated are:

$$Q_{24} = \alpha_{23} \, Q_{23}. \text{ and it is located at } -(h+4b) \text{ m.}$$

$$(3.12)$$

$$Q_{32} = (1-\alpha_{23}) \, Q_{23}, \text{ and it is located at } + (h+2b) \text{ m.}$$

$$(3.13)$$

$$Q_{25} = -\alpha_{12} \, \alpha_{23} \, Q_{23}, \text{ and it is located at } + (h+4b) \text{ m.}$$

$$(3.14)$$

$$Q_{12} = (1+\alpha_{12}) \, \alpha_{23} \, Q_{23}, \text{and it is located at } - (h+4b) \text{ m.}$$

$$(3.15)$$

Using Eq. 3.10a, then the above charges become

$$Q_{24} = -\alpha^2_{23} \, \alpha_{12} \, (1-\alpha_{12}) Q \qquad (3.12a)$$

$$Q_{32} = -\alpha_{12} \, \alpha_{23} \, (1-\alpha_{12}) \, (1-\alpha_{23}) \, Q \qquad (3.13a)$$

$$Q_{25} = \alpha^2_{12} \, \alpha^2_{23} \, (1-\alpha_{12}) \, Q \qquad (3.14a)$$

$$Q_{12} = -\alpha_{12} \, \alpha^2_{23} \, (1-\alpha^2_{12}) \, Q \qquad (3.15a)$$

The last step will be the collection of all the image charges for the three regions. Region I charges are: Q, Q_0, Q_{11}, Q_{12}, and the position of these charges are at h, -h, -(h+2b) and -(h+4b) m respectively. Using Eqs. 3.11a and 3.15a, the nth image can be generated by

$$Q_{1n} = (-\alpha_{12})^{n-1} \, (\alpha_{23})^n \, (1-\alpha^2_{12}) \, Q \qquad (3.16)$$

The corresponding position of the above charge at -(h+2nb) m. One more convention will be introduced. All parameters (charge value, distance) situated in the space z > 0 will be affected by the index (+) and all parameters situated in the space z < 0 will be affected by the index (-). Therefore, using Eqs. 3.6, 3.11a, 3.16, and with the help of Fig. 3.7, region I potential can be expressed as

$$\phi^{(1)}(x,y,z) = \frac{Q}{4\pi\varepsilon_1} \left[\frac{1}{r^+_0} + \frac{\alpha_{12}}{r^-_0} + (1-\alpha^2_{12}) \sum_{n=1}^{\infty} (-\alpha_{12})^{n-1} (\alpha_{23})^n \frac{1}{r^-_n} \right] \qquad \text{For } z \geqslant 0 \qquad (3.17)$$

where

$$r^+_0 = \sqrt{x^2 + y^2 + (z-h)^2} \qquad (3.18)$$

$$r^-_0 = \sqrt{x^2 + y^2 + (z+h)^2} \qquad (3.19)$$

and

$$r^-_n = \sqrt{x^2 + y^2 + (z+h+2nb)^2} \qquad (3.20)$$

are the distances between point p and the charges.

In region II, the charges will be divided into two groups. The first group of charges are: Q_{21}, Q_{23}, Q_{25},...etc., and the second group of charges are: Q_{22}, Q_{24}, Q_{26}....etc.

Using Eqs. 3.7, 3.10a and 3.14a, the nth term of the first group can be expressed as

$$Q^+_{2n} = (-\alpha_{12} \, \alpha_{23})^{n-1} (1-\alpha_{12}) \, Q \qquad (3.21)$$

The corresponding location is at (h+2nb) meter, where n = 1,
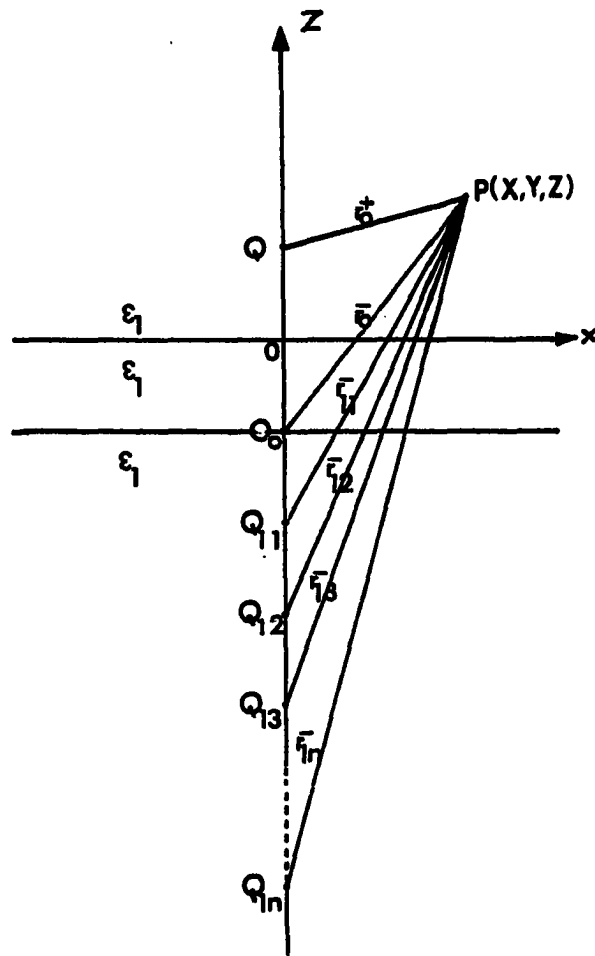
Fig. 3.7. The images location for region I field calculation

2,3,.... The nth term of the second group can then be easily written as

$$Q^-_{2n} = (-\alpha_{12})^{n-1} (\alpha_{23})^n (1-\alpha_{12}) Q \qquad (3.22)$$

The corresponding location is at $-(h+2nb)$ meter, where $n = 1,2,3,\ldots.$ Figure 3.8 shows the two groups of charges in more detail. Region II potential can then be written as

$$\Phi^{(2)}(x,y,z) = \frac{Q(1-\alpha_{12})}{4\pi\varepsilon_2} \left[\sum_{n=1}^{\infty} (-\alpha_{12}\alpha_{23})^{n-1} \frac{1}{r^+_n} + \sum_{n=1}^{\infty} (-\alpha_{23})^{n-1} (\alpha_{23})^n \frac{1}{r^-_n} \right] \qquad \text{For } -b \leqslant z \leqslant \qquad (3.23)$$

where

$$r^+_n = \sqrt{x^2 + y^2 + (z-(h+2(n-1)b))^2} \qquad (3.24)$$

and

$$r^-_n = \sqrt{x^2 + y^2 + (z+(h+2nb))^2} \qquad (3.25)$$

are the distances between point p and the charges.

In region III, the nth term of the images can be found using Eqs. 3.9a and 3.13a; therefore,

$$Q_{3n} = (-\alpha_{12}\alpha_{23})^{n-1} (1-\alpha_{12}) (1-\alpha_{23}) Q \qquad (3.26)$$

and the corresponding location will be at $(h+2(n-1)b)$ m. Therefore, the potential can then be expressed as

$$\Phi^{(3)}(x,y,z) = \frac{Q(1-\alpha_{12})(1-\alpha_{23})}{4\pi\varepsilon_3} \sum_{n=1}^{\infty} \frac{(-\alpha_{12}\alpha_{23})^{n-1}}{r^+_n}$$

$$-\infty \leqslant z \leqslant -b \qquad (3.27)$$

where

$$r^+_n = \sqrt{x^2 + y^2 + (z-(h+2(n-1)b))^2}$$
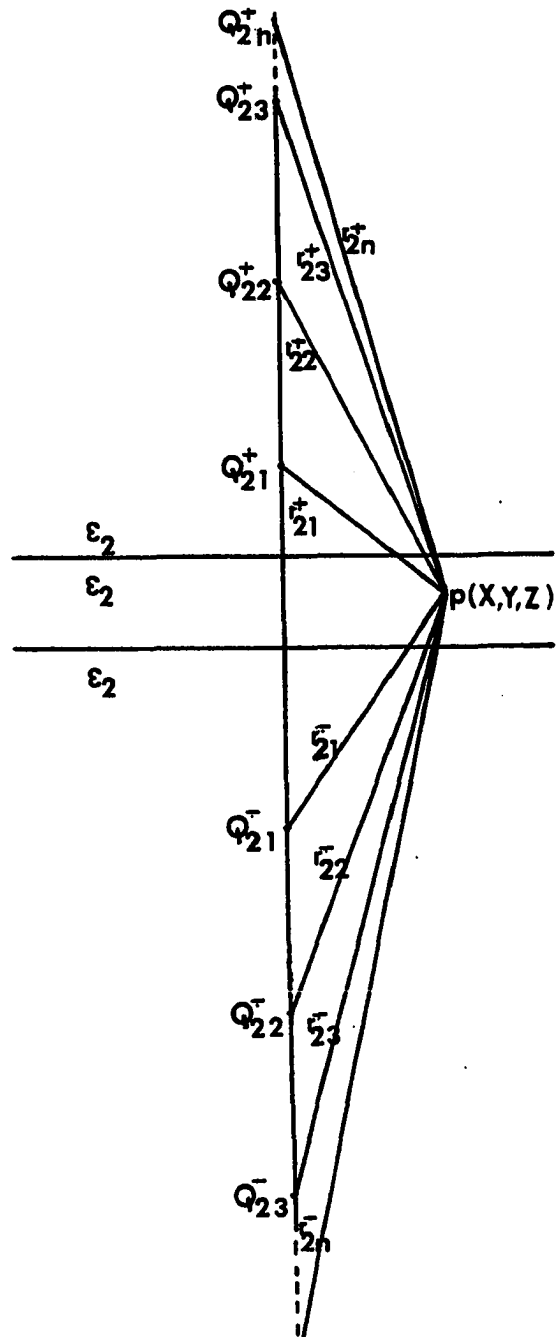
Fig. 3.8. The images location for region II field
          calculation.

Figure 3.9 shows the images location for region III.

3. Conclusion

The potential expression for the three regions of the three dielectric media are found in terms of an infinite series using the method of image technique. Another approach will be used to solve the same problem, based on writing Poisson's equation in medium I where the source is located, and Laplace's equation in regions II and III. The details of the solution will be discussed in the following section.

C. Boundary Value Problem Solution for Point Charge (in Three Dielectric Media)

A different approach will be used here to solve for the point charge case in the three dielectric media. This solution is a straightforward solution where three partial differential equations are written, one for each region. Cylindrical coordinates are chosen and symmetry is applied to simplify the final result. Consider the cylindrical configuration of Fig. 3.10.

The homogenous potential equations that describe the three dielectric media case are:

$$\nabla^2 \phi^{(1)} (\rho, z) = 0 \tag{3.28}$$

$$\nabla^2 \phi^{(2)} (\rho, z) = 0 \tag{3.29}$$

$$\nabla^2 \phi^{(3)} (\rho, z) = 0 \tag{3.30}$$
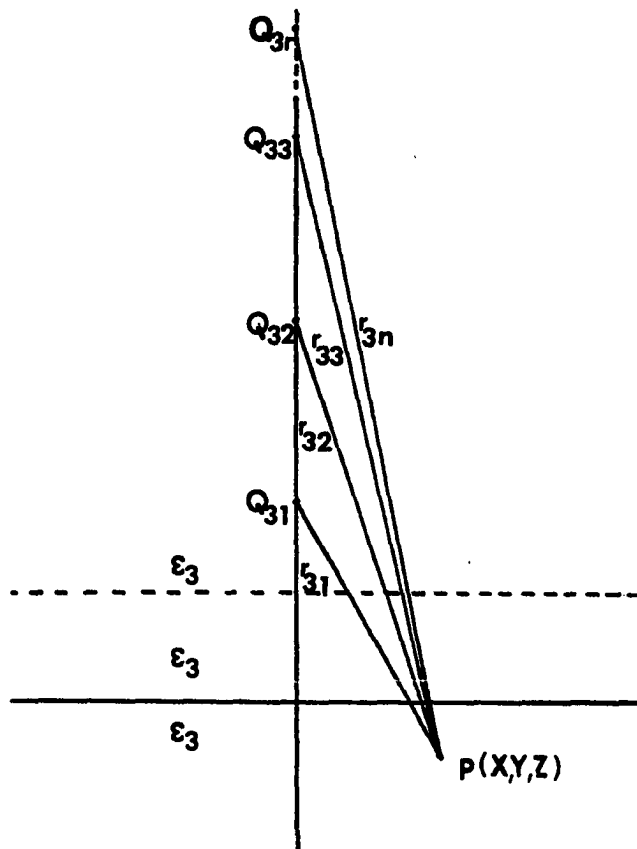
Fig. 3.9. The images location for region III field
calculation
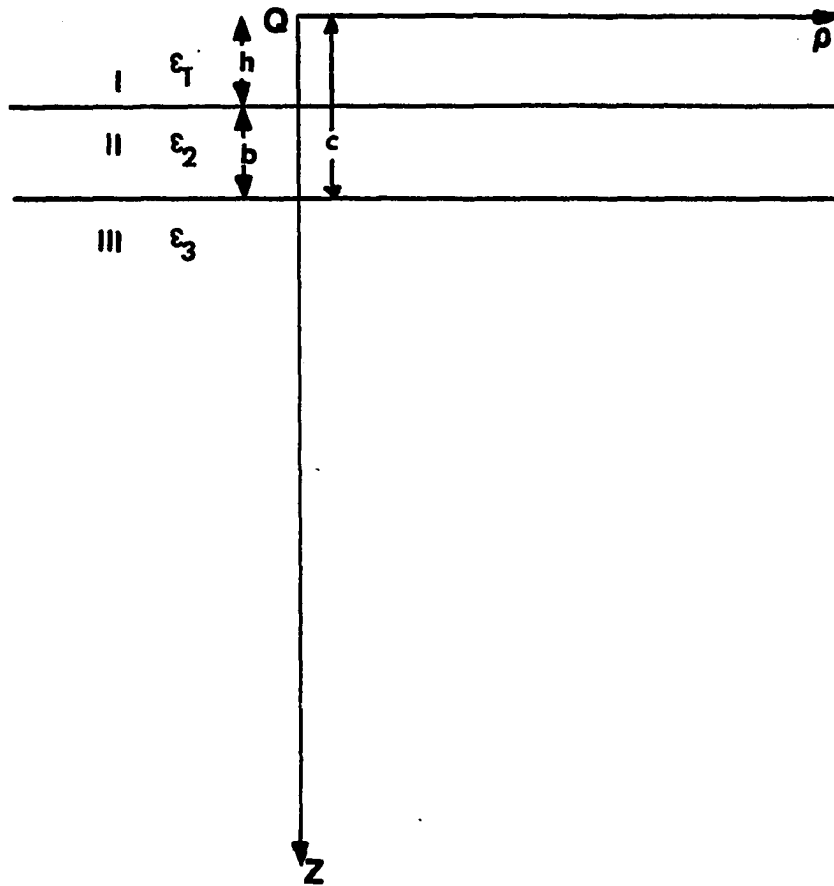
Fig. 3.10. Point charge at the origin of a cylindrical
coordinate in three dielectric media

Equations 3.28-3.30 are the Laplace's equation for the three dielectric media case. Where $\Phi^{(1)}$, $\Phi^{(2)}$ and $\Phi^{(3)}$ are the electrical potential of medium I, medium II and medium III respectively. The field boundary conditions for the above three equations are:

a) The electrical potentials at the dielectric interface are equal, i.e.,

$$\Phi^{(1)}(\rho,z)\bigg|_{z=h} = \Phi^{(2)}(\rho,z)\bigg|_{z=h} \tag{3.31}$$

and

$$\Phi^{(2)}(\rho,z)\bigg|_{z=c} = \Phi^{(3)}(\rho,z)\bigg|_{z=c} \tag{3.32}$$

b) The normal component of the flux densities at the boundary are equal, i.e.,

$$\varepsilon_1 \frac{\partial \Phi^{(1)}}{\partial z}\bigg|_{z=h} = \varepsilon_2 \frac{\partial \Phi^{(2)}}{\partial z}\bigg|_{z=h} \tag{3.33}$$

and

$$\varepsilon_2 \frac{\partial \Phi^{(2)}}{\partial z}\bigg|_{z=c} = \varepsilon_3 \frac{\partial \Phi^{(3)}}{\partial z}\bigg|_{z=c} \tag{3.34}$$

c) $\Phi^{(1)}(\rho,z) \to 0$ as $z \to -\infty$

$\Phi^{(3)}(\rho,z) \to 0$ as $z \to +\infty$ $\tag{3.35}$

Equations 3.28-3.30 can be expanded in cylindrical coordinates as follows:

$$\frac{1}{\rho} \frac{\partial}{\partial \rho} (\rho \frac{\partial \Phi^{(i)}}{\partial \rho}) + \frac{1}{\rho} \frac{\partial^2 \Phi^{(i)}}{\partial \Phi^2} + \frac{\partial^2 \Phi^{(i)}}{\partial z^2} = 0 \quad ; \quad i = 1,2,3$$

(3.28a)

Using the separation of variables technique, the solution to Eq. 3.28a is

$$\Phi (\rho,z) = Z(z) \ \Phi(\Phi) \ R(\rho)$$

(3.36)

where $Z(z)$, $\Phi(\Phi)$ and $R(\rho)$ are functions of z, the angle Φ and ρ respectively. Due to symmetry, no Φ dependence exists, i.e., $\Phi_{(\Phi)}=1$. Therefore, Eq. 3.36 becomes

$$\Phi(\rho,z) = Z(z) \ R(\rho)$$

(3.37)

The separation of variable technique gives the following solutions.

$$Z(z) = Ae^{-mz} + Be^{mz}$$

(3.38)

$$R(\rho) = C \ J_0(\rho m) + D \ N_0(\rho m)$$

(3.39)

Where A, B, C, D and m are constants to be determined by applying the boundary conditions (Eqs. 3.31-3.35), $N_0(\rho m)$ is not finite at $\rho=0$; therefore, the constant D has to be zero and Eq. 3.39 reduces to

$$R(\rho) = C \ J_0(\rho m)$$

(3.40)

Substituting Eq. 3.38 and Eq. 3.40 into Eq. 3.37, we obtain

$$\Phi(\rho,z) = (Ae^{-mz} + Be^{mz}) \ C \ J_0(\rho m)$$

(3.41)

Eq. 3.41 is the general solution of Laplace's equation. Applications of this solution to the three regions will be developed here.

1. The potential equation in region I

In region I, the potential must equal to zero at $z = -\infty$. Therefore, the constant A has to be zero in Eq. 3.41. Then, the potential equation in region I becomes

$$\phi^{(1)}(\rho,z) = B e^{mz}\ C\ J_0(\rho m)$$

Let BxC equal a new constant D_1. Then

$$\phi^{(1)}(\rho,z) = D_1\ e^{mz}\ J_0(\rho m) \tag{3.42}$$

Equation 3.42 is the solution of Laplace's equation in region I. To get the complete solution in region I, a solution due to the charge in region I has to be added. The potential due to the point charge is

$$\phi^{(1)}{}_2(\rho,z) = Q/4\pi\varepsilon_1 \sqrt{\rho^2+z^2} \tag{3.43}$$

where $\phi^{(1)}{}_2(\rho,z)$ is the second component of the general equation in region I. Using any mathematics textbook table [35], Eq. 3.43 can be expressed as

$$\Phi^{(1)}{}_2(\rho,z) = \frac{Q}{4\pi\varepsilon_1} \int_0^\infty e^{-m|z|}\ J_0(\rho m)\ dm \tag{3.44}$$

Therefore, the complete solution of region I can be found by adding Eq. 3.42 to Eq. 3.44.

$$\Phi^{(1)}(\rho,z) = \frac{Q}{4\pi\varepsilon_1} \int_0^\infty e^{-m|z|}\ J_0(\rho m)\ dm + \int_0^\infty D_1\ e^{mz}$$

$$J_0(\rho m)\ dm \tag{3.45}$$

2. The potential equation in region II

Since region II is bounded on the z direction, the two exponential terms exist in Eq. 3.41 and the region II solution can be written as a Fourier integral that is exactly similar to Eq. 3.45.

$$\Phi^{(2)}(\rho,z) = \int_0^\infty \left[C_2 e^{-mz} + D_2 e^{mz} \right] J_0(\rho m) \, dm \qquad (3.46)$$

where C_2 and D_2 are new constants to be determined and equal to the old constants AxC and BxC of Eq. 3.41 respectively.

3. The potential equation in region III

In region III, the potential must be equal to zero at z=+∞. Therefore, the constant B in Eq. 3.41 has to be zero. Thus, region IV potential becomes

$$\Phi^{(3)}(\rho,z) = \int_0^\infty D_3 e^{-mz} J_0(\rho m) \, dm \qquad (3.47)$$

where D_3 is a constant to be determined and equal to the old constant AxC of Eq. 3.41.

The next step in the solution procedure is to determine the four constants in the potential Eqs. 3.41-3.47. The boundary conditions in Eqs. 3.31-3.34 will be utilized. Substituting the boundary conditions of Eqs. 3.31 and 3.33 into Eq. 3.45 and Eq. 3.46, and neglecting the integral sign for the time being, we obtain

$$\frac{Q}{4\pi\varepsilon_1} e^{-mh} + D_1 e^{mh} = C_2 e^{-mh} + D_2 e^{mh} \qquad (3.48)$$

and

$$\frac{Q}{4\pi\varepsilon_1} e^{-mh} - D_1 e^{mh} = \frac{\varepsilon_2}{\varepsilon_1} [C_2 e^{-mh} - D_2 e^{mh}] \qquad (3.49)$$

Substituting the boundary conditions of Eqs. 3.32 and 3.34 into Eq. 3.46 and Eq. 3.47 to get

$$C_2 e^{-mc} + D_2 e^{mc} = D_3 e^{-mc} \qquad (3.50)$$

and

$$-C_2 e^{-mc} + D_2 e^{mc} = -\varepsilon_3/\varepsilon_2 D_3 e^{-mc} \qquad (3.51)$$

Therefore, Eqs. 3.48-3.51 can be solved for the constants D_1, C_2, D_2 and D_3.

Adding Eq. 3.49 to Eq. 3.48 and dividing the final result by e^{-mh}, we obtain

$$\frac{Q}{2\pi} = (\varepsilon_1 + \varepsilon_2) C_2 + (\varepsilon_1 - \varepsilon_2) D_2 e^{2mh} \qquad (3.52)$$

Subtracting Eq. 3.49 from Eq. 3.48 and dividing the final result by e^{mh}, we get

$$2D_1 = \frac{\varepsilon_1 - \varepsilon_2}{\varepsilon_1} C_2 e^{-2mh} + \frac{\varepsilon_1 + \varepsilon_2}{\varepsilon_1} D_2 \qquad (3.53)$$

Multiplying Eq. 3.50 by $\varepsilon_3/\varepsilon_2$ and adding the result to Eq. 3.51 to get

$$(\varepsilon_3 - \varepsilon_2) C_2 e^{-mc} + (\varepsilon_2 + \varepsilon_3) D_2 e^{mc} = 0 \text{ or}$$

$$D_2 = \frac{\varepsilon_2 - \varepsilon_3}{\varepsilon_2 + \varepsilon_3} C_2 \, e^{-2mc} \qquad (3.54)$$

Substituting Eq. 3.54 into Eq. 3.52 to obtain

$$C_2 = \frac{\varepsilon_2 + \varepsilon_3}{(\varepsilon_1 + \varepsilon_2)(\varepsilon_2 + \varepsilon_3) + (\varepsilon_1 - \varepsilon_2)(\varepsilon_2 - \varepsilon_3) \, e^{-2mb}} \, \frac{Q}{2\pi} \qquad (3.55)$$

where $b = c-h$ and

$$D_2 = \frac{\varepsilon_2 - \varepsilon_3}{(\varepsilon_1 + \varepsilon_2)(\varepsilon_2 + \varepsilon_3) + (\varepsilon_1 - \varepsilon_2)(\varepsilon_2 - \varepsilon_3) \, e^{-2mb}} \, \frac{Q}{2\pi} \qquad (3.56)$$

Substituting Eq. 3.55 and Eq. 3.56 into Eqs. 3.48 and 3.50 to get

$$D_1 = \frac{(\varepsilon_1 - \varepsilon_2)(\varepsilon_2 + \varepsilon_3) \, e^{-2mh} + (\varepsilon_1 + \varepsilon_2)(\varepsilon_2 - \varepsilon_3) \, e^{-2mc}}{(\varepsilon_1 + \varepsilon_2)(\varepsilon_2 + \varepsilon_3) + (\varepsilon_1 - \varepsilon_2)(\varepsilon_2 - \varepsilon_3) \, e^{-2mb}} \, \frac{Q}{4\pi\varepsilon_1} \qquad (3.57)$$

and

$$D_3 = \frac{2\varepsilon_2}{(\varepsilon_1 + \varepsilon_2)(\varepsilon_2 + \varepsilon_3) + (\varepsilon_1 - \varepsilon_2)(\varepsilon_2 - \varepsilon_3) \, e^{-2mb}} \, \frac{Q}{2\pi} \qquad (3.58)$$

Utilizing the definition of α_{12} and α_{23} described earlier, Eqs. 3.55-3.58 can be written as follows.

$$C_2 = \frac{(1 - \alpha_{12})}{1 + \alpha_{12} \, \alpha_{23} \, e^{-2mb}} \, \frac{Q}{4\pi\varepsilon_2} \qquad (3.55a)$$

$$D_2 = \frac{\alpha_{23} \, (1 - \alpha_{12})}{1 + \alpha_{12} \, \alpha_{23} \, e^{-2mb}} \, \frac{Q}{4\pi\varepsilon_2} \qquad (3.56a)$$

$$D_1 = \frac{\alpha_{12} \, e^{-2mh} + \alpha_{23} \, e^{-2mc}}{1 + \alpha_{12} \, \alpha_{23} \, e^{-2mb}} \, \frac{Q}{4\pi\epsilon_1} \tag{3.57a}$$

and

$$D_3 = \frac{(1-\alpha_{12}) \, (1-\alpha_{23})}{1 + \alpha_{12} \, \alpha_{23} \, e^{-2mb}} \, \frac{Q}{4\pi\epsilon_2} \tag{3.58a}$$

Once these constants are determined, the potential equation in each region of the three dielectric media can be written. Substituting Eqs. 3.55a-3.58a in Eqs. 3.45-3.47, we can write the final potential expressions

$$\Phi^{(1)}(\rho,z) = \frac{Q}{4\pi\epsilon_1} \left\{ \int_0^\infty \left[e^{-m|z|} + \frac{\alpha_{12} \, e^{-2mh} + \alpha_{23} \, e^{-2mc}}{1 + \alpha_{12} \, \alpha_{23} \, e^{-2mb}} \, e^{mz} \right] \right.$$

$$\left. J_0(\rho m) \, dm \right\} \qquad -\infty \leqslant z \leqslant h \tag{3.59}$$

$$\Phi^{(2)}(\rho,z) = \frac{Q}{4\pi\epsilon_2} \left\{ \int_0^\infty \left[\frac{e^{-mz} + \alpha_{23} \, e^{-2mc} \, e^{mz}}{1 + \alpha_{12} \, \alpha_{23} \, e^{-2mb}} \right] J_0(\rho m) \, dm \right\}$$

$$h \leqslant z \leqslant c \tag{3.60}$$

and

$$\Phi^{(3)}(\rho,z) = \frac{Q(1-\alpha_{12})(1-\alpha_{23})}{4\pi\epsilon_3} \left\{ \int_0^\infty \frac{e^{-mz}}{1 + \alpha_{12} \, \alpha_{23} \, e^{-2mb}} \, J_0(\rho m) \, dm \right\}$$

$$z \geqslant c \tag{3.61}$$

Equations 3.59-3.61 can, in fact, be proved to be exactly the same as Eqs. 3.17, 3.23 and 3.27 found by the

image method. The proof appears in Appendix A for the convenience of the interested reader.

D. Conclusion

In this chapter, two methods of solution of the multiple dielectric problem are presented. The first method is the application of the image technique. The second method is a straightforward solution to Poisson's equations using the separation of variables technique. Both solutions yield the same result. The second solution seems to be much easier than the image technique in this case, but this is not true in case of more than three dielectric media as will be seen in the next chapter. The potential expression underneath the integral becomes large, and the evaluation of such an integral is difficult or even impossible unless special numerical techniques are used. Therefore, it becomes necessary to find an alternative method. Such a method will be based on developing a digital computer algorithm to generate the images.

IV. THE ELECTRIC FIELD DISTRIBUTION IN FOUR AND FIVE DIELECTRIC MEDIA

A. Introduction

In the previous chapter, two methods of solution (the image technique and the boundary value problem solution) are discussed. It was pointed out that the second method is (much) easier than the first method. This statement is also true in the case of a larger number of dielectric layers but the difficulty is in the evaluation of the infinite integrals as will be shown in the case of four dielectric media. The procedure of the image method presented in Chapter III will not be followed because of the difficulty in keeping track of the images. Thus, there is a need for an alternative method. Such a method is proposed and is based on the image technique using a digital computer algorithm. The computer algorithm will be first developed for the three dielectric media case. A comparison between this method and Chapter III solution will be made. The same algorithm will then be extended to cover both the four and the five dielectric media.

B. The Four Dielectric Media Case

In this instance, one more dielectric layer will be added to Fig. 3.17. In order to be more specific, medium II

will be divided into two media as shown in Fig. 4.1, where

the dielectric constants of these two media are ε_2 and ε_3.

Let medium I, where the source is located, to be air with ε_1

its permittivity and medium IV to be the fourth layer that

may be the ground with either a finite dielectric constant

(dielectric plane) or with infinite dielectric constant

(perfect conductor). Two methods of solution are presented.

The first one is solving Poisson's equation using the

separation of variables technique to show the complexity of

the obtained integrals. The second solution will be to

develop a computer algorithm using the image method.

1. Boundary value problem solution

Consider Fig. 4.1, which is exactly the same as Fig.

3.17. The only differences are: medium II of Fig. 3.17 is

divided into two media, medium II and medium III, while

medium III becomes medium IV in this case, following exactly

the same procedure of Chapter III. The general potential

expressions for the four regions can be written, by

inspection, similar to Eqs. 3.45-3.47 as follows:

Region I
$$\Phi^{(1)}(\rho,z) = \frac{Q}{4\pi\varepsilon_1}\left[\int_0^\infty e^{-m|z|}\ J_0(\rho m)\ dm + \int_0^\infty A_1\ e^{mz}J_0(\rho m)\,dm\right] \quad (4.1)$$

Region II
$$\Phi^{(2)}(\rho,z) = \int_0^\infty [A_2\ e^{-mz} + B_2\ e^{mz}]\ J_0(\rho m)\ dm \quad (4.2)$$

Region III
$$\Phi^{(3)}(\rho,z) = \int_0^\infty [A_3\ e^{-mz} + B_3\ e^{mz}]\ J_0(\rho m)\ dm \quad (4.3)$$
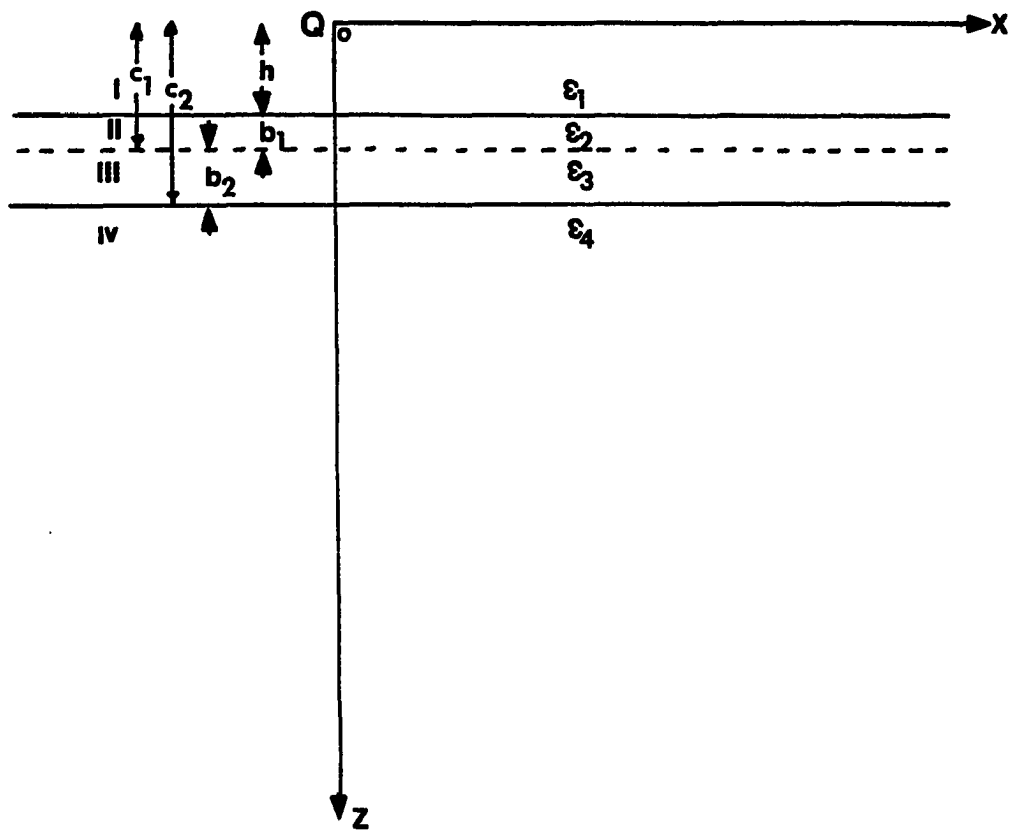
Fig. 4.1. Point charge in four dielectric media

and finally

$$\Phi^{(4)}(\rho,z) = \int_0^\infty A_4\, e^{-mz}\, J_0(\rho m)\, dm \qquad\qquad (4.4)$$

Where A_1, A_2, A_3, A_4, B_2, B_3. and B_4 are constants that can easily be determined by applying the following boundary conditions.

$$\Phi^{(1)}(\rho,z) = \Phi^{(2)}(\rho,z) \ \big|\ z = h \qquad\qquad (4.5)$$

$$\Phi^{(2)}(\rho,z) = \Phi^{(3)}(\rho,z) \ \big|\ z = c_1 \qquad\qquad (4.6)$$

$$\Phi^{(3)}(\rho,z) = \Phi^{(4)}(\rho,z) \ \big|\ z = c_2 \qquad\qquad (4.7)$$

and

$$\varepsilon_1 \frac{\partial\Phi^{(1)}}{\partial z} = \varepsilon_2 \frac{\partial\Phi^{(2)}}{\partial z} \ \bigg|_{z=h} \qquad\qquad (4.8)$$

$$\varepsilon_2 \frac{\partial\Phi^{(2)}}{\partial z} = \varepsilon_3 \frac{\partial\Phi^{(3)}}{\partial z} \ \bigg|_{z=c_1} \qquad\qquad (4.9)$$

$$\varepsilon_3 \frac{\partial\Phi^{(3)}}{\partial z} = \varepsilon_4 \frac{\partial\Phi^{(4)}}{\partial z} \ \bigg|_{z=c_2} \qquad\qquad (4.10)$$

If these boundary conditions (Eqs. 4.5-4.10) are substituted into Eqs. 4.1-4.4, the constants can be determined. The following potential equations can then be obtained easily.

Region I

$$\Phi^{(1)}(\rho,z) = \frac{Q}{4\pi\varepsilon_1} \int_0^\infty e^{-m|z|} +$$

$$\left[\frac{\alpha_{12}\, e^{-2mh} + \alpha_{12}\alpha_{23}\alpha_{34}\, e^{-2m(h+b2)} + \alpha_{23}\, e^{-2mc_1} + \alpha_{34}\, e^{-2mc_2}}{1 + \alpha_{23}\alpha_{34}\, e^{-2mb_2} + \alpha_{12}\alpha_{23}\, e^{-2mb_1} + \alpha_{12}\alpha_{34}\, e^{-2m(b_1+b_2)}} \right.$$

$$\times\, e^{mz} \quad J_0(\rho m)\, dm$$

$$(4.11)$$

Region II

$$\Phi^{(2)}(\rho,z) = \frac{Q(1+\alpha_{12})}{4\pi\varepsilon_1} \int_0^\infty$$

$$\left[\frac{(1+\alpha_{23}\alpha_{34}\,e^{-2mb_2})e^{-mz} + (\alpha_{23}\,e^{-2mc_1} + \alpha_{34}\,e^{-2mc_2})\,e^{mz}}{1 + \alpha_{23}\alpha_{34}\,e^{-2mb_2} + \alpha_{12}\alpha_{23}\,e^{-2mb_1} + \alpha_{12}\alpha_{34}\,e^{-2m(b_1+b_2)}}\right]$$

$$J_0(\rho m)\,dm \qquad\qquad (4.12)$$

Region III

$$\Phi^{(3)}(\rho,z) = \frac{Q(1+\alpha_{12})(1+\alpha_{23})}{4\pi\varepsilon_1} \int_0^\infty$$

$$\frac{(e^{-mz} + \alpha_{34}\,e^{-2mc_2}\,e^{mz})\,J_0(\rho m)\,dm}{1 + \alpha_{23}\alpha_{34}\,e^{-2mb_2} + \alpha_{12}\alpha_{23}\,e^{-2mb_1} + \alpha_{12}\alpha_{34}\,e^{-2m(b_1+b_2)}}$$

$$(4.13)$$

Region IV

$$\Phi^{(4)}(\rho,z) = \frac{Q(1+\alpha_{12})(1+\alpha_{23})(1+\alpha_{34})}{4\pi\varepsilon_1} \int_0^\infty$$

$$\frac{e^{-mz}\,J_0(\rho m)\,dm}{1 + \alpha_{23}\alpha_{34}\,e^{-2mb_2} + \alpha_{12}\alpha_{23}\,e^{-2mb_1} + \alpha_{12}\alpha_{34}\,e^{-2m(b_1+b_2)}}$$

$$(4.14)$$

If these four potential equations are tested under the following special case, when $\varepsilon_2 = \varepsilon_3$, α_{23} becomes equal to zero, then medium II and medium III become one medium. The four regions will then reduce to three regions and Eqs. 4.11-4.14 will then be exactly matched to Eqs. 3.63-3.65. If $\alpha_{23} = 0$, then Eq. 4.11 becomes

$$\Phi^{(1)}(\rho,z) = \frac{Q}{4\pi\varepsilon_1} \int_0^\infty \left[e^{-m|z|} + \frac{(\alpha_{12}\, e^{-2mh} + \alpha_{34}\, e^{-2mc_2})}{1 + \alpha_{12}\alpha_{34}\, e^{-2m(b_1+b_2)}}\, e^{mz} \right]$$

$$J_0(\rho m)\, dm \qquad\qquad (4.12a)$$

This equation is exactly the same as Eq. 3.63. Eqs. 4.12 and 4.13 become equal, since both describe the same medium.

$$\Phi^{(2)}(\rho,z) = \Phi^{(3)}(\rho,z) = \frac{Q(1+\alpha_{12})}{4\pi\varepsilon_1} \int_0^\infty \frac{e^{-mz} + \alpha_{34}\, e^{-2mc_2}\, e^{mz}}{1 + \alpha_{12}\alpha_{34}\, e^{-2mb}}$$

$$J_0(\rho m)\, dm \qquad\qquad (4.12a)$$

Equation 4.12a is in fact the same as Eq. 3.64, where

$$\frac{(1+\alpha_{12})}{\varepsilon_1} = \frac{(1-\alpha_{12})}{\varepsilon_2}$$

Finally, if $\alpha_{23} = 0$ is substituted into Eq. 4.14, the potential expression becomes

$$\phi^{(4)}(\rho,z) = \frac{Q(1+\alpha_{12})(1+\alpha_{34})}{4\pi\varepsilon_1} \int_0^\infty \frac{e^{-mz}}{1 + \alpha_{12}\alpha_{34} e^{-2mb}} J_0(\rho m)\ dm$$

(4.14a)

Equation 4.14a checks with Eq. 3.65.

2. Generation of the images by computer

a. Introduction · This method was first introduced in 1978 by Takashima and Ishibashi [36], where they looked to the point charge case and that of a spherical conductor in front of three dielectric media on a perfect conductor ground. A similar algorithm will be used to solve for the vegetation medium underneath the EHV transmission line. In this case, the vegetation (corn) will be mainly represented by two layers of uniform dielectric constants.

First, a computer algorithm will be developed for the three dielectric media. It was found much easier to start with the three media case, and then the four and the five dielectric media algorithms would follow exactly the same pattern. This algorithm will be accompanied by a schematic diagram to show the location of the image charges in the three regions.
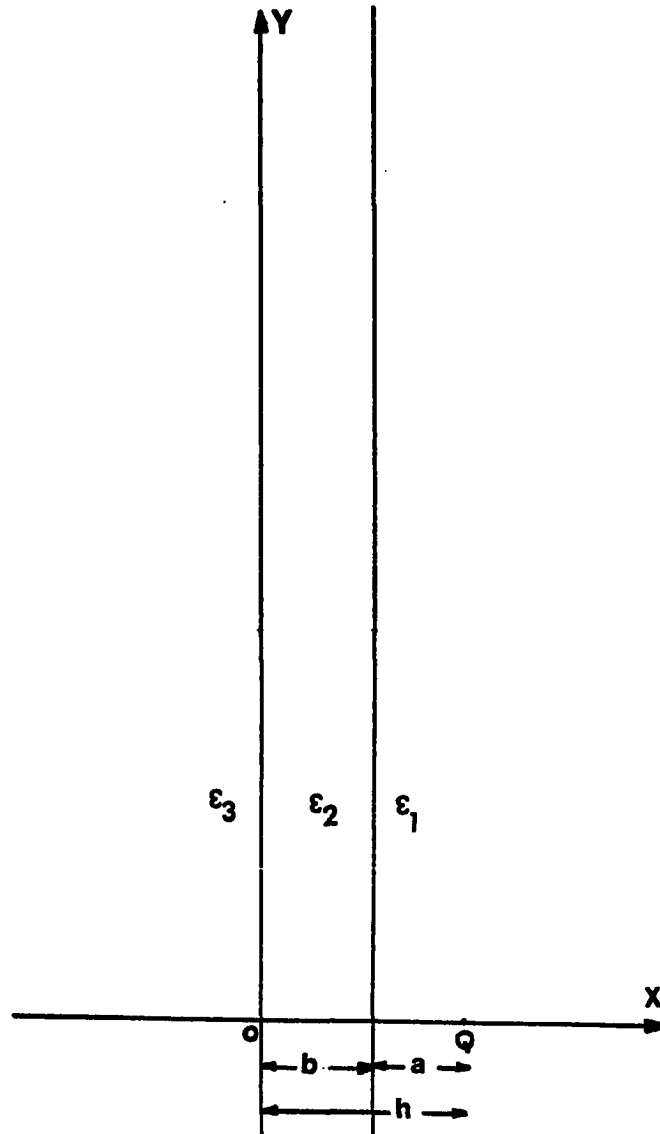
Fig. 4.2. Point charge in the three dielectric media

The developed computer algorithm will be compared to Chapter III solution and it will be shown that both solutions are exactly the same.

The three dielectric media algorithm will then be followed by the four and the five dielectric algorithms. Two examples are given at the end of this chapter for the point charge case to show the validity and the accuracy of these algorithms.

$\underline{b}$. **Point charge in three dielectric media** Let the point charge be located in medium I as shown in Fig. 4.2. The electric field due to the charge Q is symmetrical about the x-axis. By now, it is clear that if a charge Q is placed in front of a dielectric plane, two fictitious images will be generated. One is equal to $Q(\varepsilon_1-\varepsilon_2)/(\varepsilon_1+\varepsilon_2)$ and located at a distance a meters to the left of the A interface. This image together with the original charge will determine the field in medium I. The second fictitious image is equal to $(2\varepsilon_2/(\varepsilon_1+\varepsilon_2)Q$ and is located in place of the original charge or a meters to the right of the A interface. This charge will determine the field at any point in medium II, as shown in Fig. 4.3. Takashima and Ishibashi explained this problem by analogy with geometrical optics. A point charge is replaced with a point source of light. The illuminance in medium I is given by the direct light from the source Q and the reflected

light in the semitransparent plane. The reflection is expressed by an image $Q_0 = ((\varepsilon_1-\varepsilon_2)/(\varepsilon_1+\varepsilon_2))Q$. The illuminance in medium II is given by the transmitted light through the semitransparent plane. The transmission is expressed by an image $Q_{11} = (2\varepsilon_2/\varepsilon_1+\varepsilon_2)Q$. Let us follow Chapter III definitions, where $\alpha_{mn} = \varepsilon_m-\varepsilon_n/\varepsilon_m+\varepsilon_n$ is the coefficient of reflection and $\beta_{mn} = 2\varepsilon_n/(\varepsilon_m+\varepsilon_n)$ is the coefficient of transmission.

Figure 4.3 shows a schematic diagram for the images that are generated by the application of the above results. The first images due to plane A interface are Q_0 and Q_{11}, where $Q_0 = \alpha_{12}Q$ and $Q_{11} = \beta_{12}Q$. The corresponding positions of these two images are: a meters to the left of the A interface and a meters to the right of the A interface respectively.

The charge Q_{11}, which is located to the right of the A interface or (b+a) meters to the right of 0 interface, then creates two new images due to plane 0 interface; $Q_{21} = \alpha_{23}Q_{11}$ for medium II field calculation and $Q_{31} = \beta_{23}Q_{11}$ for medium III field calculation. The positions of these two images are: (b+a) meters to the left of 0, and (b+a) meters to the right of 0 respectively, as shown in Fig. 4.3.

The charge Q_{21} will then yield two new charges due to plane A interface; $Q_{12} = \alpha_{21}Q_{21}$ and $Q_{41} = \beta_{21}Q_{11}$. The positions of these two images are at (a+2b) meters to the

right of A and (a+2b) meters to the left of A interface.

Then, a summary of the above generated images is as follows.

$$Q_0 = \alpha_{12}Q$$

Let the corresponding location be named $l_0 = a$ from A to the left.

$$Q_{11} = \beta_{12}Q$$

Let the corresponding location be named $l_{11} = a$ from A to the right.

$$Q_{21} = \alpha_{23}Q_{11}$$

Let the corresponding location be named $l_{21} = l_{11} + b$ from 0 to the left.

$$Q_{31} = \beta_{23}Q_{11}$$

Let the corresponding location be named $l_{31} = l_{11} + b$ from 0 to the right.

$$Q_{12} = \alpha_{21}Q_{21}$$

Let the corresponding location be named $l_{12} = l_{21} + b$ from A to the right.

$$Q_{41} = \beta_{21}Q_{21}$$

Let the corresponding location be named $l_{41} = l_{21} + b$ from A to the left.

Figure 4.3 shows a few more steps of the generated images and their corresponding locations. Looking carefully to this schematic diagram, we would be able to notice the following:
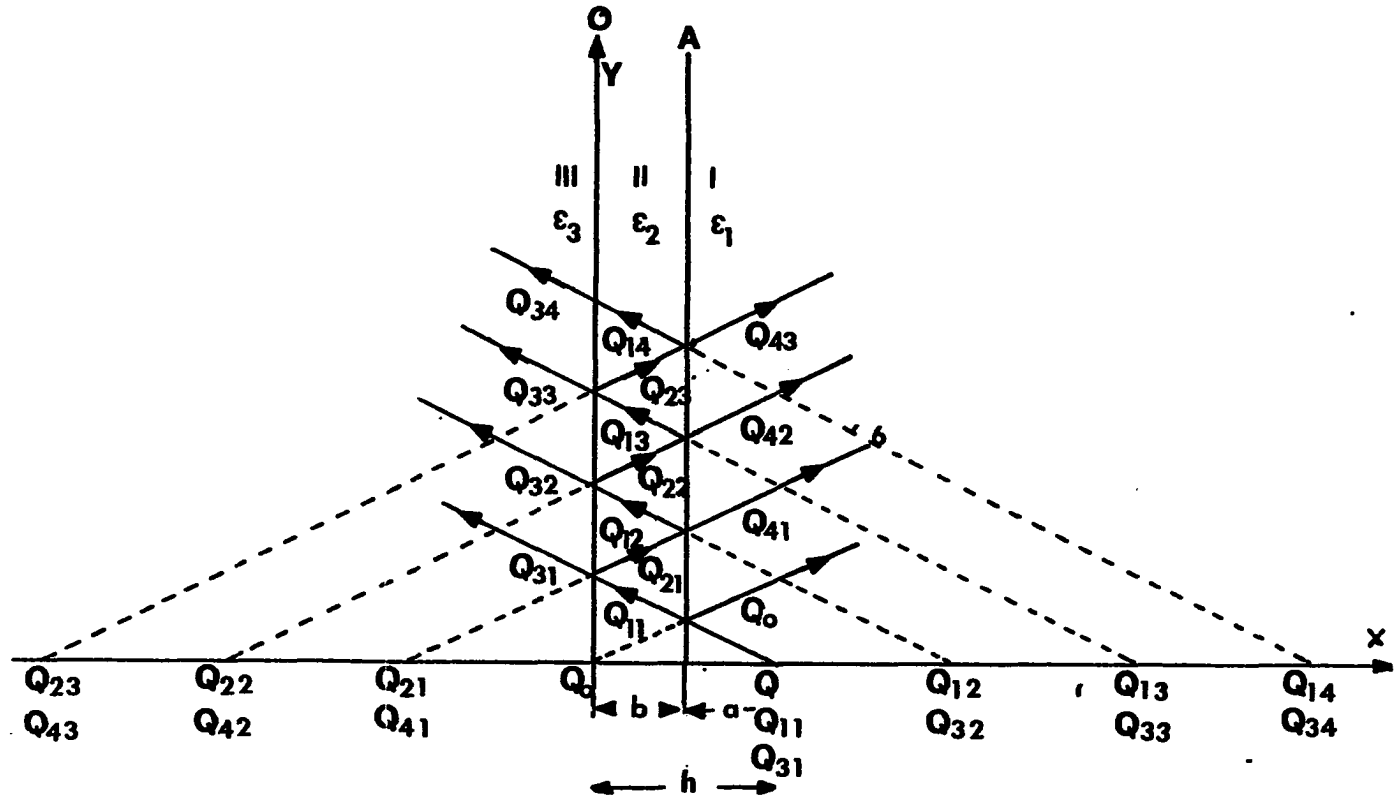
Fig. 4.3. Schematic diagram showing the position of the image charges due to point charge in front of three dielectric media case

a) Medium I charges are: Q, Q_0 and

Q_{41}, Q_{42}, $\ldots Q_{4j}$

b) Medium II charges are: Q_{11}, Q_{12}, $\ldots Q_{1n}$ and

Q_{21}, Q_{22}, $\ldots Q_{2m}$

c) Medium III charges are: Q_{31},

Q_{32}, $\ldots Q_{3i}$

where i, j, n and m are used as a counter for the images.

To start developing the computer algorithm, let us use an array notation, where the images belonging to Q_1, for example, will be stored in the Q_1 array as Q1(1), Q1(2),... Q1(j). The corresponding positions of these images will be at 11(1), 11(2),...11(j). The same notation can be applied to Q_2. Q_3. Q_4 and their corresponding positions l_2, l_3 and l_4 respectively.

Following the patterns developed in the preceding paragraphs, the use of array notation results in an algorithm that intuitively satisfies and is generally applicable.

j=1

$Q_2(j) = \alpha_{23}Q_1(j)$

$Q_3(j) = \beta_{23}Q_1(j)$

$Q_1(j+1) = \alpha_{21}Q_2(j)$

$Q_4(j) = \beta_{21}Q_2(j)$ (4.15)

and

$L_2(j) = L_1(j) + b$

$$L_3(j) = L_1(j) + b$$

$$L_1(j+1) = L_2(j) + b$$

$$L_4(j) = L_2(j) + b \qquad (4.16)$$

Increase j by 1, i.e., $(j=j+1)$, and continue the generation of images until the magnitude of the charges gets smaller and smaller. The potential expression in medium I can be written as follows:

Medium I

$$\Phi^{(1)}(x,y) = \frac{1}{4\pi\epsilon_1} \left[\frac{Q}{\sqrt{(x-h)^2+y^2}} + \frac{Q_0}{\sqrt{(x-h+2a)^2+y^2}} + \sum_{j=1}^{ni} \right.$$

$$\frac{Q_4(j)}{\sqrt{(x+L_4(j)-b)^2+y^2}} \qquad (4.17)$$

The problem was, "Could this expression be exactly similar or could it be matched to the expression given by Eq. 3.17?" In comparing Fig. 3.7 to the schematic diagram in Fig. 4.3, the position of the images is the same. A comparison of the magnitude of the charges shows the first two terms of Eqs. 4.17 and 3.17 are exactly identical. Then, a comparison of the infinite series terms is necessary for at least two terms. The first two terms are $Q_4(1)$ and $Q_4(2)$. Let $j=1$ in Eq. 4.15. The following images will then be generated:

$$Q_2(1) = \alpha_{23}Q_1(1)$$

$$Q_3(1) = \beta_{23}Q_1(1)$$

$$Q_1(2) = \alpha_{21}Q_2(1)$$

$$Q_4(1) = \beta_{21}Q_2(1) \qquad (4.18)$$

Using Eq. 4.18 together with the given charge, $Q_1(1) = \beta_{12}Q$. Therefore, $Q_4(1)$ can be written in terms of Q:

$$Q_4(1) = \beta_{21}\alpha_{23}\beta_{12}Q \qquad (4.19)$$

Utilizing the definition of β_{mn} and α_{mn} given earlier, Eq. 4.19 then becomes:

$$Q_4(1) = \alpha_{23}(1-\alpha^2_{12})Q \qquad (4.20)$$

Equation 4.20 gives the first term of the summation series given by Eq. 4.17. This checks exactly with the first term of the summation series given by Eq. 3.17.

The second term of the series given by Eq. 4.17 can be found by letting j=2; then the following images will be generated:

$$Q_2(2) = \alpha_{23}Q_1(2)$$
$$Q_3(2) = \beta_{23}Q_1(2)$$
$$Q_1(3) = \alpha_{21}Q_2(2)$$
$$Q_4(2) = \beta_{21}Q_2(2) \qquad (4.21)$$

The image $Q_4(2)$ can be written in terms of Q as follows:

$$Q_4(2) = \beta_{21}Q_2(2)$$

or

$$Q_4(2) = \beta_{21}\alpha_{23}Q_1(2) \qquad (4.22)$$

Substituting $Q_1(2)$ from relation 4.18 into Eq. 4.22, then

$$Q_4(2) = \beta_{21}\alpha_{23}\alpha_{21}Q_2(1)$$

or

$$Q_4(2) = \beta_{21}\alpha^2_{23}\alpha_{21}Q_1(1) \qquad (4.23)$$

The image $Q_4(2)$ can be written in terms of Q by utilizing the relation between $Q_1(1)$ and Q, i.e.,

$$Q_4(2) = \beta_{21}\alpha^2_{23}\alpha_{21}\beta_{12}Q$$

or

$$Q_4(2) = -\alpha_{12}\alpha^2_{23}(1-\alpha^2_{12})Q \tag{4.24}$$

This image checks exactly with the second term in the summation series of Eq. 3.17.

Continuing this comparison procedure shows all the terms in both equations are the same. Therefore, the developed computer algorithm will generate exactly the same images, and the field can be determined directly in a straightforward manner. This approach is very beneficial in the case of four or more dielectric media, where a closed form solution is difficult to obtain.

3. Point charge in four dielectric media

Consider Fig. 4.4. Image charges representing the field in all regions are shown schematically in Fig. 4.5. To be brief, the first two steps of the images generation can be written by inspection using Fig. 4.5 and the procedure of the previous section. Notice in this case, the fourth medium is chosen to be a perfect conductor, which implies $\alpha_{34} = -1$, and zero transmission coefficient.

Given Q_{11} and its position l_{11}, the remaining images can be written as follows:

$$Q_{21} = \alpha_{23}Q_{11}, \quad Q_{12} = \alpha_{21}Q_{21}, \quad Q_{41} = (-1)Q_{31}$$

$$Q_{32} = \alpha_{32}Q_{41}$$

$$Q_{31} = \beta_{23}Q_{11}, \quad Q_{51} = \beta_{21}Q_{21}, Q_{22} = \beta_{32}Q_{41} \qquad (4.25)$$

The position of the above images are

$L_{21} = L_{11} + b$, to the left of the B interface.

$L_{31} = L_{11} + b$, to the right of the B interface.

$L_{12} = L_{21} + b$, to the right of the A interface.

$L_{51} = L_{21} + b$, to the left of the A interface.

$L_{41} = L_{31} + c$, to the left of the O interface.

$L_{32} = L_{41} + c$, to the right of the B interface.

$L_{22} = L_{41} + c$, to the left of the B interface.

$$(4.26)$$

The second step of the images generation is:

$$Q_{23}=\alpha_{23}Q_{12} \qquad Q_{13}=\alpha_{21}Q_{22} \qquad Q_{42}=(-1)Q_{32} \qquad Q_{34}=\alpha_{32}Q_{42}$$

$$Q_{33}=\beta_{23}Q_{12} \qquad Q_{52}=\beta_{21}Q_{22} \qquad\qquad\qquad Q_{24}=\beta_{32}Q_{42}$$

$$(4.27)$$

The corresponding positions of the above images are:

$L_{23} = L_{12} + b$, to the left of the B interface.

$L_{33} = L_{12} + b,,$ to the right of the B interface.

$L_{13} = L_{22} + b$, to the right of the A interface.

$L_{52} = L_{22} + b$, to the left of the A interface.

$L_{42} = L_{32} + c$, to the left of the O interface.

$L_{34} = L_{42} + c$, to the right of the B interface.

$L_{24} = L_{42} + c$, to the left of the B interface.

$$(4.28)$$
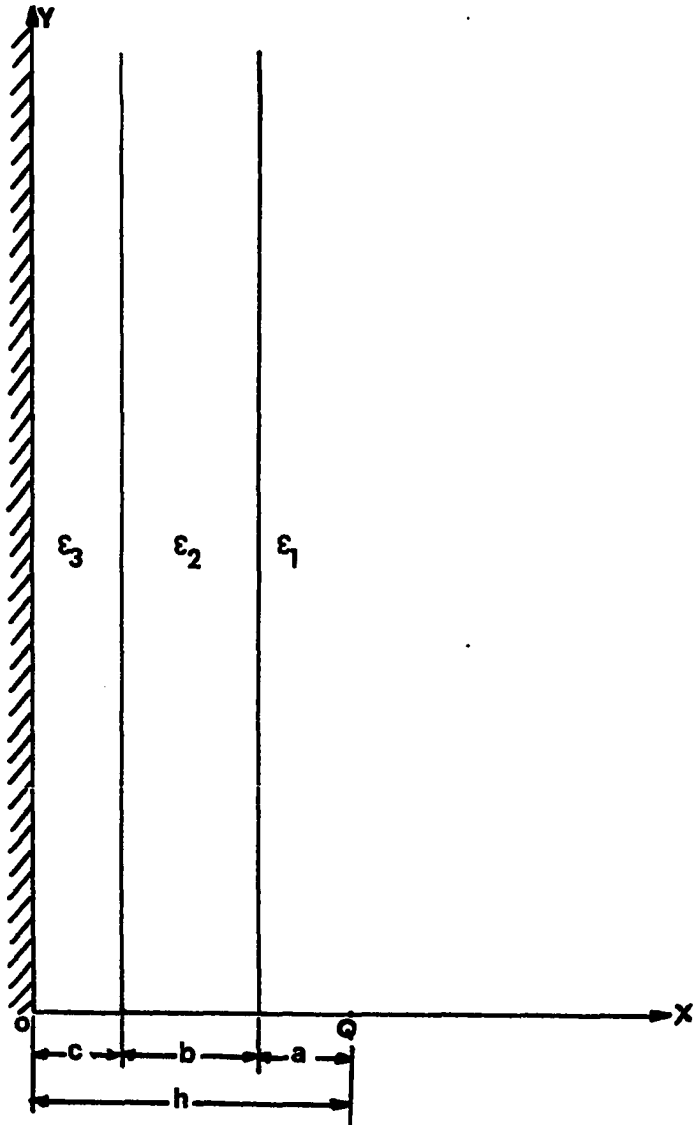
Fig. 4.4. Point charge in front of three dielectric media
on a perfect conductor ground
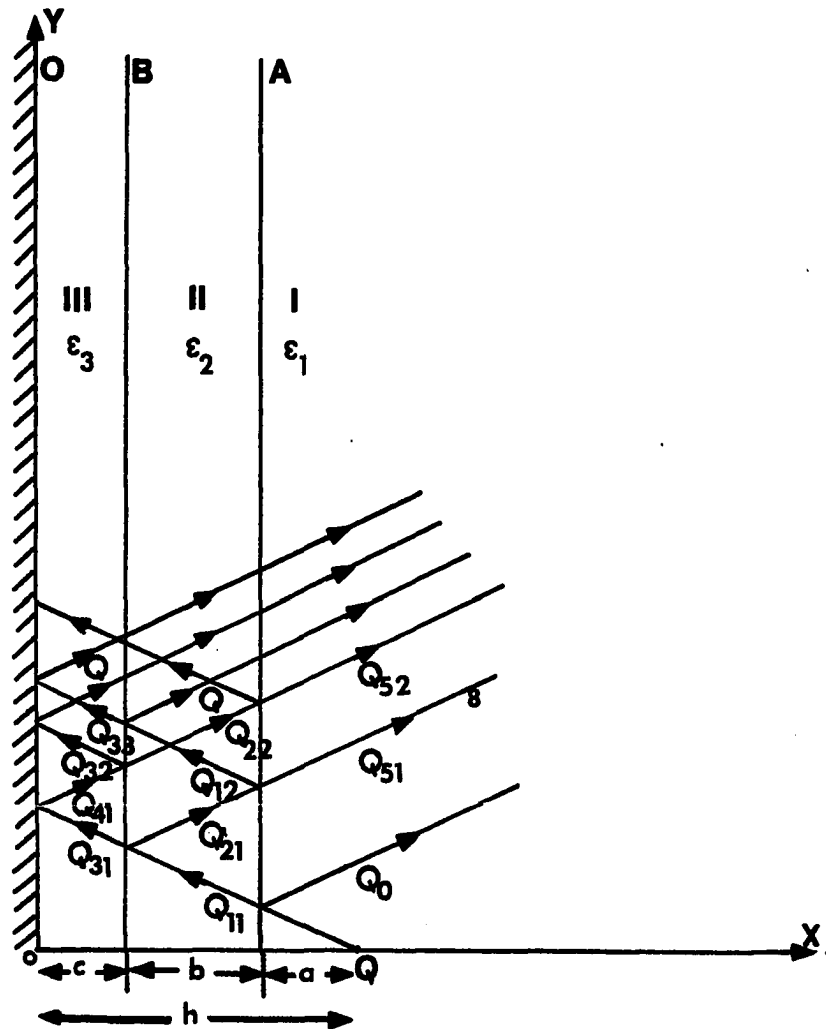
Fig. 4.5.   Schematic diagram for image generation of a
point charge in medium I

The following algorithm will be very reasonable for the most part to generate the images, where the array notation will be used similar to the three dielectric media case.

j=1

i=1

$$Q_2(i) = \alpha_{23}Q_1(j)$$

$$Q_3(i) = \beta_{23}Q_1(j)$$

$$Q_1(j+1) = \alpha_{21}Q_2(j)$$

$$Q_5(j) = \beta_{21}Q_2(j)$$

$$Q_4(j) = -Q_3(j)$$

$$Q_3(2*j) = \alpha_{32}Q_4(j)$$

$$Q_2(2*j) = \beta_{32}Q_4(j) \qquad \qquad (4.29)$$

The corresponding locations of the above images can be determined by the following algorithm:

$$L_2(i) = L_1(j) + b$$

$$L_3(i) = L_1(j) + b$$

$$L_1(j+1) = L_2(j) + b$$

$$L_5(j) = L_2(j) + b$$

$$L_4(j) = L_3(j) + c$$

$$L_3(2*j) = L_4(j) + c$$

$$L_2(2*j) = L_4(j) + c \qquad \qquad (4.30)$$

Increase i by 2, i.e., (i=i+2) and increase j by 1, i.e., (j=j+1), and continue the process of images generation. The generation will be discontinued when the images get smaller and smaller. Once the images are

generated, then the potential and the corresponding electric field can easily be determined for all regions using the following equations.

Medium I

$$\phi^{(1)}(x,y) = \frac{1}{4\pi\varepsilon_1}\left[\frac{Q}{\sqrt{(x-h)^2+y^2}} + \frac{Q_0}{\sqrt{(x-h+2a)+y^2}} + \sum_{j=1}\right.$$

$$\left.\frac{Q_5(j)}{\sqrt{(x+L_5(j)-b-c)^2+y^2}}\right] \qquad (4.31)$$

Medium II

$$\phi^{(2)}(x,y) = \frac{1}{4\pi\varepsilon_2}\left[\sum \frac{Q_1(j)}{\sqrt{(x-L_1(j)-b-c)^2+y^2}} + \sum_{k=1}\right.$$

$$\left.\frac{Q_2(k)}{\sqrt{(x+L_2(k)-c)^2+y^2}}\right. \qquad (4.32)$$

Medium III

$$\phi^{(3)}(x,y) = \frac{1}{4\pi\varepsilon_3}\left[\sum_{m=1}\frac{Q_3(m)}{\sqrt{(x-L_3(m)-c)^2+y^2}} + \sum_{m=1}\right.$$

$$\left.\frac{Q_4(m)}{\sqrt{(x+L_4(m))^2+y^2}}\right] \qquad (4.33)$$

The electric field components can simply be obtained using the negative of the gradient of the potential $(E^i_{x,y} = -\nabla \Phi^i(x,y)$, $i = 1,2,3)$. Therefore, region I field components are:

$$E^{(1)}_x(x,y) = \frac{1}{4\pi\varepsilon_1}\left[\frac{Q(x-h)}{[(x-h)^2+y^2]^{3/2}} + Q_0\frac{(x-h+2a)}{[(x-h+2a)^2+y^2]^{3/2}} + \sum_{j=1}\frac{Q_5(j)(x+L_5(j)-b-c)}{[(x+L_5(j)-b-c)^2+y^2]^{3/2}}\right] \quad (4.34)$$

$$E^{(1)}_y(x,y) = \frac{1}{4\pi\varepsilon_1}\left[\frac{Q\cdot y}{[(x-h)^2+y^2]^{3/2}} + Q_0\frac{y}{[(x-h+2a)^2+y^2]^{3/2}} + \sum_{j=1}Q_5(j)\frac{y}{[(x+L_5(j)-b-c)^2+y^2]^{3/2}}\right] \quad (4.35)$$

Similar equations can be written for the other two regions.

4. Application

A program was written for the four dielectric media, using arbitrary values for the point charge Q (one pico coulombs) and the permittivities ε_1, ε_2 and ε_3. Table 4.1 and Table 4.2 showed that at the boundaries of the dielectrics, the potential, the tangential component of the electric field (E_y), and the normal components of the flux densities (D_x) all satisfied the boundary condition with accuracy.

In general, the more images that are generated, the better the accuracy obtained. The number of images also depends upon the permittivities of the media. For example, Table 4.1 and Table 4.2 showed that the number of images required to satisfy the boundary conditions with certain accuracy is about 1800 images, while about 700 images are needed for Table 4.3 and Table 4.4. The only difference between the two cases is $\varepsilon_2 = 4$ for Tables 4.1 and 4.2, while $\varepsilon_2 = 2$ for Tables 4.3 and 4.4.

C. The Five Dielectric Media

1. Introduction

In this case, one more dielectric layer will be added to the four dielectric media model as shown in Fig. 4.6. The derivation of the computer algorithm will follow exactly

Table 4.1. Boundary condition values along the interface of media 1 and 2 (ε_1=1.0, ε_2=4.0, ε_3=1.0; a=2.0cm, b=1.0cm, c=2.0cm, h=5.0cm) (number of images = 1800)

| y
cm | Medium I | | | Medium II | | |
	$\phi^{(1)}$ volts	$D^{(1)}_x$ volt/cm	$E^{(1)}_y$ volt/cm	$\phi^{(2)}$ volts	$D^{(2)}_x$ volt/cm	$E^{(2)}_y$ volt/cm
0.0	19.3579	-34.4720	0.0000	19.3604	-34.4716	0.0000
1.0	17.2280	-24.4243	3.6566	17.2305	-24.4238	3.6566
2.0	13.2855	-11.8164	3.8446	13.2880	-11.8160	3.8446
3.0	9.8623	- 5.6507	2.9724	9.8648	- 5.6503	2.9724
4.0	7.3089	- 3.0302	2.1682	7.3115	- 3.0298	2.1682
5.0	5.4555	- 1.8421	1.5714	5.4580	- 1.8417	1.5714
6.0	4.1093	- 1.2394	1.1452	4.1117	- 1.2390	1.1452
7.0	3.1241	- 0.8969	0.8420	3.1266	- 0.8965	0.8420
8.0	2.3965	- 0.6819	0.6251	2.3989	- 0.6816	0.6251
9.0	1.8538	- 0.5362	0.4686	1.8562	- 0.5358	0.4686

Table 4.2. Boundary condition values along the interface of media 2 and 3 ($\varepsilon_1=1.0$, $\varepsilon_2=4.0$, $\varepsilon_3=1.0$; a=2.0cm, b=1.0cm, c=2.0cm and h=5.0cm; D=flux density normal to the dielectric boundary (divided by ε_0)) (number of images=1800)

y cm	Medium II			Medium III		
	$\Phi^{(2)}$ volts	$D_x^{(2)}$ volt/cm	$E_y^{(2)}$ volt/cm	$\Phi^{(3)}$ volts	$D_x^{(3)}$ volt/cm	$E_y^{(3)}$ volt/cm
0.0	1.4298	-9.5534	0.0000	1.4299	-9.5536	0.0000
1.0	1.3290	-8.5046	1.8635	1.3291	-8.5047	1.8635
2.0	1.1000	-6.4279	2.5092	1.1001	-6.4280	2.5092
3.0	0.8561	-4.6100	2.2857	0.8562	-4.6101	2.2857
4.0	0.6506	-3.3233	1.8168	0.6507	-3.3235	1.8168
5.0	0.4916	-2.4433	1.3749	0.4917	-2.4438	1.3749
6.0	0.3725	-1.8313	1.0244	0.3726	-1.8314	1.0244
7.0	0.2838	-1.3953	0.7619	0.2839	-1.3954	0.7619
8.0	0.2178	-1.0781	0.5690	0.2179	-1.0782	0.5690
9.0	0.1683	-0.8434	0.4279	0.1684	-0.8435	0.4279

Table 4.3. Boundary condition values along the interface of media 1 and 2 (ε_1=1.0, ε_2=2.0, ε_3=1.0; a=1.0cm, b=1.0cm, c=2.0cm and h=5.0cm; D=flux density normal to the dielectric boundary (divided by ε_0)) number of images = 700).

y cm	Medium I			Medium II		
	$\Phi^{(1)}$ volts	$D^{(1)}_x$ volt/cm	$E^{(1)}_y$ volt/cm	$\Phi^{(2)}$ volts	$D^{(2)}_x$ volt/cm	$E^{(2)}_y$ volt/cm
0.0	26.0852	-29.5656	0.0000	26.0852	-29.5653	0.0000
1.0	22.7954	-21.1589	5.5964	22.7954	-21.1585	5.5964
2.0	16.8883	-10.5662	5.6202	16.8883	-10.5657	5.6202
3.0	12.0179	- 5.3023	4.1021	12.0179	- 5.3176	4.0122
4.0	8.5876	- 3.0234	2.8288	8.5876	- 3.0230	2.8288
5.0	6.2269	- 1.9335	1.9504	6.2269	- 1.9331	1.9504
6.0	4.5905	- 1.3471	1.3615	4.5905	- 1.3467	1.3616
7.0	3.4400	- 0.9935	0.9649	3.4400	- 0.9932	0.9649
8.0	2.6187	- 0.7607	0.6943	2.6187	- 0.7603	0.6943

Table 4.4.   Boundary condition values along the interface of medium II and medium III (ε_1=1.0, ε_2=2.0, ε_3=1.0; a=2.0cm, b=1.0cm, c=2.0cm and h=5.0cm, D=flux density normal to the dielectric boundary (divided by ε_0)) (number of images = 700)

	Medium II			Medium III		
y cm	$\Phi^{(2)}$ volts	$D^{(2)}_x$ volt/cm	$E^{(2)}_y$ volt/cm	$\Phi^{(3)}$ volts	$D^{(3)}_x$ volt/cm	$E^{(3)}_y$ volt/cm
0.0	16.6224	-11.3347	0.0000	16.6300	-11.3343	0.0000
1.0	15.3222	- 9.9520	2.3943	15.3298	- 9.9515	2.3943
2.0	12.4111	- 7.2598	3.1537	12.4187	- 7.2594	3.1537
3.0	9.3921	- 4.9822	2.7817	9.3997	- 4.9818	2.7817
4.0	7.9345	- 3.4442	2.1293	6.9421	- 3.4443	2.1293
5.0	5.1063	- 2.4443	1.5497	5.1138	- 2.4443	1.5497
6.0	3.7871	- 1.7817	1.1119	3.7946	- 1.7813	1.1120
7.0	2.8408	- 1.3283	0.7987	2.8483	- 1.3279	0.7988
8.0	2.1588	- 1.0095	0.5783	2.1662	- 1.0091	0.5784

the same procedure of the four dielectric media. This computer algorithm could then be used not only for the five dielectric case, but also as a four, three, or even two dielectric media. This can occur by choosing some of the dielectric constants of the neighborhood regions to be equal. For example, if $\varepsilon_3 = \varepsilon_4$ in Fig. 4.6, then this figure will reduce to the four dielectric media case, and no reflection will exist at the dielectric interface separating the two media. Then the five dielectric model can be used as a four dielectric model. On the other hand, if $\varepsilon_4 = \varepsilon_3 = \varepsilon_2$, then we obtain the three media case, while the two media case can be obtained by letting $\varepsilon_1 = \varepsilon_2 = \varepsilon_3 = \varepsilon_4$.

2. Generation of the images by computer

Consider Fig. 4.4, where region III is divided into two different media by the plane separation c as shown in Fig. 4.6. Let the two media be characterized by two dielectric constants ε_3 and ε_4. Figure 4.6 also shows a schematic diagram of some of the images needed to solve for the field in the five dielectric media. Knowing the dielectric constants and the source charge Q, the following images are generated.

$$Q_{21} = \alpha_{23} Q_{11}$$
$$Q_{31} = \beta_{23} Q_{11}$$
$$Q_{12} = \alpha_{21} Q_{21}$$
$$Q_{51} = \beta_{21} Q_{21}$$
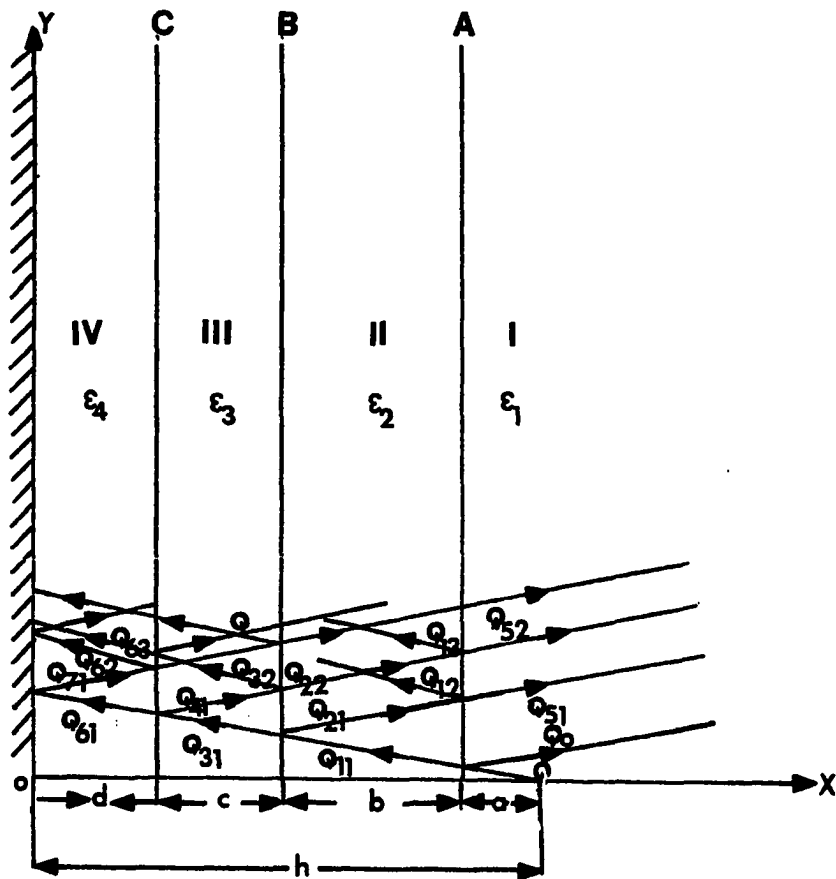
Fig. 4.6. Point charge in front of four dielectric media on a perfect conductor ground

$$Q_{41} = \alpha_{34}Q_{31}$$

$$Q_{61} = \beta_{34}Q_{31}$$

$$Q_{32} = \alpha_{32}Q_{41}$$

$$Q_{22} = \beta_{32}Q_{41}$$

$$Q_{71} = -Q_{61}$$

$$Q_{62} = \alpha_{43}Q_{71}$$

$$Q_{42} = \beta_{43}Q_{71}$$

$$Q_{43} = \alpha_{34}Q_{32}$$

$$Q_{63} = \beta_{34}Q_{32} \tag{4.36}$$

where

$$\alpha_{mn} \triangleq \frac{\varepsilon_m - \varepsilon_n}{\varepsilon_m + \varepsilon_n} \quad \text{and} \quad \beta_{mn} \triangleq \frac{2\varepsilon_n}{\varepsilon_m + \varepsilon_n} \tag{4.37}$$

Using the array notation and grouping the images together, then Eq. 4.36 can be written again, where $Q_1(1)$ and its location $l_1(1)$ are given in advance.

Images belonging to Q_1 are: $\quad Q_1(1), \ Q_1(2)$

Images belonging to Q_2 are: $\quad Q_2(1), \ Q_2(2)$

Images belonging to Q_3 are: $\quad Q_3(1), \ Q_3(2)$

Images belonging to Q_4 are: $\quad Q_4(1), \ Q_4(2), \ Q_4(3)$

Images belonging to Q_5 are: $\quad Q_5(1)$

Images belonging to Q_6 are: $\quad Q_6(1), \ Q_6(2), \ Q_6(3)$

Images belonging to Q_7 are: $\quad Q_7(1)$

$$\tag{4.38}$$

Consider Eq. 4.36 as the first step in images generation, then the next images to be generated are:

$Q_1(3)$

$Q_2(3)$, $Q_2(4)$

$Q_4(4)$, $Q_4(5)$, $Q_4(6)$

$Q_5(2)$

$Q_6(4)$, $Q_6(5)$, $Q_6(6)$

$Q_7(2)$

$Q_5(2)$ (4.39)

From the above two steps, Eqs. 4.38 and 4.39, notice the following:

a) One image is generated for Q_1, Q_7 and Q_5.

b) Two images are generated for Q_2 and Q_3.

c) Three images are generated for Q_4 and Q_6.

The following algorithm is then proposed: let j be a counter of the steps and at the same time, take care of the images belonging to Q_5 and Q_7. The index (j+1) will then belong to Q_1. The index i belongs to Q_2 and Q_3, while n belongs to Q_4 and Q_5.

i=1

j=1

n=1

$Q_2(i) = \alpha_{23} Q_1(j)$

$Q_3(i) = \beta_{23} Q_1(j)$

$Q_1(j+1) = \alpha_{21} Q_2(j)$

$Q_5(j) = \beta_{21} Q_2(j)$

$Q_4(n) = \alpha_{34} Q_3(i)$

$$Q_6(n) = \beta_{34}Q_3(i)$$

$$Q_3(2*j) = \alpha_{32}Q_4(j)$$

$$Q_2(i+1) = \beta_{32}Q_4(j)$$

$$Q_7(j) = (-1)Q_6(j)$$

$$Q_6(n+1) = \alpha_{43}Q_7(j)$$

$$Q_4(n+1) = \beta_{43}Q_7(j)$$

$$Q_4(n+2) = \alpha_{34}Q_3(2*j)$$

$$Q_6(n+2) = \beta_{34}Q_3(2*j) \tag{4.40}$$

The corresponding location of the images are:

$L_2(i) = L_1(j) + b$, to the left of the plane B interface.

$L_3(i) = L_1(j) + b$, to the right of the plane B interface.

$L_1(j+1) = L_2(j) + b$, to the right of the plane A interface.

$L_5(j) = L_2(j) + b$, to the left of the plane A interface.

$L_4(n) = L_3(i) + c$, to the left of the plane c interface.

$L_6(n) = L_3(i) + c$, to the right of the plane C interface.

$L_3(2*j) = L_4(j) + c$, to the right of the plane B interface.

$L_2(i+1) = L_4(j) + c$, to the left of the plane B interface.

$L_7(j) = L_6(j) + d$, to the left of the O interface.

$L_6(n+1) = L_7(j) + d$, to the right of the plane C interface.

$L_4(n+1) = L_3(2*j) + c$, to the left of the plane C interface.

$L_4(n+2) = L_3(2*j) + c$, to the left of the plane C interface.

$L_6(n+2) = L_3(2*j) + c$, to the right of the plane C interface.   (4.41)

Increase j by 1, i by 2 and n by 3, i.e., (j=j+1, i=i+2 and n=n+3) and repeat the above process over and over until the magnitudes of the images start to get small and smaller. With the help of Fig. 4.6, the potential expressions for the different regions are:

Region I

$$\Phi^{(1)}(x,y) = \frac{1}{4\pi\varepsilon_1} \left[\frac{Q}{\sqrt{(x-h)^2+y^2}} + \frac{Q_0}{\sqrt{(x-h+2a)^2+y^2}} + \right.$$

$$\left. \sum_{i=1} \frac{Q_5(j)}{\sqrt{(x+L_5(j)-b-c-d)^2+y^2}} \right]$$ (4.42)

Region II

$$\Phi^{(2)}(x,y) = \frac{1}{4\pi\varepsilon_2} \left[\sum_{j=1} \frac{Q_1(j)}{\sqrt{(x-L_1(j)-b-c-d)^2+y^2}} + \right.$$ (4.43)

$$\left. \sum_{j=1} \frac{Q_2(j)}{\sqrt{(x+L_2(j)-c-d)^2+y^2}} \right]$$

Region III

$$\Phi^{(3)}(x,y) = \frac{1}{4\pi\epsilon_3}\left[\sum_{j=1} \frac{Q_3(j)}{\sqrt{(x-L_3(j)-c-d)^2+y^2}} + \sum_{k=1}\right.$$

$$\left.\frac{Q_4(k)}{\sqrt{(x+L_4(k)-d)^2+y^2}}\right] \tag{4.44}$$

Region IV

$$\Phi^{(4)}(x,y) = \frac{1}{4\pi\epsilon_4}\left[\sum \frac{Q_7(k)}{\sqrt{(x-L_6(k)-d)^2+y^2}} + \sum_{i=1}\right.$$

$$\left.\frac{Q_7(i)}{\sqrt{(x+L_7(i))^2+y^2}}\right] \tag{4.45}$$

The corresponding electric field components of Eqs. 4.42-4.45 are:

$$E_x^{(1)}(x,y) = \frac{1}{4\pi\epsilon_1}\left[\frac{Q(x-h)}{[(x-h)^2+y^2]^{3/2}} + Q_0\frac{(x-h+2a)}{[(x-h+2a)^2+y^2]^{3/2}}\right.$$

$$\left.+ \sum_{j=1} \frac{Q_5(j)\ (x+L_5(j)-b-c-d)}{[(x+L_5(j)-b-c-d)^2+y^2]^{3/2}}\right] \tag{4.46}$$

$$E_y^{(1)}(x,y) = \frac{1}{4\pi\epsilon_1}\left[\frac{Q\cdot y}{[(x-h)^2+y^2]^{3/2}} + Q_0\frac{(x-h+2a)}{[(x-h+2a)^2+y^2]^{3/2}}\right.$$

$$\left.+ \sum_{j=1} \frac{Q_5(j)\ y}{[(x+L_5(j)-b-c-d)^2+y^2]^{3/2}}\right] \tag{4.47}$$

Similar equations can be written for the other electric field components of the other regions.

3. Application

A program was written using the algorithm given by Eqs. 4.40 and 4.41 for the images generation and the potential and the electric field components (Eqs. 4.42-4.47). The program is tested for the special case ($\varepsilon_3 = \varepsilon_4$) and using the following parameters as an input $Q=1pc$, $\varepsilon_1=1.0$, $\varepsilon_2=2.0$ and $\varepsilon_3=\varepsilon_4=1.0$. Similar results to Tables 4.3 and 4.4 were obtained. This shows that the proposed five dielectric model algorithm is working under the special case when the five dielectric media are reduced to four dielectric media.

D. Summary

Solution of the electric field due to a point charge in multilayer dielectric case is discussed in detail. Digital computer algorithms are developed for the three, the four and the five dielectric media case. The three dielecteic media algorithm is tested and compared with the closed form slution of Chapter III. The compared results show exact one to one correspondence. With the three dielectric media algorithm as a background, the four and the five dielectric media algorithms are then developed in a straightforward manner. The four dielectric media algorithm is then tested and compared with published results. Exact results are obtained.

A proposed extension of the four dielectric media was developed to cover the five dielectric media case. The proposed algorithm was then tested for the special case when the five media reduced to four media and good results were obtained. The computer algorithm technique is very beneficial for the case of more than three dielectric layers, where a closed form solution is difficult to obtain.

In Chapter.V, all the developed computer algorithms will be applied to the case of vegetation underneath the three-phase transmission line. The expressions of the point charge field will be modified to the line charge case.

V. ELECTRIC FIELD DISTRIBUTION THROUGH MULTILAYER VEGETATION UNDERNEATH THE EHV TRANSMISSION LINE

A. Introduction

Transmission facilities tie the power together so that generating capacity at various locations may be made available to the system load. Power can be generated at various locations and, through the high voltage network, supply various loads at various locations. Through such a network, excess capacity can be transmitted where it is needed. Capacity interchange and economic use of excess capacity is made possible. Thus, high voltage transmission provides the most important ingredient for large scale economic pooling of generation resources combined with better reliability of power supply. Both population and per capita output will increase in the future years and afford a basis for forecasting energy requirements. The tremendous use of the electrical energy in the U.S.A. and the rest of the industrial world in the coming years will dictate the expansion in both the 500 kV and the 765 kV system. In any high voltage system, there are many factors that affect its type, potential level, and growth. These factors include [22]:

a) Distance involved in transmitting the power.

b) Load growth and its pattern.

c) The amount of power to be transmitted.

d) Fuel availability on regional basis. .

e) Power losses in the network.

As far back as the 1920s, a 220 kV transmission line
has been used to cover long distances. Today, voltages
ranging from 420-1500 kV are either being used or are in the
preparation stages. As a matter of definition [22], the
different potential levels are divided into three major
categories:

a) High voltage (HV), up to 100 kV.

b) Extra high voltage (EHV), between 100 kV-380 kV.

c) Ultra high voltage (UHV), 400 kV and above.

Increasing the voltage of a network is associated with
a large number of design criteria for the transmission and
distribution system. A discussion of all of the criteria
involved in the design of EHV and UHV transmission lines is
beyond the scope of this work. Any limitation of the more
important design criteria should include:

a) The cross section of the conductor.

b) The number of subconductors per phase. This is
    necessary to meet the restriction on radio
    frequency interference (RFI).

c) Insulation level and, therefore, the tower
    dimensions.

d) Polluted conditions, especially at higher voltages beyond 1,000 kV.

e) The maximum allowable voltage gradient both at the conductor surface where corona phenomena will be prevalent, and in the vicinity of the ground where people, livestock, mobile equipment or vegetation may exist in the EHV transmission line environment.

The vegetation problem is our main topic of discussion in this chapter.

Vegetation grows in the rural areas where EHV lines cross such regions. The electric field characteristics in such regions behave differently from those in free space due to the difference in the permittivities between the air medium compared to the vegetation medium. In order to determine the electric field distribution in any region, the permittivity of the region has to be known. In case of vegetation, it is not an easy task to know the value of the permittivity due to the large number of parameters involved, such as:

a) The difference in the heights of the plants.

b) The nonuniform distribution of leaves.

c) The difference in the size of leaves.

d) The difference in water content in vegetation.

e) The ground level.

f) The moisture content in the ground.

These are some of the parameters that affect the determination of the vegetation dielectric constant.

In this study, the vegetation was assumed first as one single layer of uniform homogeneous dielectric constant. The value of the dielectric constant of such a layer is not known. Different arbitrary values will be assumed and a computer simulation will be done using the three dielectric media models. These three dielectric media represent air, vegetation and the perfect conductor ground. Then the electric field distribution from the computer output will be compared to the measured field.

Two other representations were also investigated. In the first case, the vegetation will be modeled as two layers with different dielectric constants, and where the four dielectric media model is used; in the second case, where the vegetation was modeled as three dielectric layers, and where five dielectric media model was used. A computer simulation was done for arbitrary values of the dielectric constants that have to be chosen to get computer output that will fit the measured data. But before deriving the electric field for these cases, a review of the basic relationship will follow.

B. Electrostatic Field

Consider two infinite parallel line charges separated a distance 2 s as shown in Fig. 5.1, and placed parallel to the z-axis. The y=0 plane will be an equipotential surface (Φ=0). It can be shown [3, 19, 22, 38] that the potential surfaces of such a system are given by:

$$\Phi(x,y) = \frac{q}{4\pi\epsilon} [\ln \frac{s}{R_2} - \ln \frac{s}{R_2}] = \text{constant} \qquad (5.1)$$

Where R_1 and R_2 are the distances between the sources to the position where Φ is measured, see Fig. 5.1.
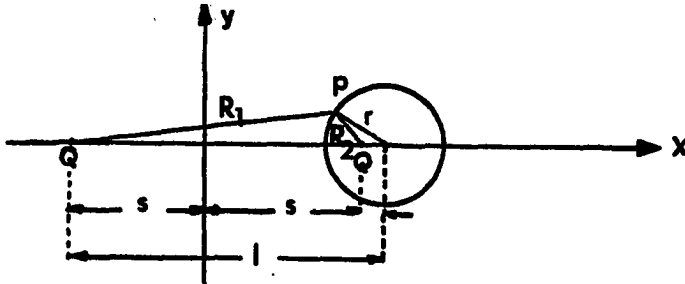
Fig. 5.1. Cylindrical condition in front of perfect conductor plan

The above equation can be written in another way:

$$\Phi(x,y) = \frac{q}{2\pi\epsilon} \ln \frac{R_1}{R_2} = \text{constant}$$

It can be shown that the locus of this equipotential surface is defined by:

$$\left[x - s \left(\frac{1+k^2}{1-k^2}\right) \right]^2 + y^2 = \left[\frac{2sk}{k^2-1} \right]^2 \tag{5.2}$$

where

$$k = \frac{R_2}{R_1} = \exp \left(\frac{2\pi\varepsilon}{q} \phi\right) \tag{5.3}$$

This is an equation of a cylinder with its center located at:

$$x_1 = s \frac{1+k^2}{1-k^2} \; ; \; \text{and} \; y_1 = 0 \tag{5.4}$$

and the radius of this cylinder is

$$r = \frac{2ks}{k^2-1} \tag{5.5}$$

Thus, two line charges satisfy the equipotential surface condition at the conductor surface.

1. Two parallel conductors

As in the case of a single line, the equipotential surface produced by such a line can be thought of as if it was produced by the line and its image. Such a relationship

is a simple geometrical relationship and can be expressed as

$$x.l - r^2_{1};$$

(5.6)

where x and l are defined in Fig. 5.2.
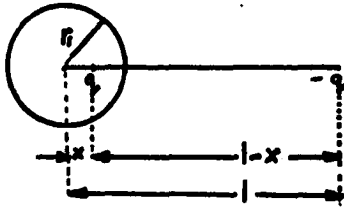
Fig. 5.2. Line charge and its image

This relationship is sometimes referred to as "inversion" and the presence of q and its image insures that the cylinder of radius r_1 is an equipotential surface.

2. Single wire above ground

This study will deal primarily with a horizontal configuration with bundle conductors in each phase; however, the general method in computing the line charges is also applied. This general method will be given shortly, but it is first necessary to look at the simplest open wire line, a single conductor over a conducting ground plane.

Assuming a perfectly conducting ground, any charge q placed at y=h above ground will produce an image charge (-q)

in the ground plane that will appear to be on a conductor at
y=-h. The line charges will be slightly eccentric to the
cylinder axis at a height determined by the ratio of the
radius squared to the separation between conductors.

The potential of the conductor with respect to the
ground will be:

$$\Phi = \frac{q}{2\pi\epsilon} \ln \left[\frac{2h}{d} + \sqrt{\left(\frac{2h}{d}\right)^2 + 1} \right] \tag{5.7}$$

If the potential Φ is fixed, then we can solve for the
charge q.

$$q = \frac{2\pi\epsilon\Phi}{\ln \left[\frac{2h}{d} + \sqrt{\frac{2h}{d}^2 + 1} \right]} \tag{5.8}$$

Since the conductor is far from its image and so small
in diameter, then the electric field can be obtained by
assuming that the equivalent charge is concentric with the
conductor, so that $(2h/d)^2 \gg 1$. This allows the capacitance
to be determined from the following simplified equation

$$c = \frac{2\pi\epsilon}{\ln \frac{4h}{d}}$$

$$= \frac{2\pi\epsilon}{\ln \frac{2h}{r}} \tag{5.9}$$

where r is the radius of the conductor.

C. The General Method of Charge Computation

1. Basic equations

The overhead high voltage transmission creates an electrostatic field whose boundaries are the conductors and the ground. The voltage gradient at ground level expresses the intensity of this field close to ground and is difficult to compute if the terrain is irregular or a different media from air exists underneath the lines. Such is the vegetation in the problem at hand. In the following, the ground can have either a finite dielectric constant (plane dielectric), where the images will be modified by a factor as discussed in Chapter III, or it can have an infinite dielectric constant (perfect conductor), and where the image factor will be (-1).

This general method of computation is valid in most general cases, and for any kind of line configuration, including multiple circuits. Each conductor of the transmission line, including wires at ground potential, must be considered. In the case of a regular bundle, it is sufficient to consider an equivalent single conductor having diameter or an equivalent radius given by

$$R_{eq} = \frac{D}{2} \sqrt[n]{\frac{nd}{D}} \qquad\qquad (5.10)$$

where D is the bundle diameter, that is to say, the diameter of the circle in which the subconductors lie, n is the number of subconductors, and d is the diameter of the subconductor. The charges q on the conductors are determined through the voltages Φ and the Maxwell potential coefficients p [11, 22] as follows:

$$[p] \ [q] = [\Phi] \tag{5.11}$$

or

$$[q] = [p]^{-1} \ [\Phi] \tag{5.12}$$

Both voltages and charges can be represented by complex quantities and the above matrix relationship is intended for both the real and the imaginary part [11].

$$[q] = [q_r] + j[q_i] \tag{5.13}$$

$$[\Phi] = [\Phi_r] + j[\Phi_i] \tag{5.14}$$

Substituting Eqs. 5.13 and 5.14 into Eq. 5.12, we obtain

$$[q_r] = [p]^{-1} \ [\Phi_r] \tag{5.15}$$

$$[q_i] = [p]^{-1} \ [\Phi_i] \tag{5.16}$$

The elements of the matrix [p] are given by

$$P_{xx} = \frac{1}{2\pi\epsilon} \ln \frac{4H_x}{dx} \tag{5.17}$$

$$P_{xy} = \frac{1}{2\pi\epsilon} \ln \frac{L'_{xy}}{L_{xy}} \tag{5.18}$$

where H_x is the height of conductor x above gound, d_x is the

conductor diameter, L_{xy} is the distance between conductor x

and conductor y, and L'_{xy} is the distance between conductor

x and the image of conductor y. (See Fig. 5.3.)
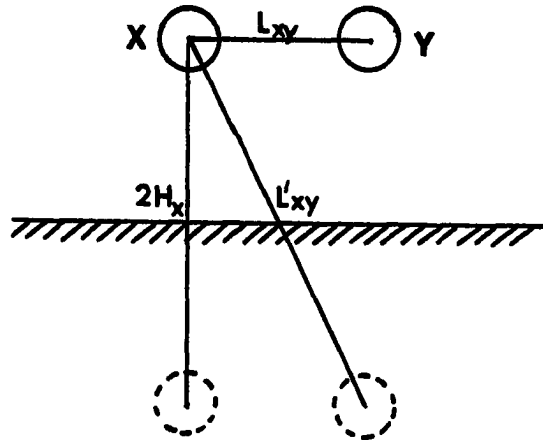
Fig. 5.3. Two conductors and their images in a plane

2. Line charges calculation

The data used for this study are largely based upon a

standard three-phase transmission line configuraion that is

referred to as the "base case." This base case is used in

making comparisons with data obtained from other

configurations that represent modifications of the various

dimensions from the standard case shown in Fig. 5.4.

The base case transmission line is a flat horizontal

configuration at nominal height of 12.5 m[1] above ground

plane. The nominal horizontal phase separation D, between

the centers of the conductor bundle, is shown as 7.5 m. For

----

[1] This configuration and the above data were used by
the author of reference [5].
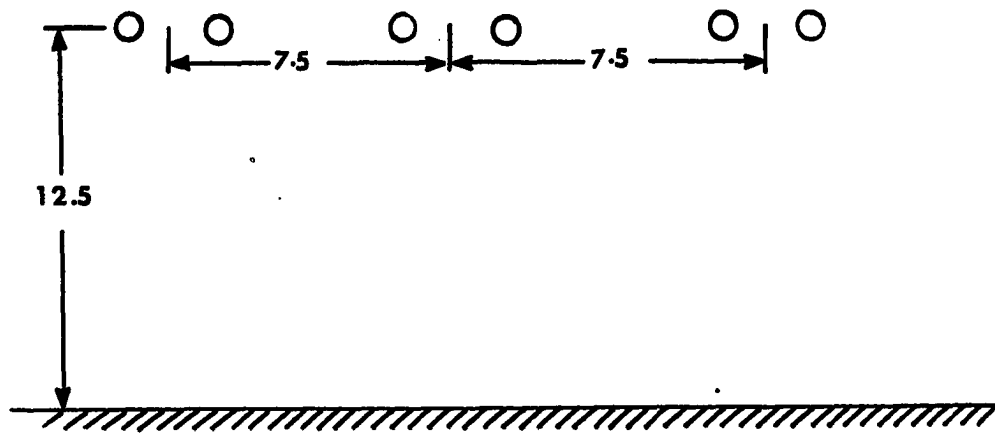
Fig. 5.4. Dimension for base case

the base case, the bundles consist of two subconductors with
a diameter of three centimeters and with a horizontal
separation s between the subconductor centers of fifty
centimeters.

For the purpose of this study, a balanced three-phase
system with nominal 345 kV line to line, 60 Hz were used as
an input data to the two media program. The following
approximate values for the three-phase line charges have
been found.

$q_a = (2.3510 + j0.23582)*10^{-6}$ col/m

$q_b = (-1.28144 - j0.221917)*10^{-6}$ col/m

$q_c = (-0.971285 + j0.215395)*10^{-6}$ col/m where q_a, q_b

amd q_c are the equivalent line charges for phases a, b and c
of the three-phase system. These values will be used in the
next section as the source line charges for the analysis.

D. Application of the Three Dielectric Models to Three-Phase Transmission Line

1. Introduction

The problem of a point charge in front of a multilayer dielectric was discussed in detail in the previous chapters. This chapter is mainly concerned with applying the same algorithm to the line charge case after some modifications. Application of the line charge in the case of two dielectric media was solved by Cowan [5] where he applied it to the case of three-phase transmission line when the ground is a dielectric plane. Let us extract the potential expression and the corresponding electric field components from [5].

$$\phi^{(1)}_{(x,y)} = \frac{q}{2\pi\epsilon_1} \left[\ln \frac{h}{g_1} + \alpha_{12} \ln \frac{h}{g_2} \right] \qquad (5.19)$$

where q is the line charge (col/m) and h, g_1 and g_2 are defined in Fig. 5.5. The corresponding electric field components are:

$$E_x^{(1)}(x,y) = \frac{q}{2\pi\epsilon_1} \left[\frac{(x-h)}{[(x-h)^2+y^2]} + \alpha_{12} \frac{x+h}{[(x+h)^2+y^2]} \right] \quad (5.20)$$

and

$$E_y^{(1)}(x,y) = \frac{q}{2\pi\epsilon_1} \left[\frac{y}{[(x-h)^2+y^2]} + \alpha_{12} \frac{y}{[(x+h)^2+y^2]} \right] \quad (5.21)$$
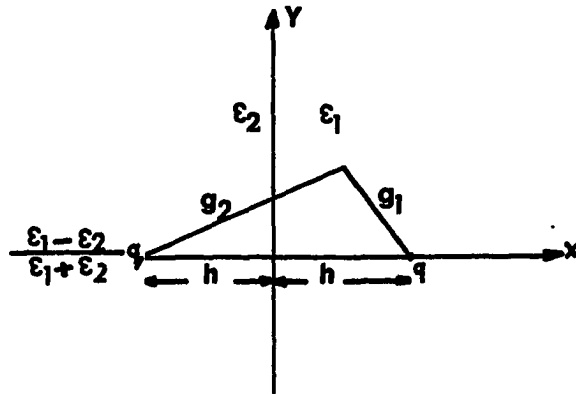
Fig. 5.5. Image of line charge in dielectric plane

Since the main concern is the calculation of the electric field close to ground, each phase of the transmission line can be represented by a single line of charge. The location of such a charge is at the center of an equivalent conductor as discussed in section C. Therefore, the total electric field components due to the three-phase line can be determined using Eqs. 5.20 and 5.21 and the principles of superposition.

$$E_x^{(1)}(x,y) = \sum_{i=1}^{3} \frac{q_i}{2\pi\varepsilon_1} \left\{ \frac{(x-h_i)}{[(x-h_i)^2+(y-y_i)^2]} + \alpha_{12} \right.$$

$$\left. \frac{x+h_i}{[(x+h_i)^2+(y-y_i)^2]} \right\} \qquad (5.22)$$

and

$$E_y^{(1)}(x,y) = \sum_{i=1}^{3} \frac{q_i}{2\pi\varepsilon_1} \left\{ \frac{(y-y_i)}{[(x-h_i)^2+(y-y_i)^2]} + \alpha_{12} \right.$$

$$\left. \frac{y-y_i}{[(x+h_i)^2+(y-y_i)^2]} \right\} \qquad (5.23)$$

2. Two media application

The electric field profiles are computed at two different heights; at ground and 4.0 meters above ground using the general method of charge computation presented in section C, and Eqs. 5.22 and 5.23. These profiles are exactly similar to the ones obtained by [5], where the author of [5] represented each conductor with n line charges. Figure 5.6 shows the magnitude of the electric field profiles at ground and 4.0 m above it. The electric field at the ground is mainly due to the normal component because the tangential (horizontal) component is zero. The maximum value of the electric field at ground is found to be 3.5 kV/m at a distance of approximately 10 m measured horizontally from the center line of the system. This field illustrates a typical electric field distribution along the ground beneath a flat horizontal transmission line.
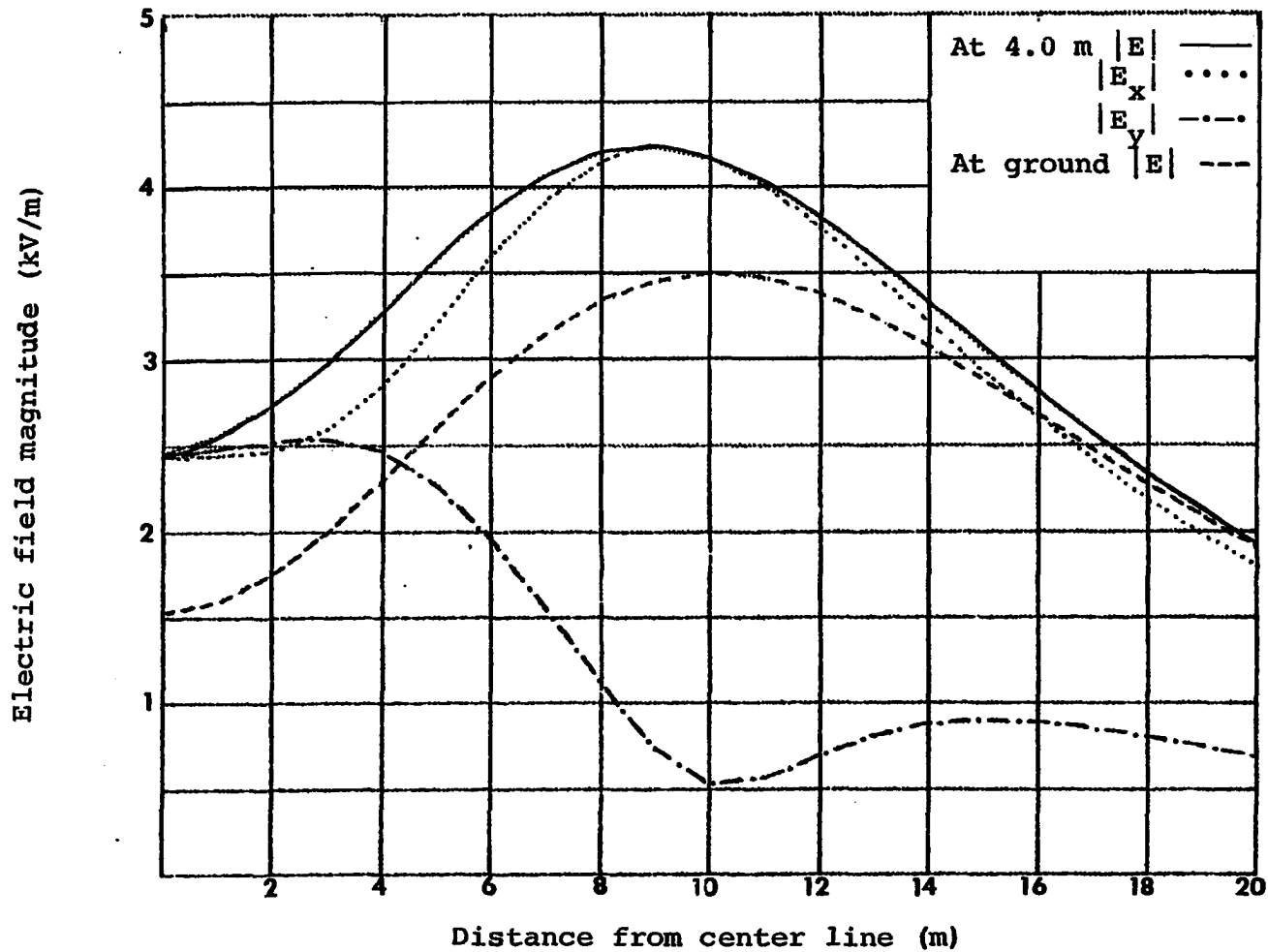
Fig. 5.6. Electric field contour at the ground and 4.0 m height using the free
space perfect conductor ground (two media)

Figure 5.6 also shows the electric field profile at 4.0 m above ground. When examined, this figure shows an increase in the maximum vertical component to 4.2 kV/m and a significant horizontal component 2.5 kV/m. Comparing both fields (at the ground and 4.0 m above it), it can be seen that the electric field magnitude at the edge of the right of way (ROW) is not changed appreciably with height, although an increase of 50% in the electric field can be seen along the center line.

3. Three dielectric media cases

a. Single line charge   The field due to a single line charge in three dielectric media can be written by inspection based on the derived models in the previous two chapter and the line expression given by [5, 18, 22]. Silvester [33], Takashima and Ishibashi [37] gave an expression for the line charge case. The electric field components in the three regions can be written as follows:

Region I

$$E_x^{(1)}(x,y) = \frac{q}{2\pi\varepsilon_1} \left\{ \frac{x-h}{[(x-h)^2+y^2]} + \alpha_{12} \frac{x+h}{[(x+h)^2+y^2]} + \right.$$

$$(1-\alpha_{12}^2) \sum_{n=1}^{\infty} (\alpha_{23})^n (-\alpha_{12})^{n-1}$$

$$\left. \frac{(x-h+2nb)}{[(x-h+2nb)^2+y^2]} \right\}$$

(5.24)

and

$$E_y^{(1)}(x,y) = \frac{q}{2\pi\epsilon_1} \left\{ \frac{y}{[(x-h)^2+y^2]} + \alpha_{12} \frac{y}{[(x+h)^2+y^2]} + \right.$$

$$(1-\alpha_{12}^2) \sum_{n=1}^{\infty} (-\alpha_{12})^{n-1} (\alpha_{23})^n$$

$$\left. \frac{y}{[(x-h+2nb)^2+y^2]} \right\} \qquad\qquad (5.25$$

Where the charge q is located at (h, y), b is the thickness of medium II, and α_{12} and α_{23} are the coefficients of reflection as defined before.

Region II

$$E_x^{(2)}(x,y) = \frac{q(1+\alpha_{12})}{2\pi\epsilon_2} \left\{ \sum_{n=1}^{\infty} (\alpha_{23})^n (-\alpha_{12})^{n-1} \right.$$

$$\frac{(x+h+2nb)}{[(x+h+2nb)^2+y^2]} - \sum_{n=1}^{\infty} (-\alpha_{12}\alpha_{23})^{n-1}$$

$$\left. \frac{(h-x+2(n-1)b)}{[(h-x+2(n-1)b)^2+y^2]} \right\} \tag{5.26}$$

and

$$E_y^{(2)}(x,y) = \frac{q(1+\alpha_{12})}{2\pi\epsilon_2} \left\{ \sum_{n=1}^{\infty} (\alpha_{23})^n (-\alpha_{12})^{n-1} \right.$$

$$\frac{y}{[(x+h+2nb)^2+y^2]} + \sum_{n=1}^{\infty} (-\alpha_{12}\alpha_{23})^{n-1}$$

$$\left. \frac{y}{[(h-x+2(n-1)b)^2+y^2]} \right\} \tag{5.27}$$

And finally, Region III:

$$E_x^{(3)}(x,y) = \frac{q(1+\alpha_{12})(1+\alpha_{23})}{2\pi\epsilon_1} \cdot \sum_{n=1}^{\infty} - (-\alpha_{12}\alpha_{23})^{n-1}$$

$$\frac{(h-x+2(n-1)b)}{[(h-x+2(n-1)b)^2+y^2]} \tag{5.28}$$

and

$$E_y^{(3)}(x,y) = \frac{q(1+\alpha_{12})(1+\alpha_{23})}{2\pi\varepsilon_1} \sum_{n=1}^{\infty} (-\alpha_{12}\alpha_{23})^{n-1}$$

$$\frac{y}{[(h-x+2(n-1)b)^2+y^2]} \qquad (5.29)$$

b. **Three-phase** **case**   Equations 5.24-5.29 describe the electric field components due to a single line charge in three dielectric media. Thus, if three line charges exist instead, the total electric field components can be written in a form similar to Eqs. 5.22 and 5.23.

A program was written for the three-phase transmission line in the three dielectric media case. This program was then tested for the special case when $\varepsilon_2=\varepsilon_1=$ the free space dielectric constant, and ε_3 was taken to be infinite (perfect conductor). The computer calculation matched exactly with the two media results. The results are shown in Fig. 5.7. Three curves are plotted: the electric field magnitude at ground, 2.5 m, and 4.0 m above it.

The three media program was then run for an arbitrary value of medium II dielectric constant. Tables 5.1-5.4 show the computed results. Both the tangential electric field and the normal flux density components are satisfied at the boundaries.
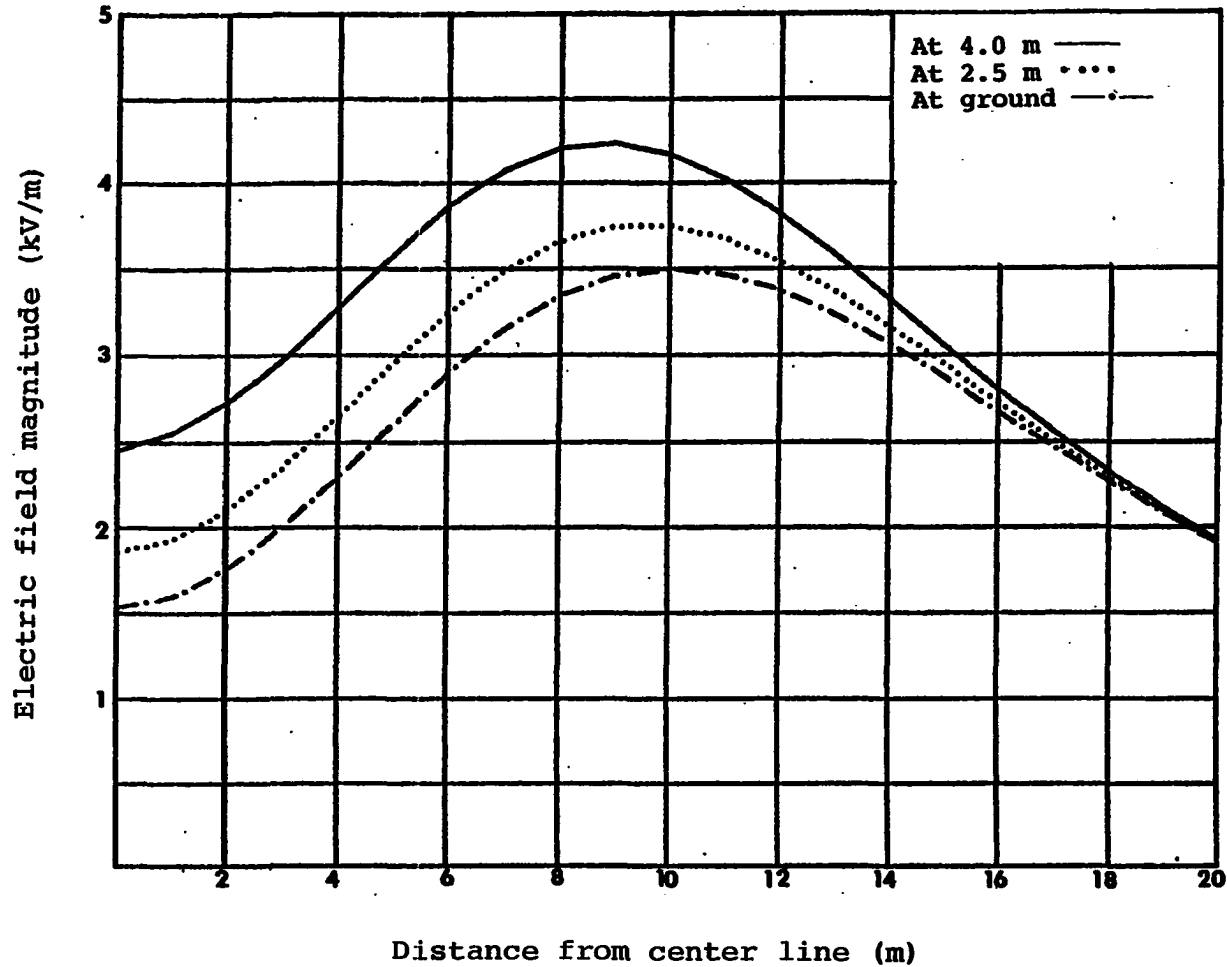
Fig. 5.7. Variation of the electric field magnitude with height above ground using the three dielectric media ($\varepsilon_1 = \varepsilon_2 = 1.0$, $\varepsilon_3 = \infty$)

Table 5.1. Boundary condition values for the tangential electric field and the normal flux density at media I-II interface ($\varepsilon_1 = 1.0$, $\varepsilon_2 = 2.0$, $\varepsilon_3 = \infty$)

| y | Medium I | | Medium II | |
m	$|E^{(1)}_y|$ kV/m	$|D^{(1)}_x|$ kV/m	$|E^{(2)}_y|$ kV/m	$|D^{(2)}_x|$ kV/m
0.0	0.8479	2.2518	0.8476	2.2518
2.0	0.8612	2.3918	0.8623	2.3917
4.0	0.8289	2.9332	0.8286	2.9358
6.0	0.6595	3.6358	0.6595	3.6358
8.0	0.3921	4.1688	0.3922	4.1688
10.0	0.1950	4.2607	0.1950	4.2607
12.0	0.2420	3.9593	0.2420	3.9594
14.0	0.3101	3.4493	0.3101	3.4494
16.0	0.3186	2.8937	0.3186	2.8938
18.0	0.2894	2.3822	0.2893	2.3823
20.0	0.2459	1.9473	0.2459	1.9474

Table 5.2. Boundary condition values for the tangential electric field and the normal flux density at media II-III interface ($\varepsilon_1 = 1.0$, $\varepsilon_2 = 2.0$, $\varepsilon_3 = \infty$) (number of images used $\cong 10$)

y m	Medium II		Medium III	
	$\|E^{(2)}_y\|$ kV/m	$\|D^{(2)}_x\|$ kV/m	$\|E^{(3)}_y\|$ kV/m	$\|D^{(3)}_x\|$ kV/m
0.0	0.0	1.8532	0.0	1.8502
2.0	0.0	2.0752	0.0	2.0718
4.0	0.0	2.6511	0.0	2.6468
6.0	0.0	3.3268	0.0	3.3214
8.0	0.0	3.8180	0.0	3.8118
10.0	0.0	3.9670	0.0	3.9606
12.0	0.0	3.7853	0.0	3.7792
14.0	0.0	3.3885	0.0	3.3830
16.0	0.0	2.9055	0.0	2.9008
18.0	0.0	2.4279	0.0	2.4240
20.0	0.0	2.0023	0.0	1.9991

Table 5.3. Electric field values at the boundary of
media I-II interface ($\varepsilon_1=1.0$, $\varepsilon_2=5.0$, $\varepsilon_3=\infty$)
(number of images used $\cong$ 16)

y m	Medium I		Medium II	
	$\|E^{(1)}_y\|$ kV/m	$\|D^{(1)}_x\|$ kV/m	$\|E^{(2)}_y\|$ kV/m	$\|D^{(2)}_x\|$ kV/m
0.0	0.3740	2.5818	0.3740	2.5817
2.0	0.3832	2.7008	0.3832	2.7008
4.0	0.3722	3.2139	0.3716	3.2139
6.0	0.2953	4.0061	0.2952	4.0060
8.0	0.1727	4.5823	0.1728	4.5824
10.0	0.0881	4.6515	0.0880	4.6516
12.0	0.1151	4.2740	0.1152	4.2739
14.0	0.1440	3.6716	0.1441	3.6715
16.0	0.1446	3.0343	0.1446	3.0342
18.0	0.1285	2.4618	0.1285	2.4617
20.0	0.1070	1.9856	0.1070	1.9856

Table 5.4. Electric field values at the boundary of media II-III interface ($\varepsilon_1 = 1.0$, $\varepsilon_2 = 5.0$, $\varepsilon_3 = \infty$) (number of images $\cong$ 16)

y	Medium II		Medium III	
	$|E^{(2)}_y|$	$|D^{(2)}_x|$	$|E^{(3)}_y|$	$|D^{(3)}_x|$
m	kV/m	kV/m	kV/m	kV/m
0.0	0.0	2.1169	0.0	2.1198
2.0	0.0	2.3347	0.0	2.3378
4.0	0.0	2.9305	0.0	2.9345
6.0	0.0	3.6558	0.0	3.6608
8.0	0.0	4.1815	0.0	4.1872
10.0	0.0	4.3195	0.0	4.3254
12.0	0.0	4.0854	0.0	4.0899
14.0	0.0	3.6136	0.0	3.6185
16.0	0.0	3.058	0.0	3.0623
18.0	0.0	2.5210	0.0	2.5245
20.0	0.0	2.0522	0.0	2.0550

E. Experimental Field Measurements

A set of electric field strength measurements was taken for several positions beneath an existing 345 kV transmission line. This line is used by the Iowa Test and Evaluation Facility (ITEF) of Iowa State University to provide a realistic environment for EHV research projects. Three sections of this line are accessible for a distance of approximately 1 km, with a large variation in height. The line runs north and south adjacent to a country road with minimum ground clearances in the three sections of 12 m, 15.5 m and 22 m from the south to the north.

A transverse set of electrical field measurements was taken with a Monroe model 238A-1 a.c. field strength meter inside the cornfield. These measurements were taken at four different heights inside the cornfield. One set of measurements was taken at 2.5 m above ground, almost at the surface of the corn. The second set of measurements was taken at 2.0 m above ground. The third set was taken at 1 m above ground and, finally, the fourth set was taken at ground level. All these measurements were made at a distance 435 m from the northern tower (see Fig. 5.8). The above four sets of measurements were taken twice: the first during the first week of September 1981 and the second two weeks later, in order to check the accuracy of the two sets. The meter used was held at about 2.5 m from the observer in

order to minimize the field disturbance caused by holding the meter. It was always oriented to read the vertical component of the electric field which, close to ground, coincides with the maximum component of the electric field. At any other heights above the ground plane, the instrument can be oriented to read both the vertical component and the horizontal component. Tables 5.5 and 5.6 show the measured electric field components inside the vegetation medium (corn) at 2.0 m, 2.5 m and 1.0 m above ground. Figure 5.9 shows a plot of the magnitude of the electric field profile in the cornfield at three different positions: 2.5 m, 2 m and 1 m above ground.

F. Application of the Four Dielectric Media Models to the Three-Phase Transmission Line

1. Single line charge case

The electric field components, due to a single line of charge in front of three dielectric media on top of perfect conductor ground, can be written using the line charge field expression plus the field due to its images. The images' magnitudes and positions can be found using the point charge algorithm where the line charge q (col/m) replaces the point charge Q (col). The electric field in region I can then be written similar to Eq. 4.33 and Eq. 4.34. The field in the other two regions would follow the same pattern.
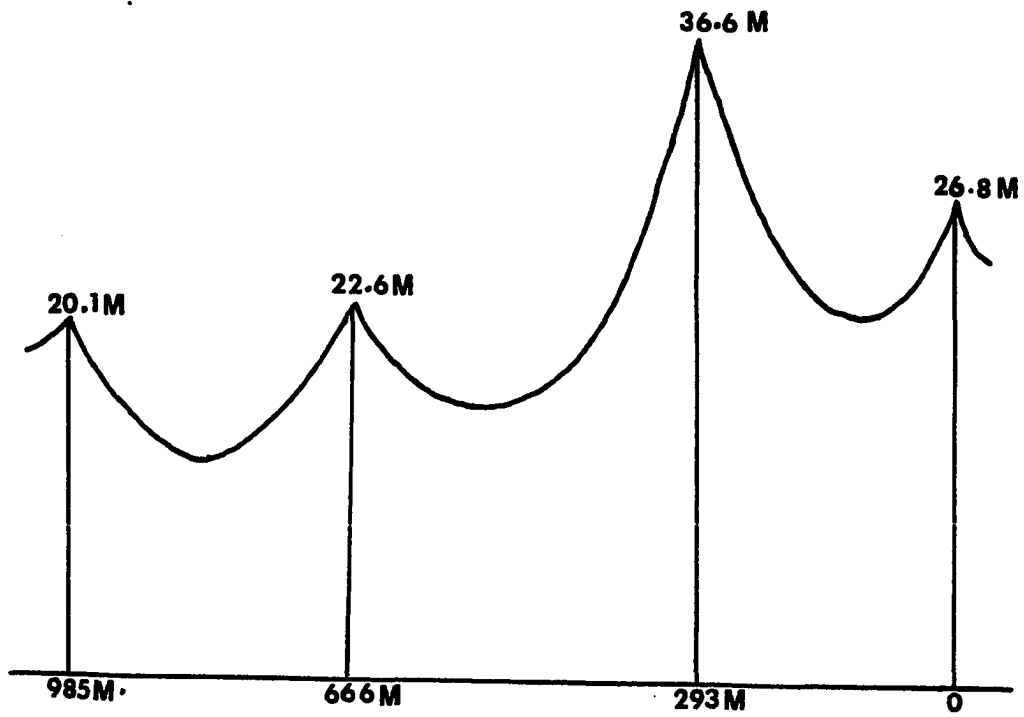
Fig. 5.8.   Profile of 345 kV transmission line at ITEF [5]

Table 5.5. Electric field measurement inside the vegetation
medium (cornfield) underneath EHV line (345 kV
transmission line at ITEF), first set[a]

Distance from Center Line (m)	2.0 m Above Ground		2.5 m Above Ground	
	Horizontal Electric Field Components E_H kV/m	Vertical Electric Field Components E_V kV/m	Horizontal Electric Field Components E_H kV/m	Vertical Electric Field Components E_V kV/m
0.0	0.2	1.2	0.5	1.7
3.0	0.1	1.3	0.3	1.8
5.0	0.1	1.6	0.3	2.1
7.0	0.1	1.8	0.5	2.7
9.0	0.0	2.1	0.3	3.5
12.0	0.1	1.7	0.2	3.1
16.0	0.0	1.2	0.3	2.5

[a]Zero readings were observed at ground level and 1 m.
above ground inside the vegetation medium (cornfield).
The meter used was a Monroe a.c. field meter, model
238 A.1, serial no. +335839003.

Table 5.6.   Electric field measurements inside the vegetation
medium (cornfield) underneath EHV line (345 kV
transmission line at ITEF), second set[a]

| | 2.0 m Above Ground | | 2.5 m Above Ground | |
Distance from Center Line (m)	Horizontal Electric Field Components E_H kV/m	Vertical Electric Field Components E_V kV/m	Horizontal Electric Field Components E_H kV/m	Vertical Electric Field Components E_V kV/m
0.0	0.1	1.2	0.3	1.8
3.0	0.1	1.3	0.3	1.9
5.0	0.0	1.6	0.3	2.0
7.0	0.0	1.9	0.5	2.8
9.0	0.0	2.0	0.3	3.6
12.0	0.1	1.8	0.1	3.1
16.0	0.0	1.3	0.3	2.7

[a] Zero readings were observed at ground level and 1 m
above ground inside the vegetation medium (cornfield).
The meter used was a Monroe a.c. field meter, model 238 A.1,
serial no. +335839003.
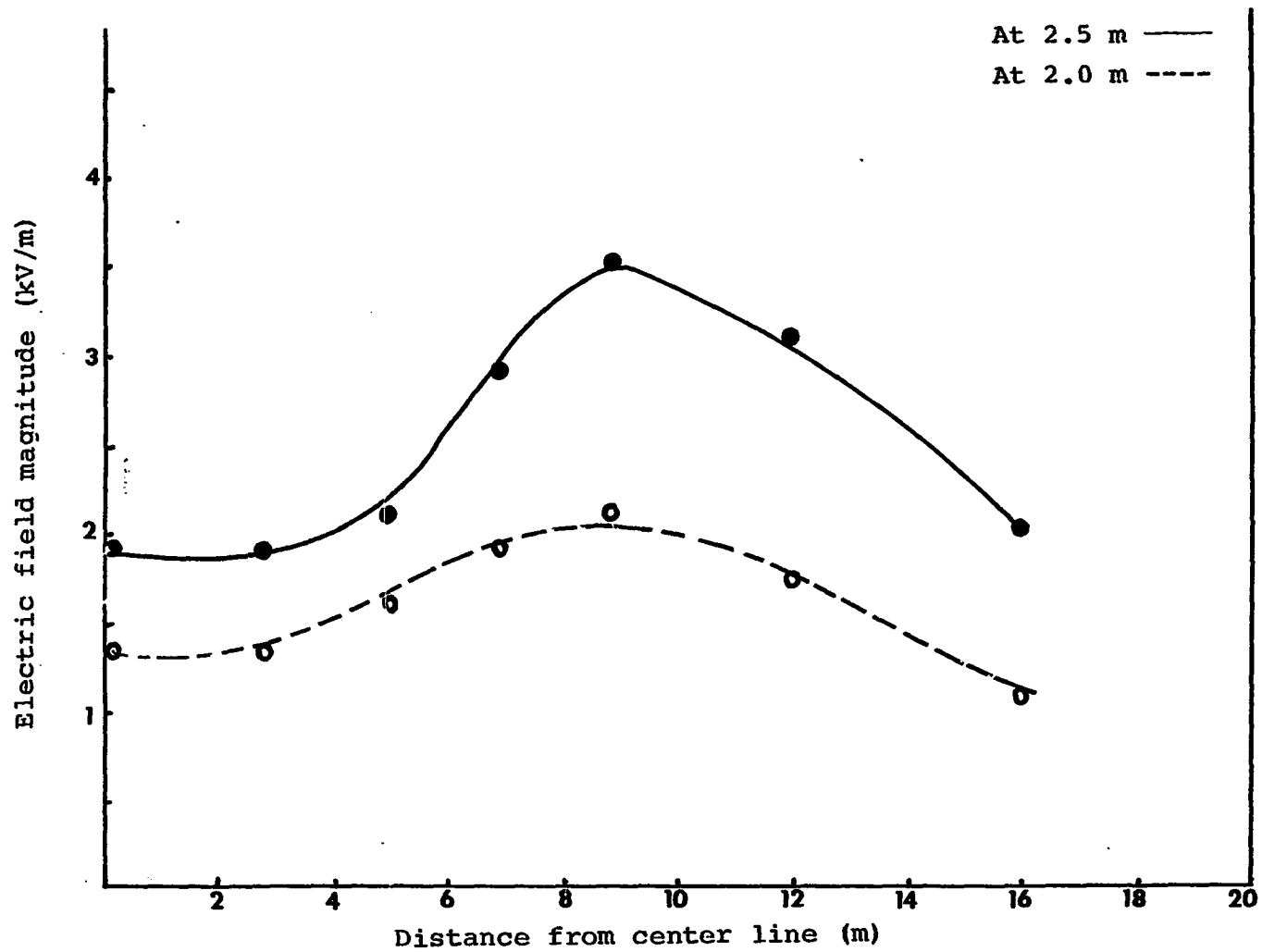
Fig. 5.9. Variation of the measured electric field magnitude with height above ground inside the cornfield

Region I

$$E_x^{(1)}(x,y) = \frac{1}{2\pi\varepsilon_1} \left[q\frac{(x-h)}{[(x-h)^2+y^2]} + q_0\frac{(x-h+2a)}{[(x-h+2a)^2+y^2]} + \right.$$

$$\left. \sum_{j=1} q_5(j)\frac{(x+L_5(j)-b-c)}{[(x+L_5(j)-b-c)^2+y^2]} \right. \qquad (5.30)$$

and

$$E_y^{(1)}(x,y) = \frac{1}{2\pi\varepsilon_1} \left[q\frac{y}{[(x-h)^2+y^2]} + q_0\frac{y}{[(x-h+2a)^2+y^2]} + \right.$$

$$\left. \sum_{j=1} q_5(j)\frac{y}{[(x+L_5(j)-b-c)^2+y^2]} \right] \qquad (5.31)$$

Region II field

$$E_x^{(2)}(x,y) = \frac{1}{2\pi\varepsilon_2} \left[\sum_{j=1} q_1(j)\frac{(x-L_1(j)-b-c)}{[(x-L_1(j)-b-c)^2+y^2]} + \right.$$

$$\left. \sum_{k=1} q_2(k)\frac{(x+L_2(k)-c)}{[(x+L_2(k)-c)^2+y^2]} \right] \qquad (5.32)$$

and

$$E_y^{(2)}(x,y) = \frac{1}{2\pi\varepsilon_2} \left[\sum_{j=1} q_1(j) \frac{y}{[(x-L_1(j)-b-c)^2+y^2]} + \right.$$

$$\left. \sum_{k=1} q_2(k) \frac{y}{[(x+L_2(k)-c)^2+y^2]} \right] \qquad (5.33)$$

Region III field

$$E_x^{(3)}(x,y) = \frac{1}{2\pi\varepsilon_3} \left[\sum_{m=1} q_3(m) \frac{(x-L_3(m)-c)}{[(x-L_3(m)-c)^2+y^2]} + \right.$$

$$\left. \sum_{j=1} q_4(j) \frac{(x+L_4(j))}{[(x+L_4(j))^2+y^2]} \right] \qquad (5.34)$$

and

$$E_y^{(3)}(x,y) = \frac{1}{2\pi\varepsilon_3} \left[\sum_{m=1} q_3(m) \frac{y}{[(x-L_3(m)-c)^2+y^2]} \right.$$

$$\left. \sum_{j=1} q_4(j) \frac{y}{[(x+L_4(j))^2+y^2]} \right] \qquad (5.35)$$

Region IV field components are zero because it is a perfect conductor region.

2. Three-phase transmission line

The electric field components due to a three-phase transmission line can be written by applying the superposition principles to Eqs. 5.30-5.34. Let the line charges be q_1, q_2 amd q_3 (col/m), located at (h_1, y_1), (h_2, y_2) and (h_3, y_3) or simply $(q_i$ at (h_i, y_i), $i=1,2,3)$. Therefore, region I electric field components are:

$$E_x^{(1)}(x,y) = \sum_{i=1}^{3} \frac{1}{2\pi\epsilon_1} \left[q_i \frac{(x-h_i)}{[(x-h_i)^2+(y-y_i)^2]} + q_{0i} \right.$$

$$\frac{(x-h_i+2a)}{[(x-h_i+2a)^2+(y-y_i)^2]} + \sum_{j=1}^{\Sigma} q_{5i}(j)$$

$$\left. \frac{(x+L_{5i}(j)-b-c)}{[(x+L_{5i}(j)-b-c)^2+(y-y_i)^2]} \right] \tag{5.36}$$

and

$$E_y^{(1)}(x,y) = \sum_{i=1}^{3} \frac{1}{2\pi\epsilon_1} \left[q_i \frac{(y-y_i)}{[(x-h_i)^2+(y-y_i)^2]} + q_{0i} \right.$$

$$\frac{(y-y_i)}{[(x-h_i+2a)^2+(y-y_i)^2]} + \sum_{j=1}^{\Sigma} q_{5i}(j)$$

$$\left. \frac{(y-y_i)}{[(x+L_{5i}(j)-b-c)^2+(y-y_i)^2]} \right] \tag{5.37}$$

Following the same procedure, Eqs. 5.32-5.35 can be written in the same manner.

3. Four dielectric media application

The four dielectric model is used to solve for the field distribution inside a cornfield underneath an EHV transmission line. The vegetation is modeled as two dielectric layers. The total height of the vegetation medium is taken to be 2.5 m, as shown in Fig. 5.10. The interface which divides the vegetation medium into two dielectric layers is chosen at an arbitrary height c m above ground. The other two regions of the four dielectric media are the air and the perfect conductor ground. Using the values of the line charges that have been found in section C and the four media program for the special case when vegetation does not exist, $\varepsilon_1 = \varepsilon_2 = \varepsilon_3 =$ free space dielectric constant. The electric field profiles of Fig. 5.6 and Fig. 5.11 are now similar.

The same program is then run for different combinations of ε_2 which represent the vegetation dielectric layers. Better results are obtained at the boundary if the number of images is increased. At least 1,000 images are needed for an accuracy of 0.001 for the boundary condition field components. For the purpose of simplicity, the magnitude of the electric field is plotted for some values of the given permittivities, as shown in Figs. 5.12, 5.13 and 5.14. The
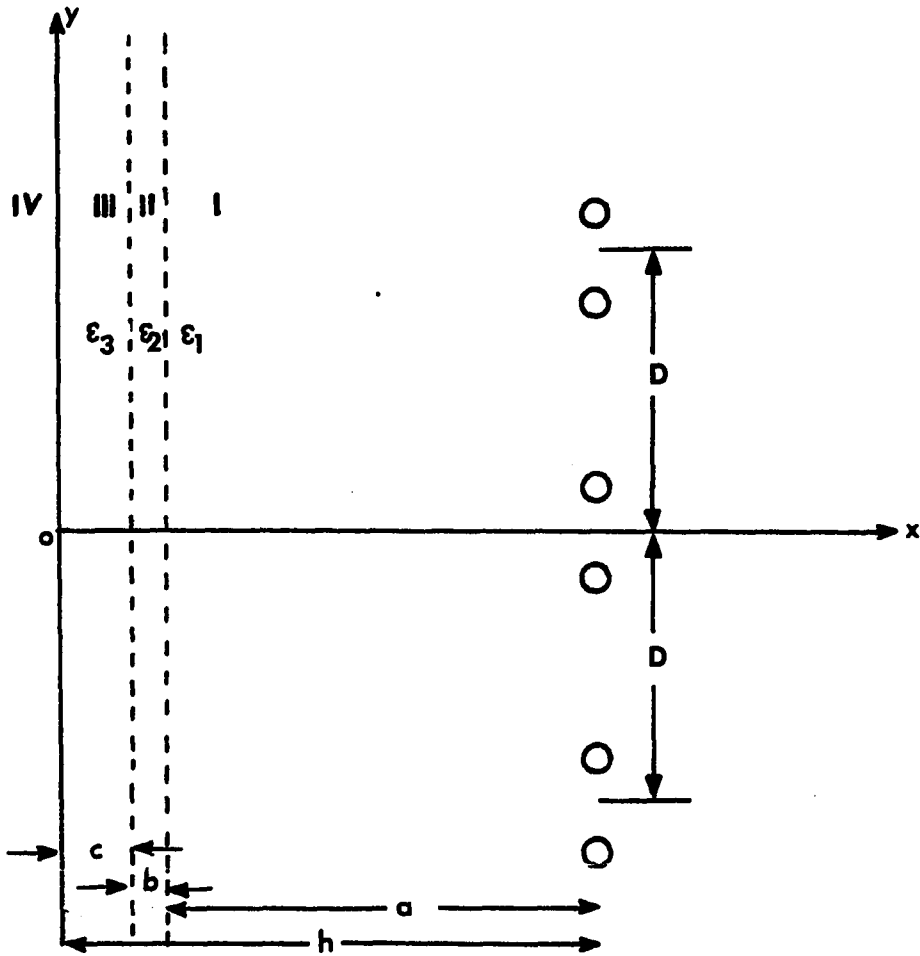
Fig. 5.10.   The vegetation medium underneath 345 kV line:
region I is the air region, region II and III
are the vegetation dielectric layers, and
region VI is the perfect conductor ground
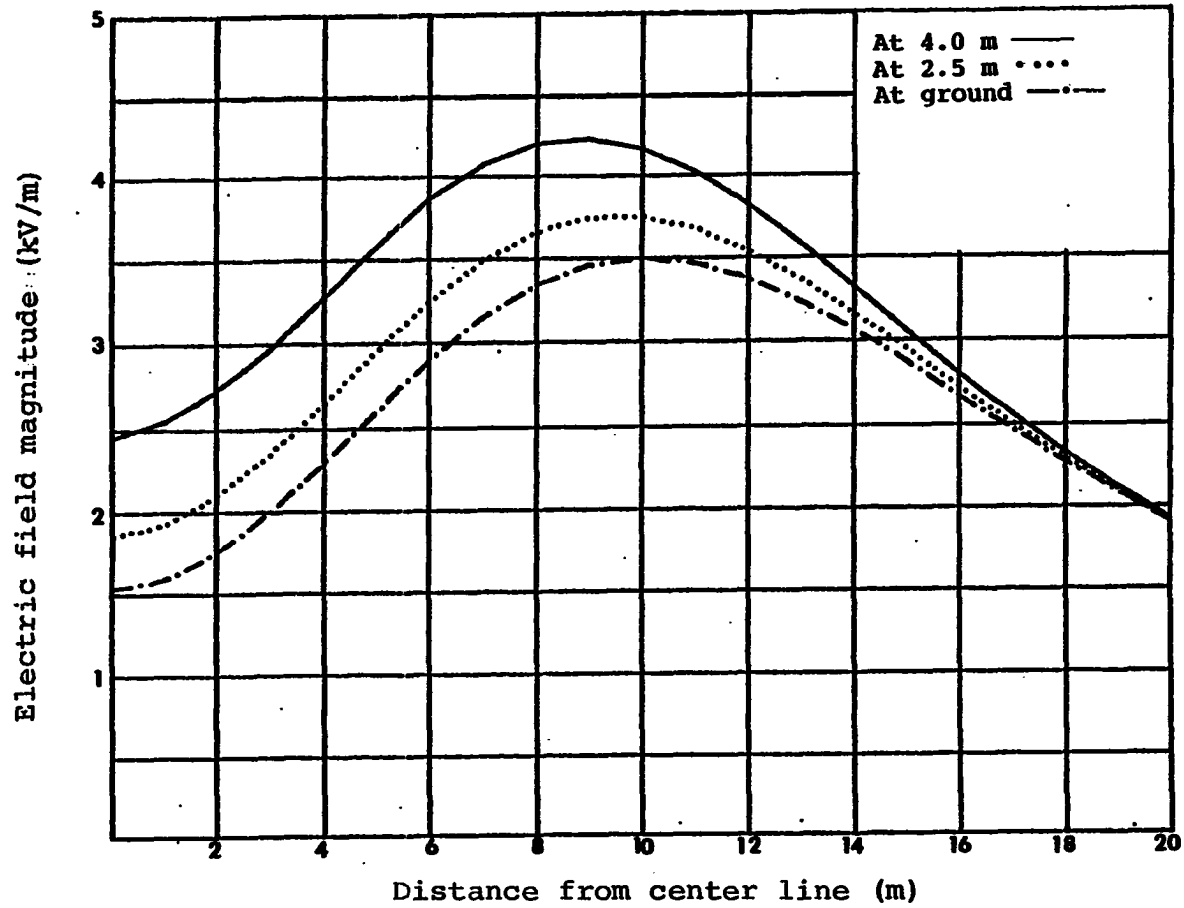
Fig. 5.11. Variation of the electric field magnitude with height above ground
using the four dielectric media ($\varepsilon_1 = \varepsilon_2 = \varepsilon_3 = 1.0$)

measured field data are plotted on the same graphs.

The profiles of the measured field data followed the same pattern as the computer simulation. The measured data at the 2.5 m height are closer to the computer simulation for the given choice of the dielectric constants which represent the outermost vegetation layer. However, there is a big difference in the results between the calculated and the measured data at the 2.0 m height. Therefore, representing the corn by two dielectric layers is not enough and the need for at least one more dielectric layer to be added to the previous model is a must. The vegetation is then modeled as three dielectric layers and together with the air and the perfect conductor ground form the five dielectric media.

G. Application of the Five Dielectric Media to Three-Phase Transmission Line

The point charge in five dielectric media was discussed in Chapter IV. The images were generated by a computer algorithm. A similar algorithm is used here where the point charge Q is replaced by the line charge q. The position of the images is given exactly by the same algorithm. The total electric field components due to the three-phase transmission line can be written similar to Eqs. 4.46 and 4.47 after using the correct field expression for the line
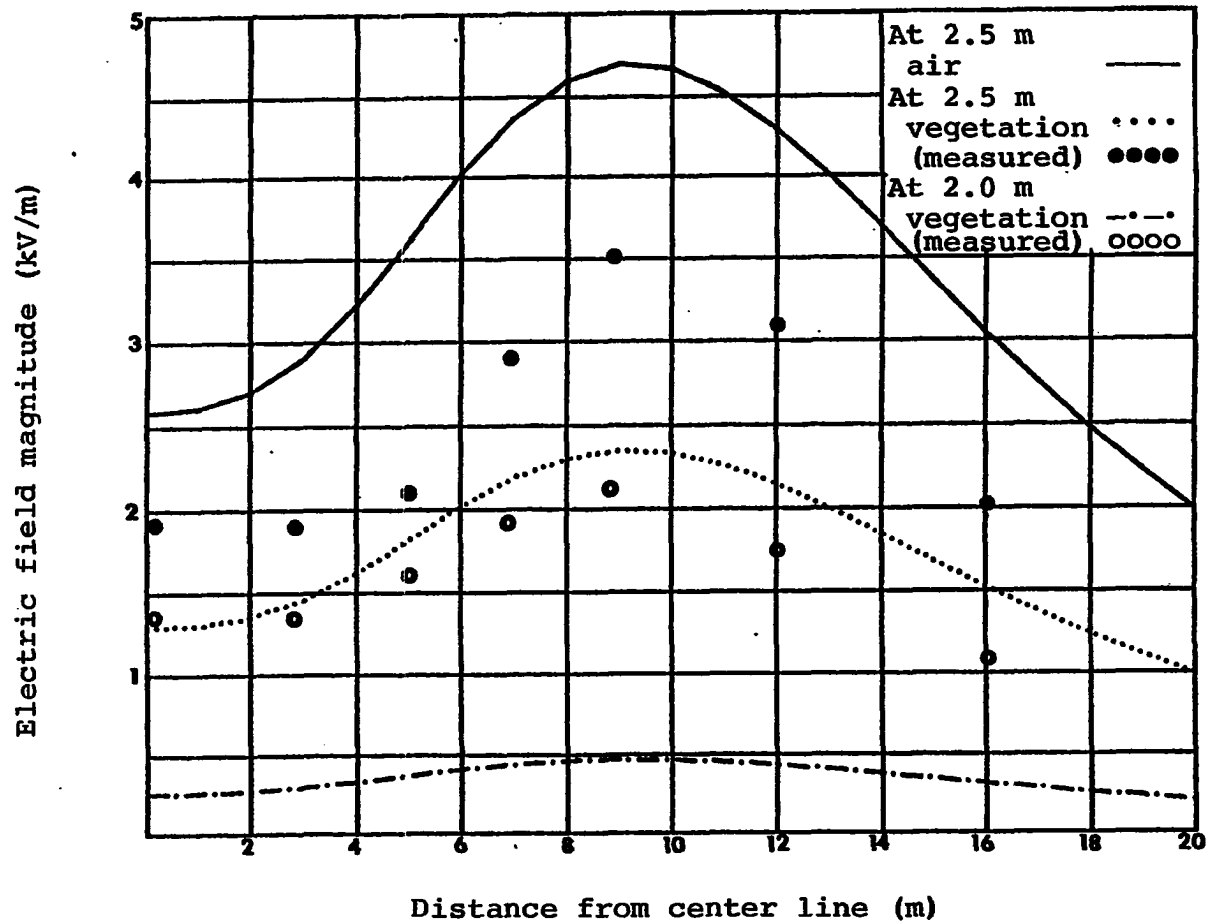
Fig. 5.12. Variation of the electric field magnitude with height above ground inside the cornfield using the four dielectric media (ε_1=1.0, ε_2=2.0, ε_3= 10.0)
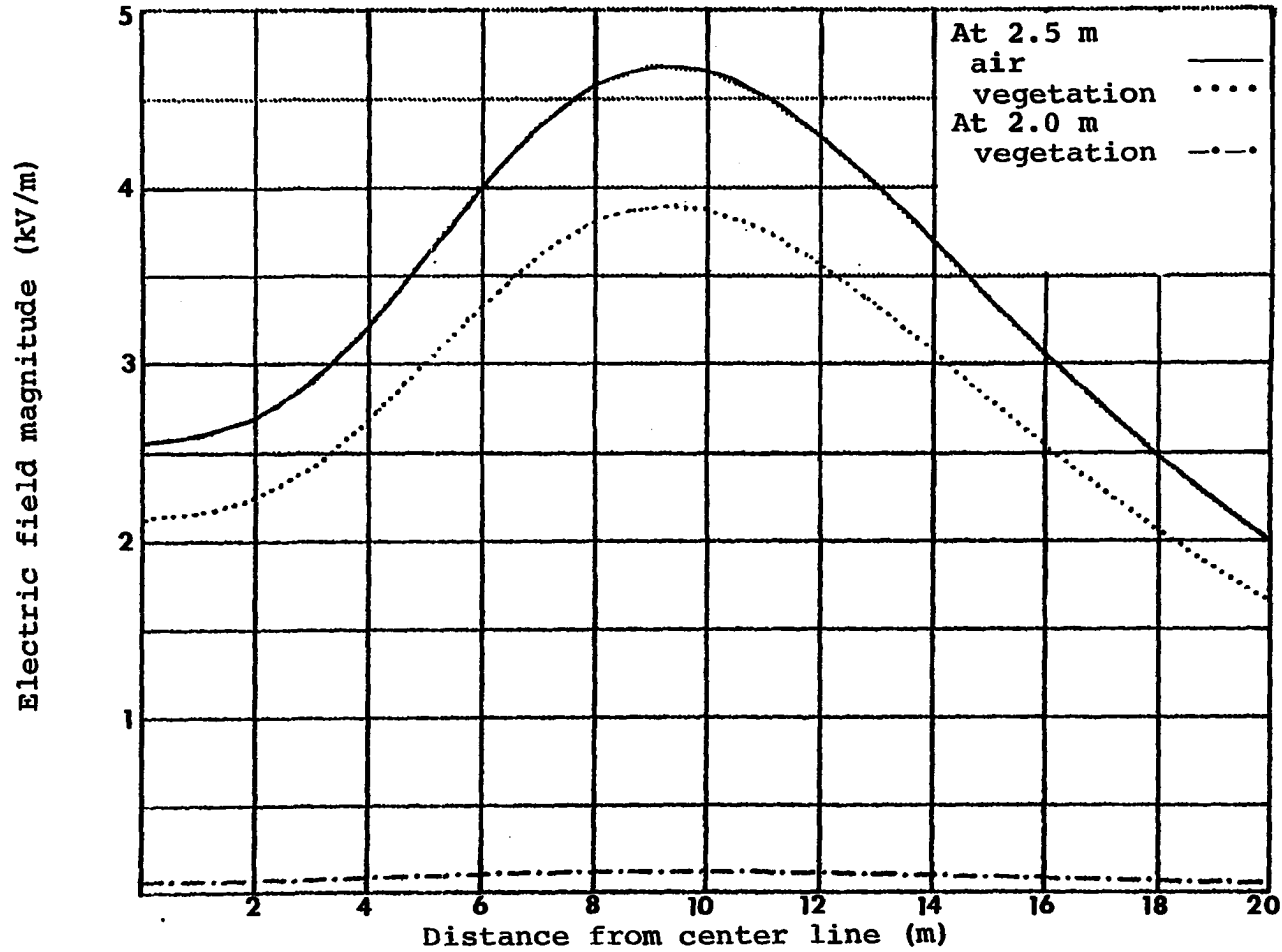
Fig. 5.13. Variation of the electric field magnitude with height above ground using the four dielectric media ($\varepsilon_1=1.0$, $\varepsilon_2=1.2$, $\varepsilon_3=40.0$)
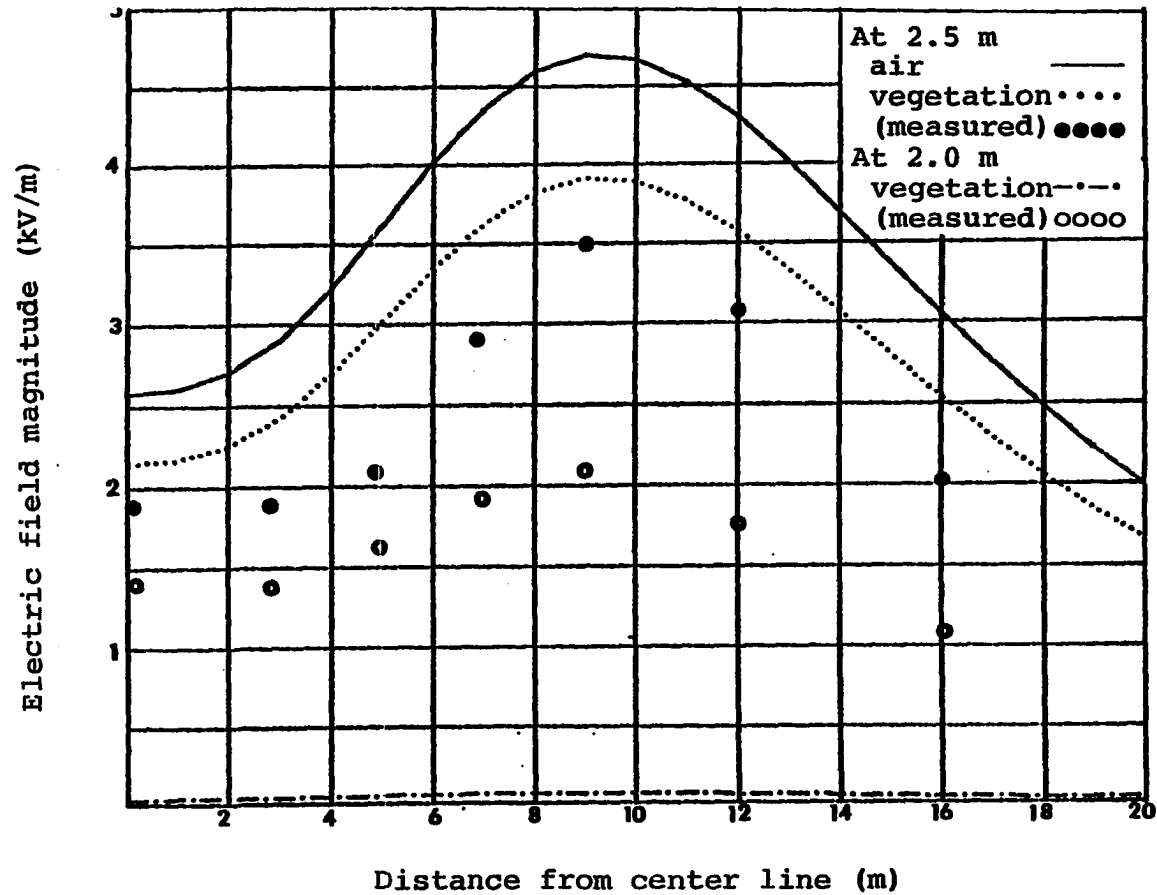
Fig. 5.14. Variation of the electric field magnitude with height above ground inside the cornfield using the four dielectric media (ε_1=1.0, ε_2=1.2, ε_3= 80.0)

charge. Thus, region I field components can be written as follows:

$$E_x^{(1)}(x,y) = \frac{1}{2\pi\varepsilon_1} \sum_{i=1}^{3} \left[q_i \frac{(x-h_i)}{[(x-h_i)^2+(y-y_i)^2]} + q_{0i} \right.$$

$$\frac{(x-h_i+2a)}{[(x-h_i+2a)^2+(y-y_i)^2]} + \sum_{j=1} q_{5i(j)}$$

$$\left. \frac{(x+L_{5i}(j)-b-c-d)}{[(x+L_{5i}(j)-b-c)^2+(y-y_i)^2]} \right] \qquad (5.38)$$

and

$$E_y^{(1)}(x,y) = \frac{1}{2\pi\varepsilon_1} \sum_{i=1}^{3} \left[q_i \frac{(y-y_i)}{[(x-h_i)^2+(y-y_i)^2]} + q_{0i} \right.$$

$$\frac{(y-y_i)}{[(x-h_i+2a)^2+(y-y_i)^2]} + \sum_{j=1} q_{5i(j)}$$

$$\left. \frac{(y-y_i)}{[(x+L_{5i(j)}-b-c-d)^2+(y-y_i)^2]} \right] \qquad (5.39)$$

Region II electric field components are:

$$E_x^{(2)}(x,y) = \frac{1}{2\pi\epsilon_2} \sum_{i=1}^{3} \left[\sum_{j=1}^{} q_{1i(j)} \frac{(x-L_{1i(j)}-b-c-d)}{[(x-L_{1i(j)}-b-c-d)^2+(y-y_i)^2]} \right.$$

$$\left. + \sum_{j=1}^{} q_{2i(j)} \frac{(x+L_{2i(j)}-c-d)}{[(x+L_{2i(j)}-c-d)^2+(y-y_i)^2]} \right] \quad (5.40)$$

and

$$E_y^{(2)}(x,y) = \frac{1}{2\pi\epsilon_2} \sum_{i=1}^{3} \left[\sum_{j=1}^{} q_{1i(j)} \frac{(y-y_i)}{[(x-L_{1i(j)}-b-c-d)^2+(y-y_i)^2]} \right.$$

$$\left. + \sum_{j=1}^{} q_{2i(j)} \frac{(y-y_i)}{[(x+L_{2i(j)}-c-d)^2+(y-y_i)^2]} \right] \quad (5.41)$$

Region III electric field components are:

$$E_x^{(3)}(x,y) = \frac{1}{2\pi\epsilon_3} \sum_{i=1}^{3} \left[\sum_{j=1}^{} q_{3i(j)} \frac{(x-L_{3i(j)}-c-d)}{[(x-L_{3i(j)}-c-d)^2+(y-y_i)^2]} \right.$$

$$\left. + \sum_{k=1}^{} q_{4i(k)} \frac{(x+L_{4i(k)}-d)}{[(x+L_{4i(k)}-d)^2+(y-y_i)^2]} \right] \quad (5.42)$$

and

$$E_y^{(3)}(x,y) = \frac{1}{2\pi\epsilon_3} \sum_{i=1}^{3} \left[\sum_{j=1}^{} q_{3i(j)} \frac{(y-y_i)}{[(x-L_{3i(j)}-c-d)^2+(y-y_i)^2]} \right.$$

$$\left. + \sum_{k=1}^{} q_{4i(k)} \frac{(y-y_i)}{[(x+L_{4i(k)}-d)^2+(y-y_i)^2]} \right] \quad (5.43)$$

Finally, region IV electric field components are:

$$E_x^{(4)}(x,y) = \frac{1}{2\pi\epsilon_4} \sum_{i=1}^{3} \left[\sum_{k=1}^{} q_{6i(k)} \frac{(x-L_{6i(k)}-d)}{[(x-L_{6i(k)}-d)^2+(y-y_i)^2]} \right.$$

$$\left. + \sum_{m=1}^{} q_{7i(m)} \frac{(x+L_{7i(m)})}{[(x+L_{7i(m)})^2+(y-y_i)^2]} \right] \qquad (5.44)$$

and

$$E_y^{(4)}(x,y) = \frac{1}{2\pi\epsilon_4} \sum_{i=1}^{3} \left[\sum_{k=1}^{} q_{6i(k)} \frac{(y-y_i)}{[(x-L_{6i(k)}-d)^2+(y-y_i)^2]} \right.$$

$$\left. + \sum_{m=1}^{} q_{7i(m)} \frac{(y-y_i)}{[(x+L_{7i(m)})^2+(y-y_i)^2]} \right] \qquad (5.45)$$

Application of the five dielectric media model to the vegetation case will be done as follows: the vegetation will be modeled as three dielectric layers. The height of these layers is shown in Fig. 5.15. Each layer has its own unique dielectric constant. The other two regions of the five dielectric media are the air and the perfect conductor ground. This model can be used also for the case of four, three or even two dielectric media. This can occur by letting some of the neighborhood dielectric regions remain the same.
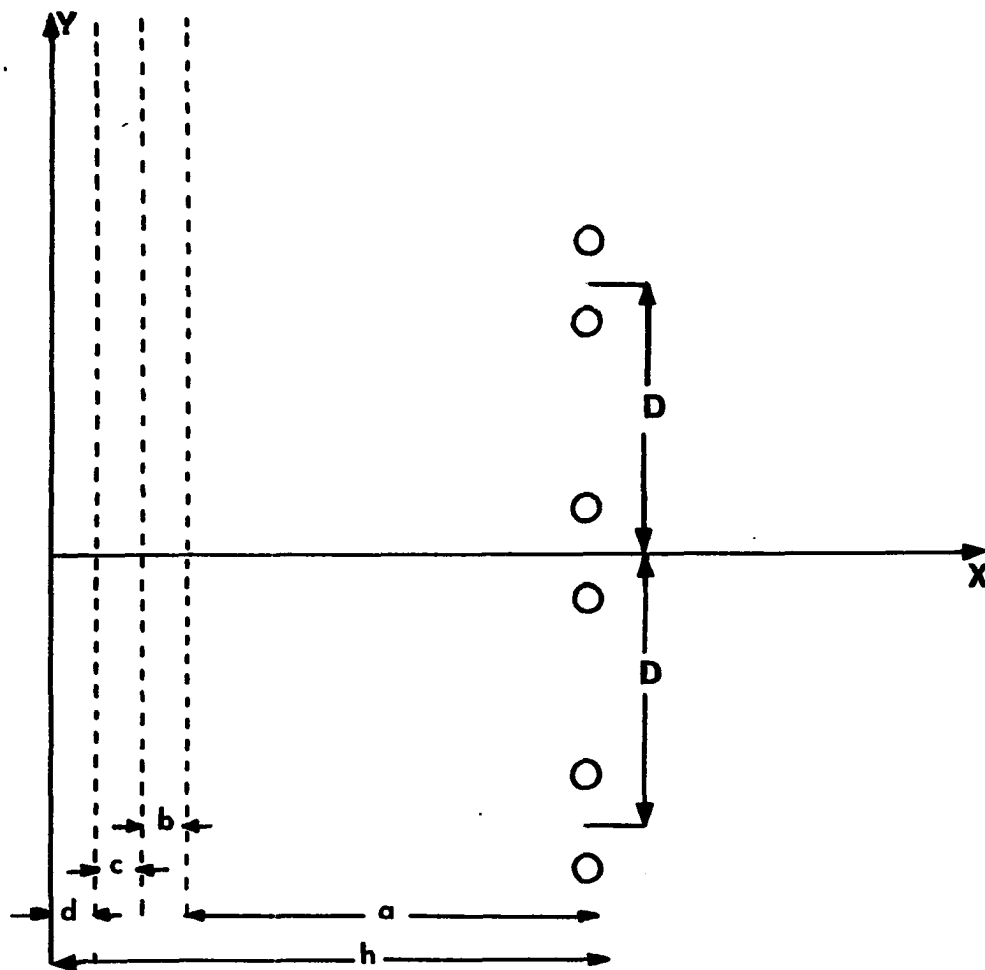
Fig. 5.15. The five dielectric model representation for the cornfield
underneath 345 kV line

A general program was written for the five dielectric media. This program was tested under three special cases:

1. $\varepsilon_1=\varepsilon_2=\varepsilon_3=\varepsilon_4$; the results of this program should give exactly the same results as the two media results.

2. $\varepsilon_2=\varepsilon_3=\varepsilon_4$; the results of this should match the results of the three dielectric media.

3. $\varepsilon_3=\varepsilon_4$; this case should correspond to the four media case.

The above three cases were tried and the results were plotted in the following figures: Fig. 5.16 shows the first case, Fig. 5.17 shows the second case, while Fig. 5.18 shows the third case. Comparison of these figures with Figs. 5.7, 5.19 and 5.20 indicates good agreement.

The same program was then run many times for different combinations of the permittivities (ε_2, ε_3, ε_4), that represent the dielectric layers. Figures 5.21-5.24 show a sample of the generated computer output graph. In looking at these figures very carefully, the following observations can be made.

1. The computer output graphs using this model (five dielectric) seem to fit very closely with the measured data.

2. The measured data seemed always to be lower than the computer output. This seemed to be very
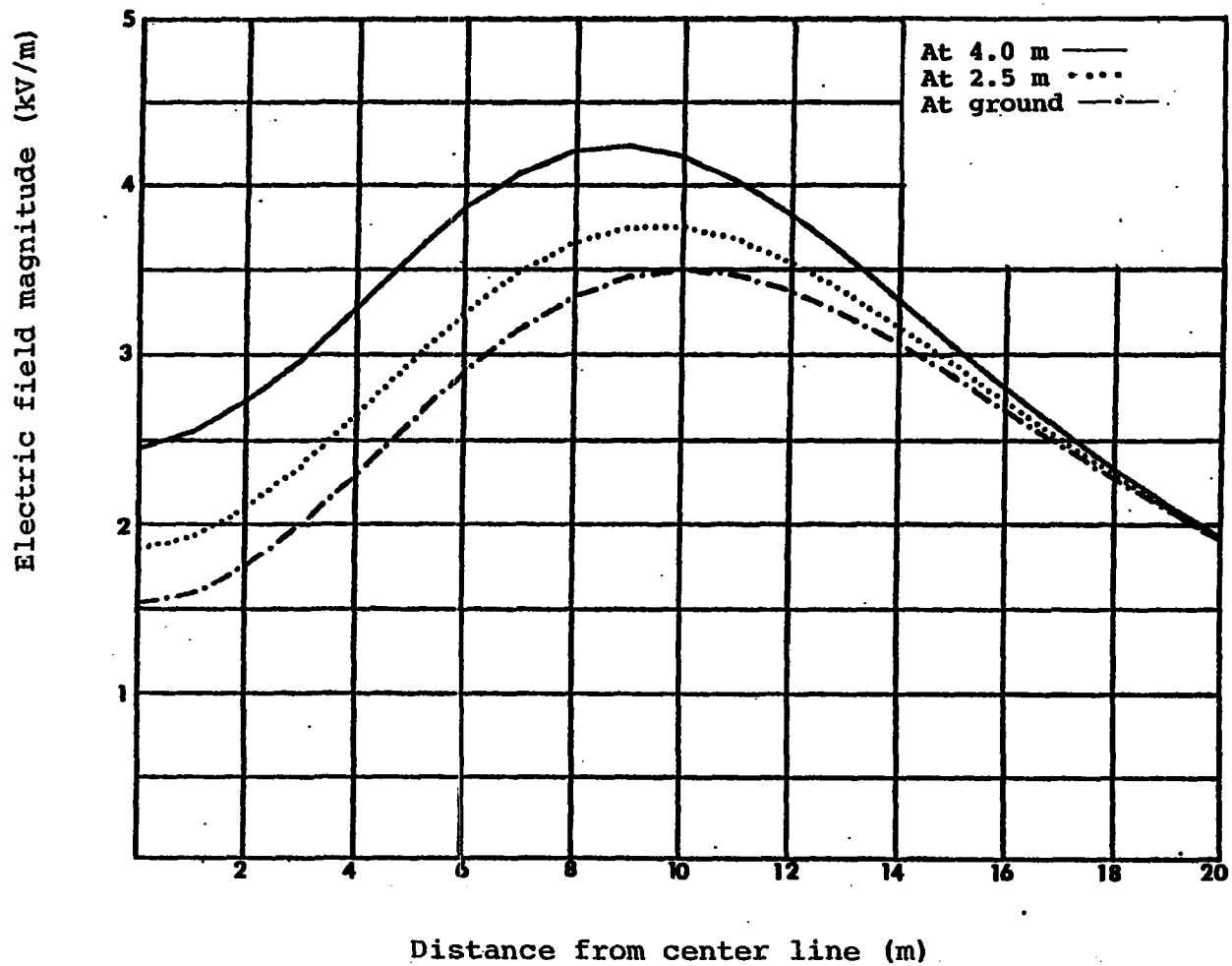
Fig. 5.16. Variation of the electric field magnitude with height (using the five dielectric media as two media)
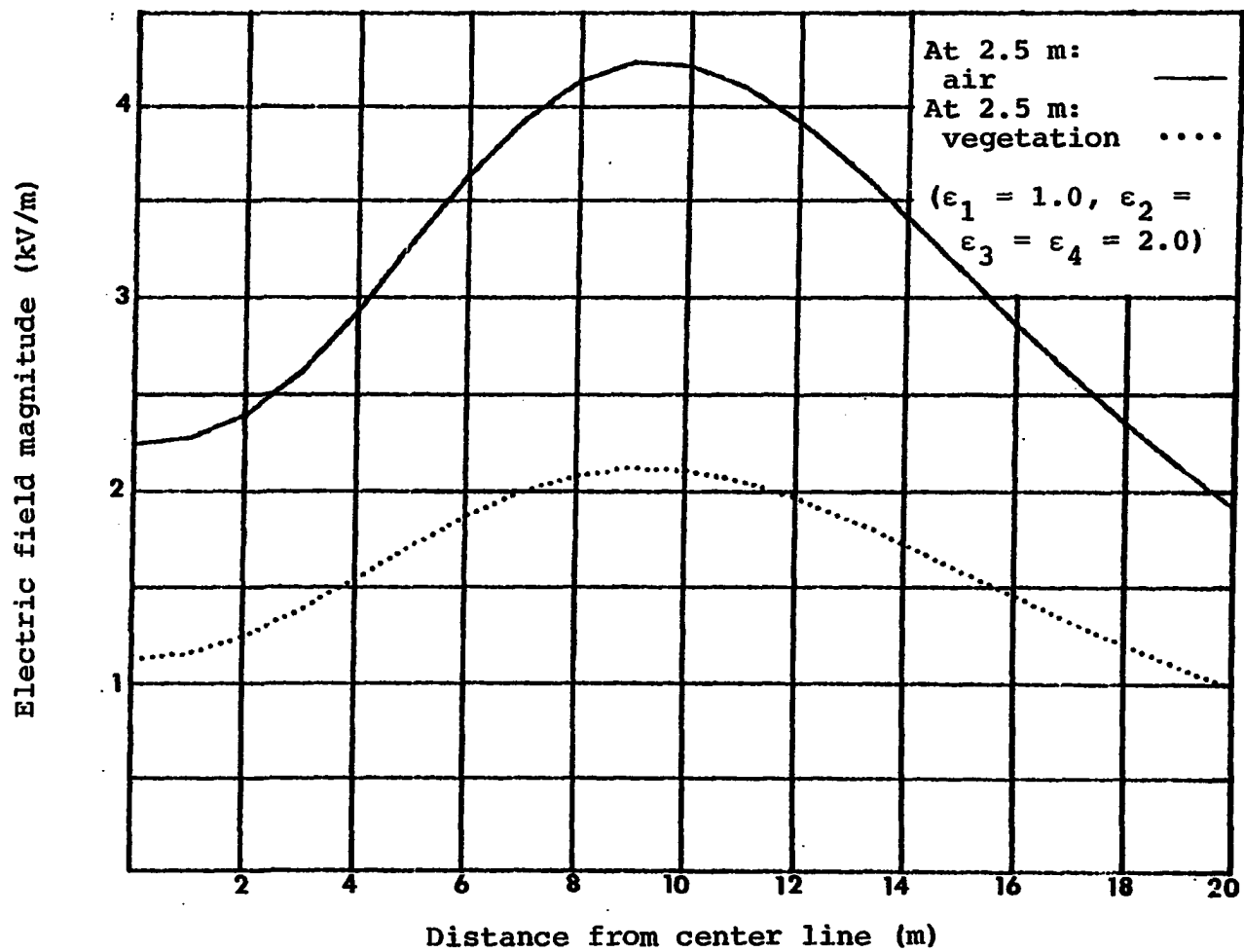
Fig. 5.17. Variation of the electric field magnitude with height above ground (using the five dielectric media as a three media)
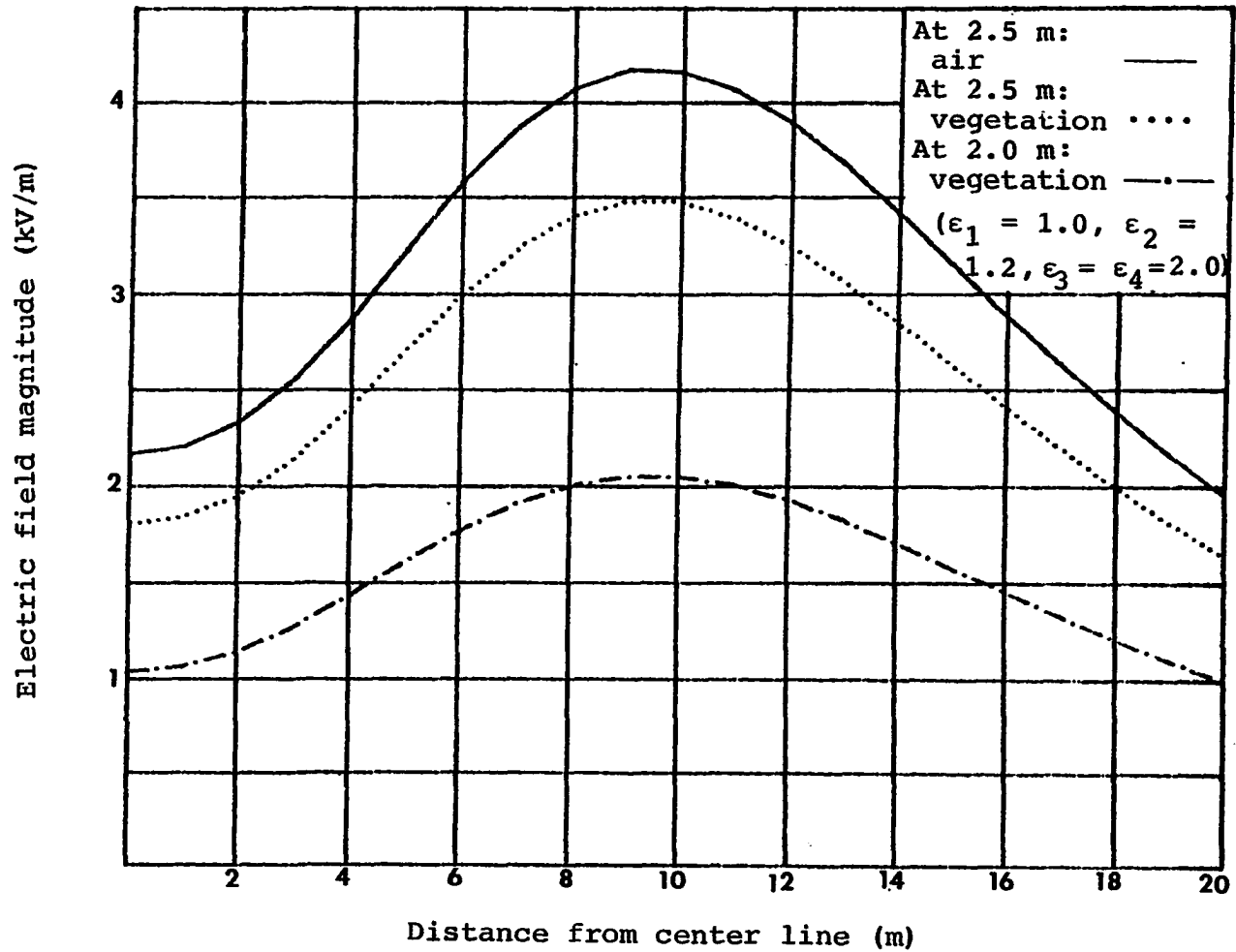
Fig. 5.18. Variation of the electric field magnitude with height above ground (using the five dielectric media as a four media)
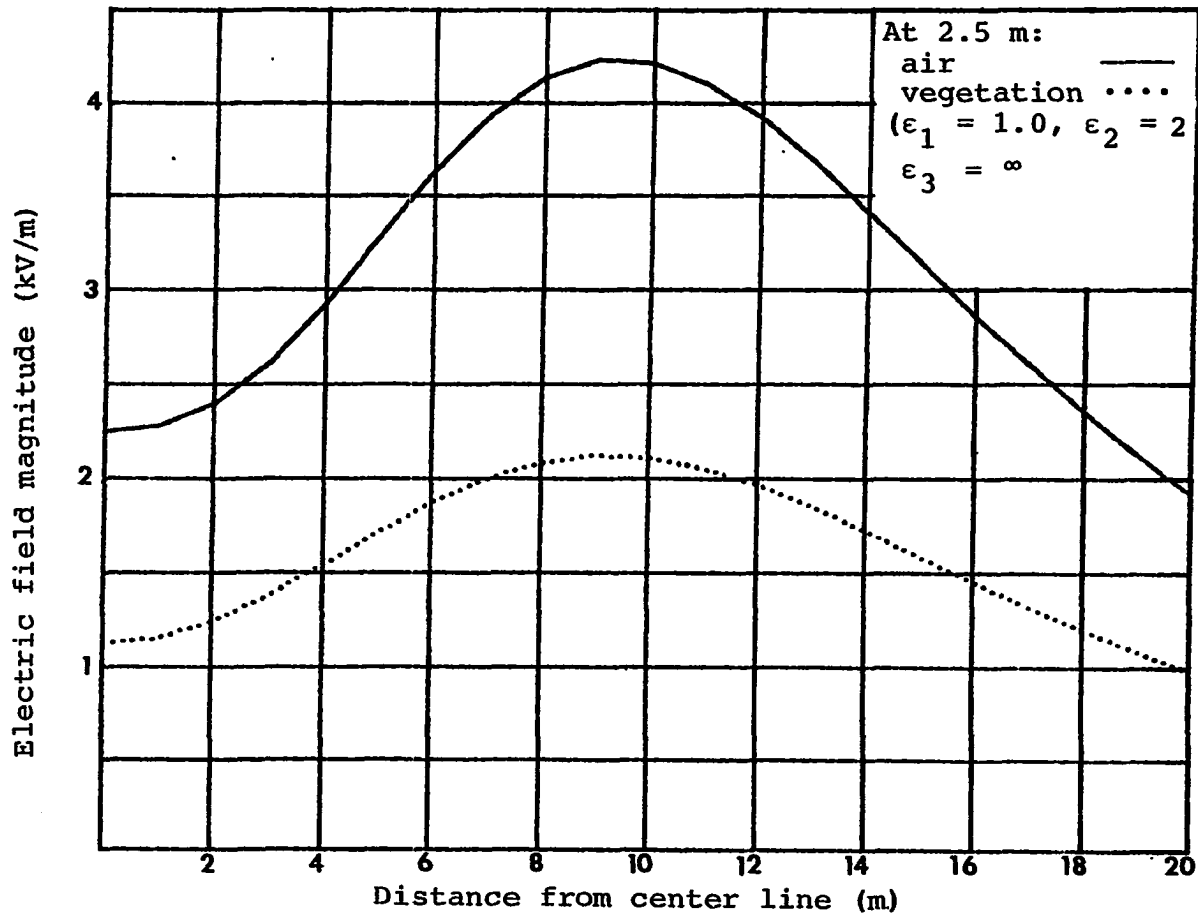
Fig. 5. 19. Variation of the electric field magnitude with height (using the three dielectric media)

Distance from center line (m)
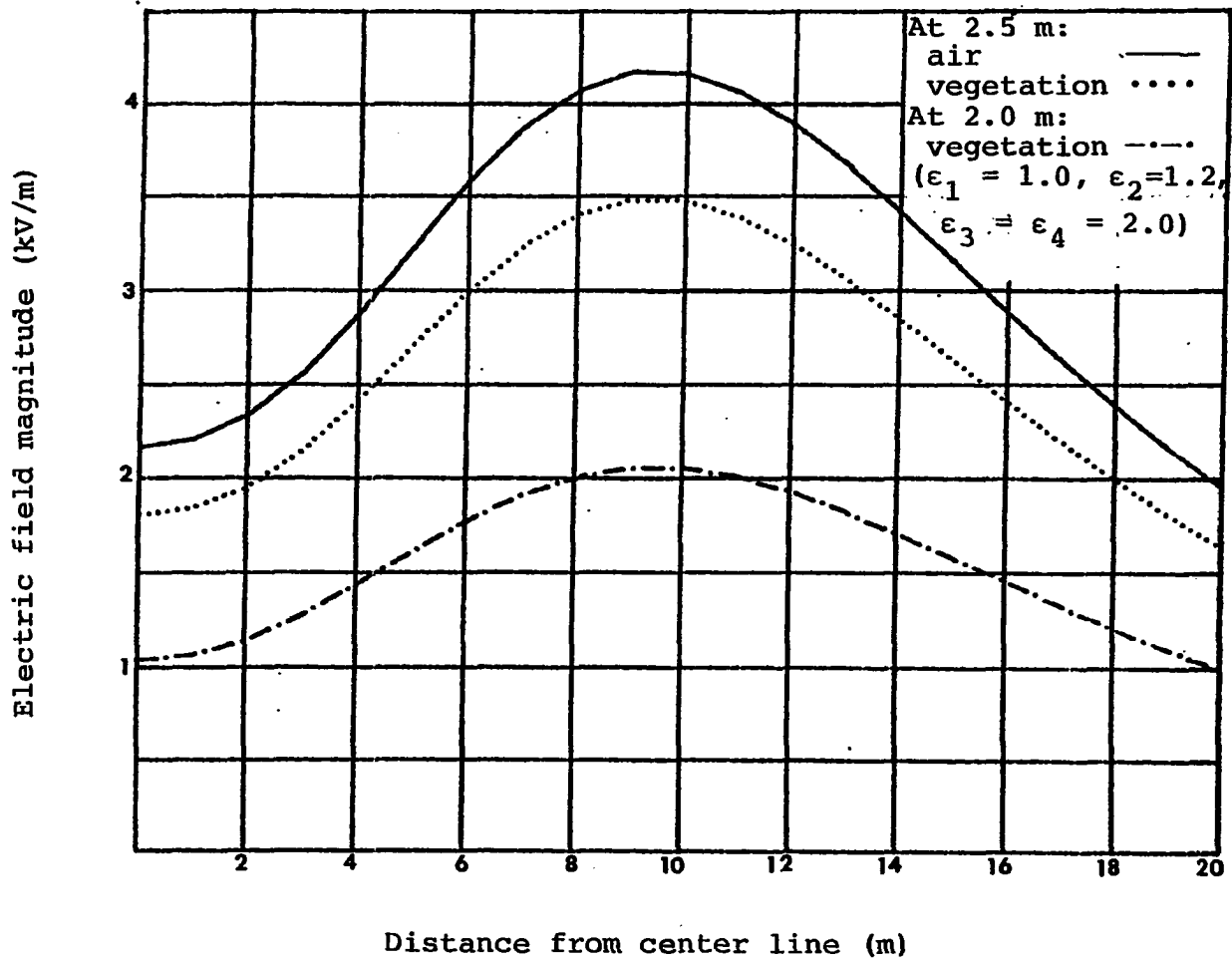
Fig. 5.20. Variation of the electric field magnitude with height (using the four dielectric media)

consistent with the literature even under the two

media case [5, 8].

The discrepancy between the computer generated graph and the measured data can be attributed to many factors. Not the least of these factors is a lack of exact height dimensions of the line that change with system load and environmental conditions. The catenarian shape of the transmission line conductor spans might also have contributed to the errors obtained by an assumption of a perfectly horizontal configuration. The assumption of using the line charges of the two media case for the multilayer dielectric case ignores the fact that the charges may vary under these conditions.

The measured data could also have some errors, because holding the meter steadily at the exact height inside the cornfield was not easy, especially at the 2.0 m height and above. Keeping the position of the meter perpendicular to the line was difficult, too, especially inside the vegetation field.

In spite of these difficulties, the contour of both the calculated and the measured fields does agree. After so many runs of the computer program, the following representation of the cornfield gave a result that fit very closely to the measured data.
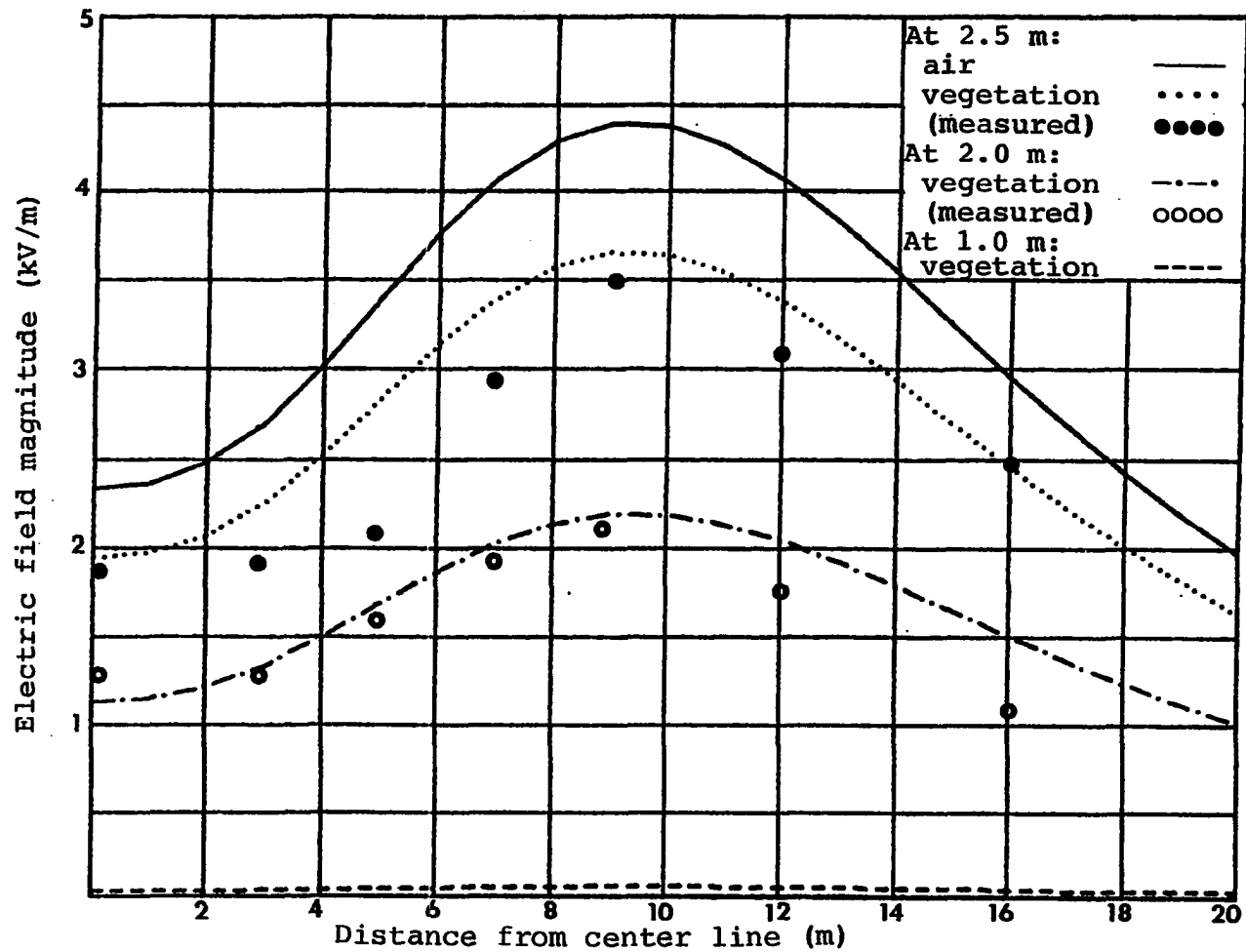
Fig. 5.21. Variation of the electric field magnitude with height inside a cornfield (ε_1=1.0, ε_2=1.2, ε_3=2.0, ε_4=80.0)
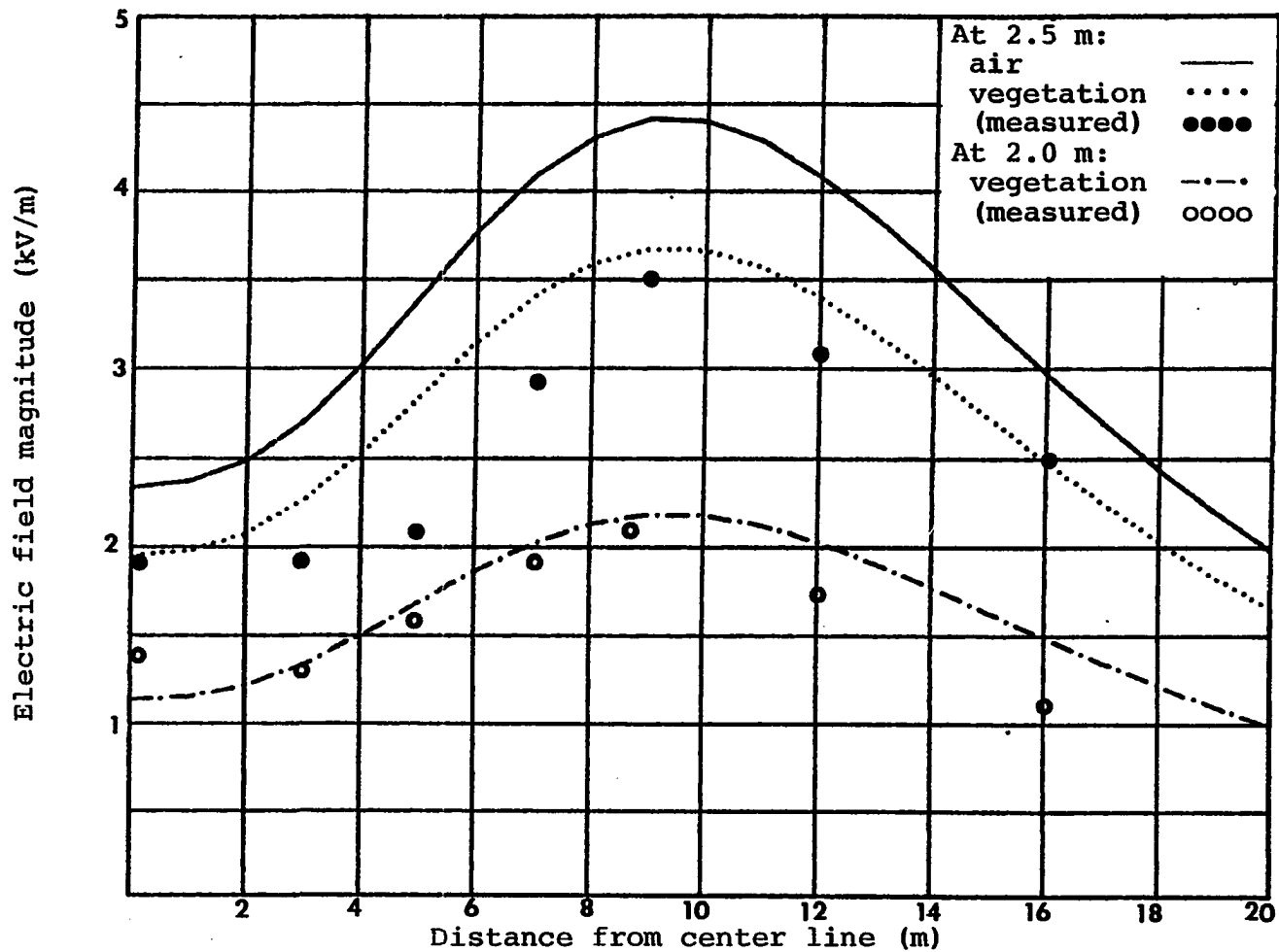
Fig. 5.22. Variation of the electric field magnitude with height inside a cornfield (ε_1=1.0, ε_2=1.2, ε_3=2.0, ε_4=infinity)
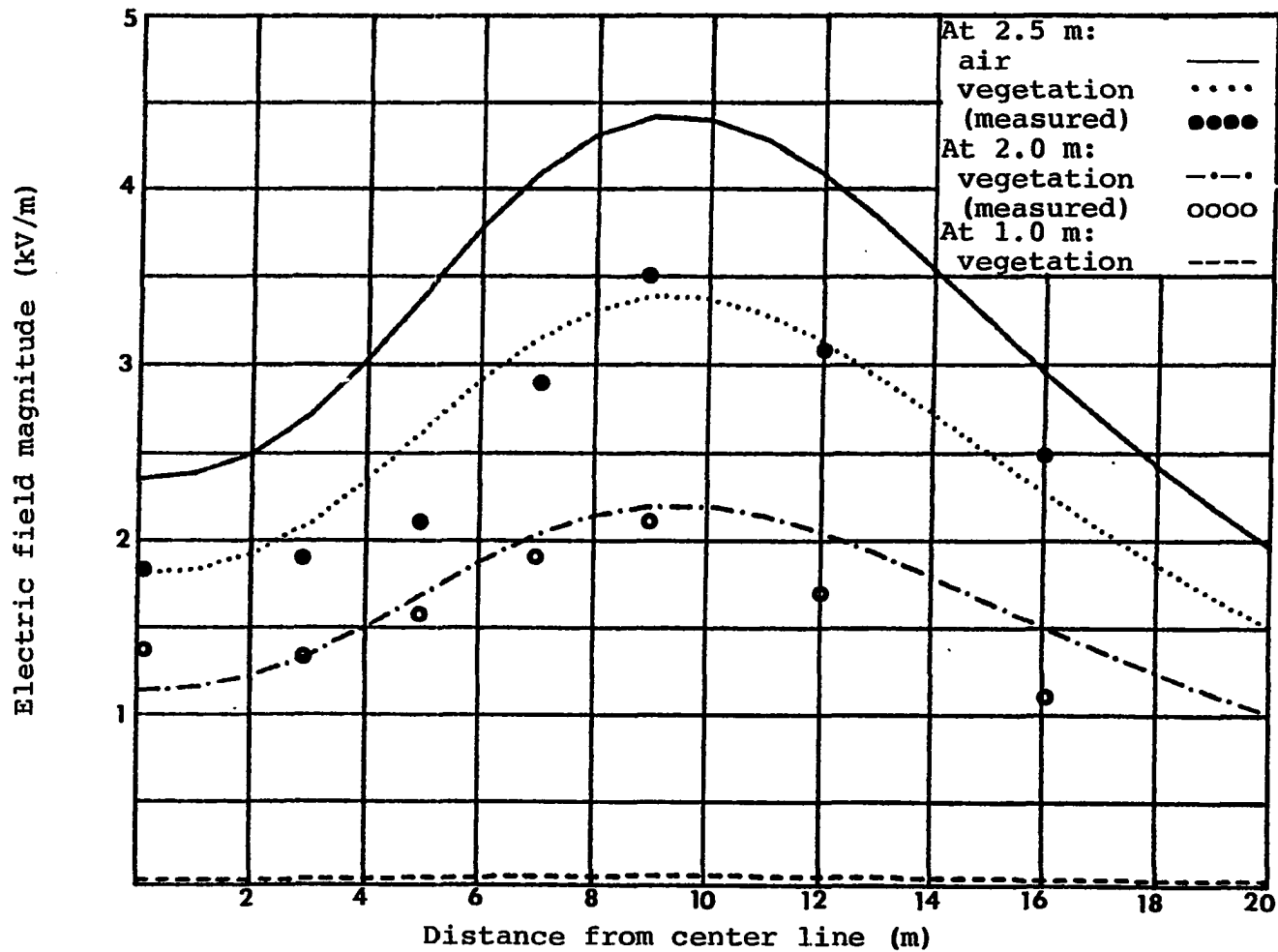
Fig. 5.23. Variation of the electric field magnitude with height inside a cornfield ($\varepsilon_1=1.0$, $\varepsilon_2=1.3$, $\varepsilon_3=2.0$, $\varepsilon_4=80.0$).
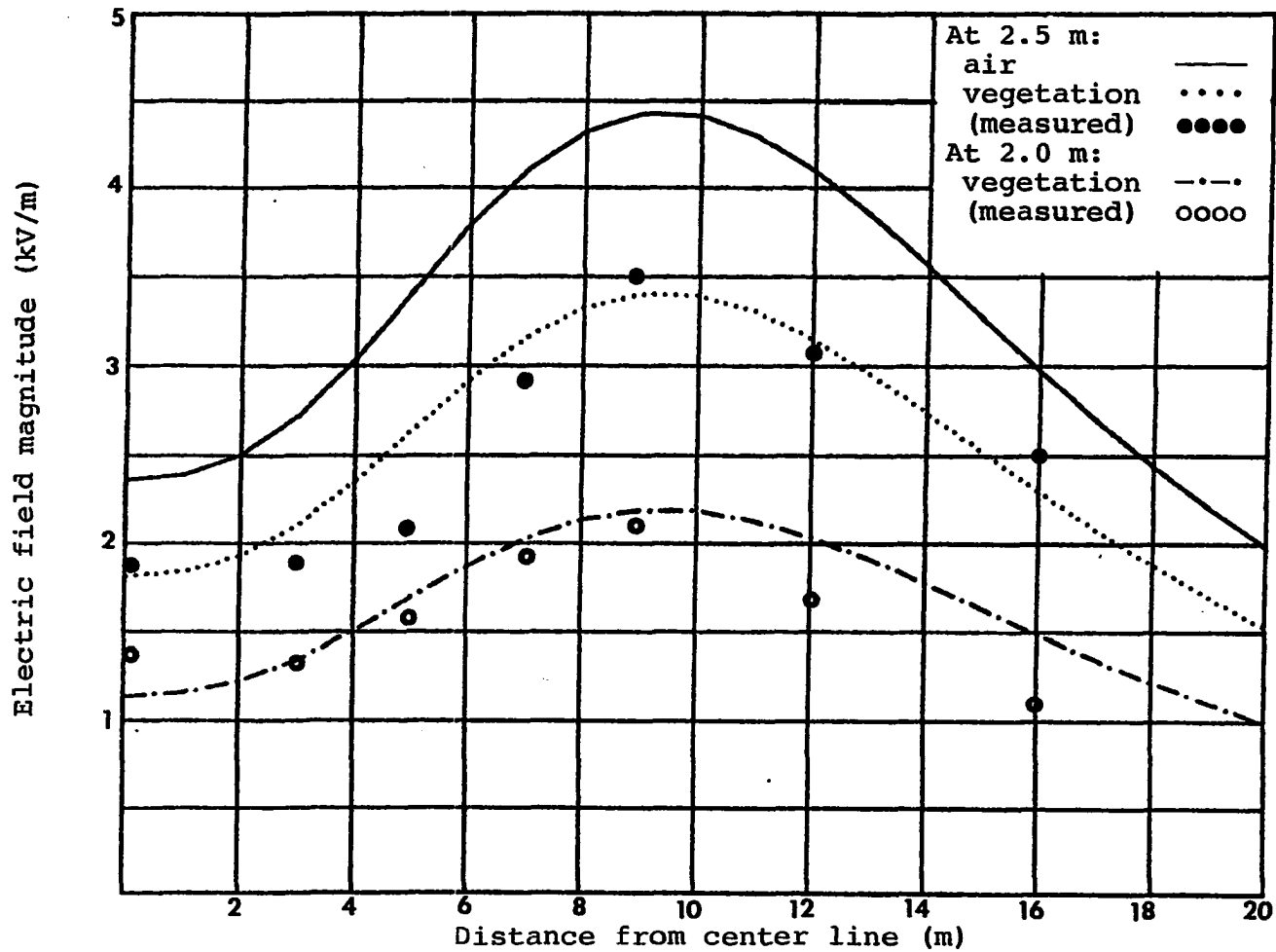
Fig. 5.24. Variation of the electric field magnitude with height inside a cornfield (ε_1=1.0, ε_2=1.3, ε_3=2.0, ε_4=infinity)

1. The top layer, or the outermost dielectric layer should have a thickness of 50 cm and a relative dielectric constant of 1.3.

2. The second layer from the top of the corn surface should have a thickness of 100 cm and a relative dielectric constant of 2.0.

3. The third layer should have a thickness of 100 cm and a relative dielectric equal to 80 or larger.

VI. CONCLUSIONS AND SUMMARY

The solution of the electric field distribution near high voltage lines and in the presence of vegetation medium can be solved by characterization of the electric field in a multilayer dielectric environment. Methods for solving the electric field problem in multilayer dielectrics have been investigated and examined in detail. It was found that the multilayer dielectric problem can be divided into three major models.

The first model was the three dielectric media case. In this three media case, three methods of solution have been presented. The first method is based on image analysis and is analyzed using a step-by-step derivation for the images. This approach was shown to be very lengthy. However, it yielded a better understanding of the image technique and its limitations.

The second method was based on solving Poisson's equations using the separation of variables technique. This approach was used to verify the accuracy of the result of the image technique and to show that both methods yield the same result.

The third method of solution was to develop a digital computer algorithm based on the image technique. This

approach is much easier than the other methods and, with the availability of a digital computer, gives a promising technique to solve problems much more complex.

The second and the third models of the multilayer dielectric problem deal with the extension of the three dielectric media computer algorithm to cover both the four and the five dielectric media. Application of these · algorithms to an arbitrary values of the dielectric constants showed that the tangential electric field component and the normal flux density component boundary conditions are very well-satisfied. The same algorithms are then modified for the line charge case.

All of the above models (three dielectric, four dielectric and five dielectric media) were used to solve for the electric field distribution in the case of the presence of vegetation medium (cornfield) that exists underneath high voltage transmission lines.

The vegetation medium is a very complex media to model due to the large number of variables involved. For this reason, the vegetation medium under high voltage lines was modeled as a multilayer dielectric. These dielectric layers are assumed to be homogenous, isotropic and linear. In the three dielectric model, the vegetation was represented in its simplest form as one single dielectric layer. In the four and the five dielectric models, the vegetation was

represented by two and three dielectric layers respectively, where the air medium and the perfect conductor ground represent the other two media. The value of the dielectric constants of each of the vegetation layers was assumed as an arbitrary value. Using the previously derived models for solving multilayer dielectric, a solution for the above three cases are obtained. The simulation of vegetation by three layers in the five dielectric model resulted in a close agreement with the measured data (corn). The thickness and the dielectric constants of the vegetation three dielectric layers were found to be represented by a top layer of 0.5 m thickness and a dielectric constant equal to 1.3. The second layer from the top has a thickness of 1.0 m and a dielectric constant equal to 2.0. The third layer has a thickness of 1.0 m and a dielectric constant equal to 80.0 or larger. These results indicated that the top layer has a relative dielectric constant close to the air. The second layer has a dielectric constant twice as much as the air. The third layer, or the bottom layer which is in contact with the ground, has the highest dielectric constant and came to be equal to the water dielectric constant.

Analysis of these results show that they are reasonable, since the lower part of the vegetation is dominated by the stems of the corn and, at the same time, is in contact with the ground, away from exposure to the sun,

and is generally rich with moisture. Therefore, the water content will be the highest in this region. The top two layers are mainly dominated by leaves exposed to the sun and wind movement, increasing the chances of water absorption and evaporation. Less water content means lower dielectric constant.

In effect, the presence of vegetation appears to change the electric field distribution near ground and along the height of the plant. Since the electric field has been shown to be drastically reduced in areas of 1 m vegetation height, the actual clearance between the three-phase conductors and the ground will vary. This will result in a change in the line of charges ordinarily used with no vegetation. In the single phase conductor case, the change in height in the presence of vegetation may significantly alter the line charge. However, in the case of three-phase transmission lines the line charges are mainly dominated by the phase separation rather than the height above ground. Therefore, the increase in the line charges caused by the raised virtual ground due to vegetation medium is much less for three phase than for single phase. The increase in the line charges was calculated and found to be 0.6% for the phases a and c, and no change for phase b for the horizontal configuration. These are negligible and justify the assumption of a constant line of charges in the three phase case.

VII. BIBLIOGRAPHY

1. Adams, A. T. and J. R. Mautz. "Computer Solution of Electrostatic Problems by Matrix Inversion." Proceedings of the National Electronic Conference 25 (1969): 198-201.

2. Bhattacharryya, B. "Electromagnetic Induction in a Two-Layer Earth." J. Geophys. Res. 60 (1955): 279-288.

3. Boast, W. B. Vector Fields. New York: Harper and Row, Publishers, 1964.

4. Clements, J. C., R. P. Clayton and A. T. Adams. "A Computation of the Capacitance Matrix for System of Dielectric Coated Cylindrical Conductors." IEEE Transactions EC-25 (1975): 238-248.

5. Cowan, C. D. "Analysis and Sensitivity of Electromagnetic Fields on High Voltage Transmission Lines." Ph.D. dissertation, Iowa State University, Ames, Iowa, 1980.

6. Dawalibi, F. and D. Mukhedkar. "Optimum Design of Substation Grounding in a Two-Layer Earth Structure." Part I, Analytical Study. IEEE Transactions PAS-95 (1975): 252-261.

7. Deno, D. W. "Current Induced in the Human Body by High Voltage Transmission Line Electric Field Measured and Calculation of the Distribution and Doze." IEEE Transactions PAS-96 (1977): 1517-1527.

8. Deno, D. W. and L. E. Zaffanella. "Electrostatic and Electromagnetic Effect of Ulta-High Voltage Transmission Line." Final report. Palo Alto: Electric Power Research Institute (1978).

9. Dey, A. and S. H. Ward. "Inductive Sounding of a Layered Earth with a Horizontal Magnetic Dipole." Geophysics 35 (1970): 660-703.

10. Durand, E. Electrostatique. Paris: Masson, 1966.

11. Electric Power Research Institute. Transmission Line Reference Book, 345 kV and Above. Palo Alto: Electric Power Research Institute, 1979.

12. Evans, H. P. "Two-Dimensional Boundary Value Problem for the Transmission of Alternating Currents through a Semi-Infinite Heterogeneous Conducting Media." Physical Review 36 (1930): 1579-1588.

13. Friedman, Bernard. Principles and Techniques of Applied Mathematics. New York: John Wiley & Sons, Inc., 1956.

14. Giao, T. N. and M. P. Sarma. "Effect of a Two-Layer Earth on the Electric Field Near HVDC Ground Electrode." IEEE Transactions PAS-91 (1972): 2356-2365.

15. Hague, B. Electromagnetic Problems in Electrical Engineering. Oxford, England: Oxford University Press, 1929.

16. Hammond, P. "Electric and Magnetic Images." Proceedings IEE 37 (1960): 250-260.

17. Harrington, R. F. Time Harmonic Electromagnetic Field. New York: McGraw-Hill, Inc., 1961.

18. Ianovici, M. and Y. J. Morf. "Calculation of the Potential Distribution Around a Charge or Current in the Presence of Three Dielectric Media." IEEE Transactions on Electrical Insulation EI-12 (1977): 165-170.

19. Jeans, Sir James. Electricity and Magnetism. Cambridge, England: Cambridge University Press, 1925.

20. Kelvin, Lord. Reprint of Papers on Electrostatic and Magnetism. New York: Macmillan Publishing Company, Inc., 1972.

21. Koefoed, O., D. P. Gosh and G. J. Polman. "Computation of Type Curves for Electromagnetic Depth Sounding with a Horizontal Transmitting Coil by Means of a Digital Linear Filter." Geophys. Prospect. 20 (2973): 406-420.

22. Mahmoud, A. A. EE 641 Class Notes. Iowa State University, 1979.

23. Maxwell, J. C. Treatise on Electricity and Magnetism. Vol. I, 3rd edition. Oxford, England: Clarendon Press, 1904.

24. Mullineux, N. and J. R. Reed. "Image of Line Charge and Currents." Proceedings IEE 3 (1964): 1343-1346.

25. Parekh, H. J. "Computation of Electrical Field for EHV and UHV Transmission Line." Ph.D. dissertation, Iowa State University, Ames, Iowa, 1974.

26. Ramo, S., J. R. Whinnery and T. Duzzer. Field and Waves in Communication Electronics. New York: John Wiley & Sons, Inc., 1965.

27. Raodh, J. R., V. L. Charitia and F. M. Dietrich. "Experimental Oxident Production Rates for EHV Transmission Line and Theoretical Estimates of Ozone Near Operating Line." IEEE Transactions PAS-93 (1974): 647-657.

28. Ryu, J., H. F. Morrison and S. H. Ward. "Electromagnetic Fields about a Loop Source of Current." Geophys. 38 (1973): 894-919.

29. Scheren, H. M., B. J. Ware and C. H. Shih. "Gaseous Effluents Due to EHV Transmission Line Corona." IEEE Transactions PAS-93 (1973): 1043-1049.

30. Schneiber, K. H. "Displacement Current to the Human Body by Dielectric Field Under Overhead Transmission Line." Int. Conf. Proc. Large High Voltage Electrical Systems, CIGRE, 25th Session, II (August 1974): 36-40.

31. Searle, G. F. C. "On the Magnetic Field Due to a Current in a Wire Placed Parallel to the Axis of a Cylinder of Iron." The Electrician (Jan. 28, 1898): 453-510.

32. Shun, D. H. and S. Y. King. "Solution of Field Problems in Composite Media." F.I.E. Institute of Engineering, Sydney, Australia, 1978.

33. Silvester, P. "Tem Wave Properties of Microstrip Transmission Line." Proceedings IEE 115 (1968): 43-48.

34. Smyth, W. R. Static and Dynamic Electricity. New York: McGraw-Hill, Inc., 1950.

35. Spiegel, M. R. Mathematical Handbook of Formulas and Tables. New York: McGraw-Hill, Inc., 1968.

36. Takashima, T. and R. Ishibashi. "Electric Field in Dielectric Multilayers Calculated by Digital Computer." IEEE Transactions on Electrical Insulation EI-13 (1978): 37-44.

37. Takashima, T. and R. Ishibashi. "Expression of Electric Fields for Systems of Dielectric Coated Cylindrical Conductors." IEEE Transactions PAS-97 (1978): 1847-1852.

38. Torre, E. D. and C. V. Long. The Electromagnetic Field. Boston: Allyn and Bacon, Inc., 1969.

39. Wait, J. R. Electromagnetic Waves in Stratified Media. New York: Macmillan Publishing Company, Inc., 1969.

40. Weber, E. Electromagnetic Field. New York: John Wiley & Sons, Inc., 1965.

41. Weinberger, H. F. A First Course in Partial Differential Equations. New York: John Wiley & Sons, Inc. 1965.

VIII. ACKNOWLEDGMENTS

The author wishes to express his sincere appreciation to Dr. Aly A. Mahmoud and Dr. Robert E. Post for their special encouragement and guidance during the work leading to this thesis. During the research period, Dr. Mahmoud and Dr. Post have continuously encouraged me at time of trouble and also directed me to various articles which helped expand my understanding of the subject. My thanks also are extended to Dr. Charles D. Cowan for his valuable discussion in using and checking the image method in the three media case.

The author also wishes to thank Dr. K. C. Kruempel, Dr. R. J. Lambert and Dr. J. D. Musil who provided helpful comments and useful advice during his graduate work, and to Ms. Gretchen Triplett for typing the manuscript.

Acknowledgment must also be made to the Iowa Test and Evaluation Facility for measurement on an active EHV circuit.

Special thanks are also due to the author's wife, Shafika, for her understanding, patience and encouragement, without which this work would not have been possible, and to the author's son, Akrum, who was born during this work.

IX. APPENDIX A: DERIVATION OF THE INFINITE SERIES SOLUTION FROM THE INTEGRALS SOLUTION

The integral expressions of the potential Eqs. 3.63-3.65 can be written in infinite series forms as follows:

$$\Phi^{(1)}(\rho,z) = \frac{Q}{4\pi\epsilon}\left\{\int_0^\infty\left[e^{-m|z|} + \frac{(\alpha_{12}e^{-2mh} + \alpha_{23}e^{-2m(h+b)})}{1 + \alpha_{12}\alpha_{23}e^{-2mb}}e^{mz}\right]J_0(\rho m)\,dm\right\} \quad (3.63)$$

$$\Phi^{(2)}(\rho,z) = \frac{Q(1-\alpha_{12})}{4\pi\epsilon_2}\left\{\int_0^\infty\left[\frac{e^{-mz}+\alpha_{23}e^{-2m(h+b)}e^{mz}}{1 + \alpha_{12}\alpha_{23}e^{-2mb}}\right]J_0(\rho m)\,dm\right\} \quad (3.64)$$

and

$$\Phi^{(3)}(\rho,z) = \frac{Q(1-\alpha_{12})(1-\alpha_{23})}{4\pi\epsilon_3}\left\{\int_0^\infty\frac{e^{-mz}}{1 + \alpha_{12}\alpha_{23}e^{-2mb}}\right\}J_0(\rho m)\,dm \quad (3.65)$$

Equations 3.63-3.65 have a common denominator under the integral sign $(1+\alpha_{12}\alpha_{23}e^{-2mb})$. Let us write this term in the numerator as $(1+\alpha_{12}\alpha_{23}e^{-2mb})^{-1}$ and then expand it using the binomial theorem.

$$(1+\alpha_{12}\alpha_{23}e^{-2mb})^{-1} = 1-\alpha_{12}\alpha_{23}e^{-2mb} + (\alpha_{12}\alpha_{23})^2 e^{-4mb} - (\alpha_{12}\alpha_{23})^3 e^{-6mb} + \cdots \quad (A.1)$$

Substitute Eq. A.1 into Eqs. 3.63-3.65 and manipulate the terms.

$$\Phi^{(1)}(\rho,z) = \frac{Q}{4\pi\epsilon_1} \left\{ \int_0^\infty e^{-m|z|} J_0(\rho m)\, dm + \int_0^\infty (\alpha_{12}e^{-2mh} + \right.$$
$$\alpha_{23}e^{-2m(h+b)})e^{mz} \cdot (1-\alpha_{12}\alpha_{23}e^{-2mb} + (\alpha_{12}\alpha_{23})^2$$
$$\left. e^{-4mb}\cdots) \cdot J_0(\rho m)\, dm \right\} \tag{A.2}$$

$$\Phi^{(2)}(\rho,z) = \frac{Q(1-\alpha_{12})}{4\pi\epsilon_2} \left\{ \int_0^\infty (e^{-mz}+\alpha_{23}e^{-2m(h+b)}e^{mz}) \right.$$
$$\left. (1-\alpha_{12}\alpha_{23}e^{-2mb} + (\alpha_{12}\alpha_{23})^2 e^{-4mb}\cdots) J_0(\rho m)\, dm \right\} \tag{A.3}$$

and

$$\Phi^{(3)}(\rho,z) = \frac{Q(1-\alpha_{12})(1-\alpha_{23})}{4\pi\epsilon_3} \left\{ \int_0^\infty e^{-mz} (1-\alpha_{12}\alpha_{23}e^{-2mb} + \right.$$
$$\left. (\alpha_{12}\alpha_{23})^2 e^{-4mb}\cdots) J_0(\rho m)\, dm \right\} \tag{A.4}$$

Equations A.2-A.4 can be simplified as follows. Let us begin with Eq. A.2.

Multiply the two brackets underneath the second infinite integral together and collect equal exponential terms together. Equation A.2 then becomes

$$\Phi^{(1)}(\rho,z) = \frac{Q}{4\pi\epsilon_1} \left\{ \int_0^\infty e^{-m|z|} J_0(\ m)\, dm + \int_0^\infty \alpha_{12}\, e^{-m(2h-z)} \right.$$

$$J_0 (\rho m) \, dm + \int_0^\infty \alpha_{23} (1-\alpha_{12}^2) \, e^{-m(2h-z+2b)} J_0 (\rho m) \, dm$$

$$- \int_0^\infty \alpha_{23}^2 \alpha_{12} (1-\alpha_{12}^2) e^{-m(2h-z+4b)} J_0 (\rho m) \, dm + \int_0^\infty \alpha_{23}^3$$

$$\alpha_{12}^2 (1-\alpha_{12}^2) \, e^{-m(2h-z+6b)} J_0 (\rho m) \, dm \cdots \qquad \text{(A.5)}$$

In order to compare Eq. A.5 to Eq. 3.17, two more steps must be completed.

1. The derivation of Eqs. 3.63-3.65 was based on the coordinate shown in Fig. 3.10., while the derivations of Eqs. 3.17, 3.23 and 3.27 were based on the coordinate shown in Fig. 3.3. Figure 3.10. and Figure 3.3 were repeated for convenience. Thus, a transformation must be done for the z coordinate.

2. As the first step is completed, then the definition of the definite integral involving Bessel's function must be used.

The transformation between Fig. 3.10 and Fig. 3.3 is

$$z' = -z+h \qquad \text{(A.6)}$$

where z' is the z coordinate of Fig. 3.3.

Substituting Eq. A.6 into Eq. A.5, we have

$$\Phi^{(1)} (\rho, z') = \frac{Q}{4\pi\varepsilon_1} \left\{ \int_0^\infty e^{-m(z'-h)} J_0 (\rho m) \, dm + \alpha_{12} \int_0^\infty e^{-m(z'+h)} \right.$$

$$J_0 (\rho m) \, dm + \alpha_{23} (1-\alpha_{12}^2) \int_0^\infty e^{-m(z'+h+2b)} J_0 (\rho m) \, dm$$

$$- \alpha_{23}^2 \alpha_{12} (1-\alpha_{12}^2) \int_0^\infty e^{-m(z'+h+4b)} J_0(\rho m) \, dm \cdots \quad (A.7)$$

And, from the definition of definite integral involving Bessel function we have

$$\int_0^\infty e^{-ax} J_0(bx) \, dx = \frac{1}{\sqrt{a^2+b^2}} \quad (A.8)$$

Substitute Eq. A.8 into Eq. A.7 and it becomes

$$\Phi^{(1)}(\rho,z) = \frac{Q}{4\pi\epsilon_1} \left[\frac{1}{\sqrt{\rho^2+(z'-h)^2}} + \alpha_{12} \frac{1}{\sqrt{\rho^2+(z'+h)^2}} \right.$$

$$+ \alpha_{23}(1-\alpha_{12}^2) \frac{1}{\sqrt{\rho^2+(z'+h+2b)^2}} - \alpha_{23}^2 \alpha_{12}(1-\alpha_{12}^2)$$

$$\left. \frac{1}{\sqrt{\rho^2+(z'+h+4b)^2}} \cdots \right] \quad (A.9)$$

Equation A.9 can be written in a more compact form as shown:

$$\Phi^{(1)}(\rho,z) = \frac{Q}{4\pi\epsilon_1} \left[\frac{1}{\sqrt{\rho^2+(z'-h)^2}} + \alpha_{12} \frac{1}{\sqrt{\rho^2+(z'+h)^2}} + \right.$$

$$(1-\alpha_{12}^2) \sum_{n=1}^\infty (\alpha_{23})^n (-\alpha_{12})^{n-1}$$

$$\left. \frac{1}{\sqrt{\rho^2+(z'+h+2nb)^2}} \right] \quad (A.10)$$

Equation A.10 is exactly the same as Eq. 3.17.

Following the same procedure, we would be able to prove that Eqs. 3.64 and 3.65 are exactly the same as Eqs. 3.23 and 3.27.
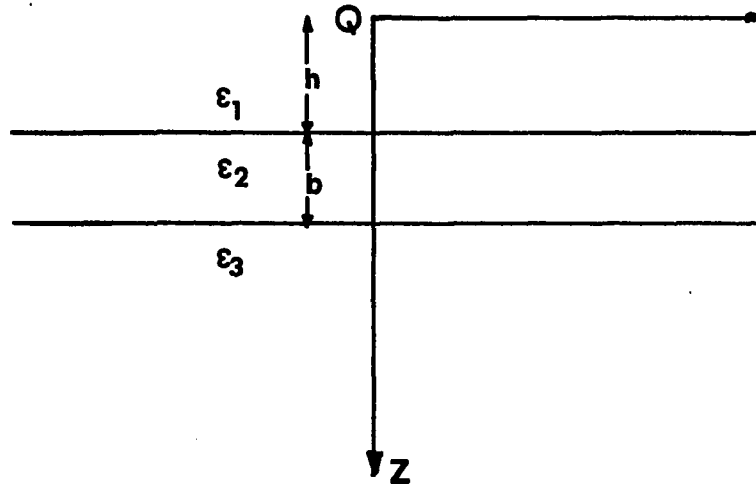
Fig. 3.10. Point charge at the origin of a cylindrical coordinate in three dielectric media
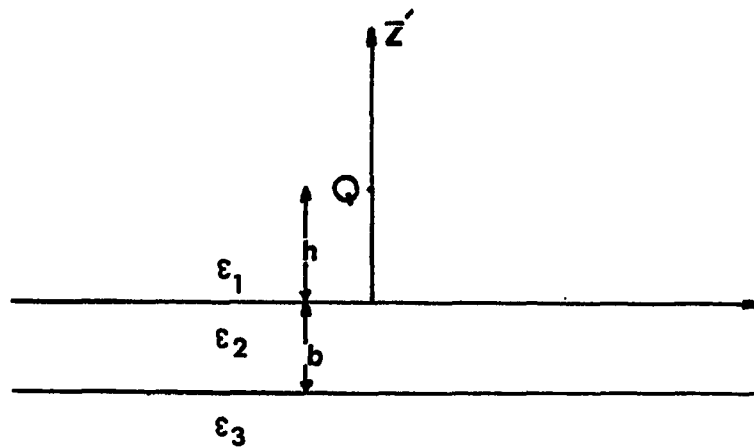
Fig. 3.3. Point charge in three dielectric media

X. APPENDIX B: APPLICATION OF THE IMAGE METHOD
IN THE COMPLEX MEDIA CASE

The method of images is not restricted by any means to the case of multilayer dielectric. A general equation will be derived in case of complex media where the source is an alternating current and the medium has both a conductivity and dielectric constant.

A. Alternating Current Point Source

Let an alternating current point source $I = I_0 \exp(jwt)$ be located in a homogenous medium with conductivity σ and permittivity ϵ, as shown in Fig. B.1. The current supplied from the source flows into the surrounding medium. Now consider the field due to this current source. Let J be the current density at any point p, and let s be the surface area of a sphere with the center at 0 and of radius r. Using Gauss's Law, we obtain

$$I = \iint J \cdot ds = 4\pi r^2 J \cdot a_r \tag{B.1}$$

which results in

$$J = \frac{I}{4\pi r^2} a_r = J a_r \tag{B.2}$$

where a_r is a unit vector in the r direction. On the other hand, suppose that the electric field intensity is given by

$$E = E_0 \exp(jwt) a_r \tag{B.3}$$

Using Maxwell's equations,

$$J = \sigma E + \varepsilon \frac{\partial E}{\partial t}$$

$$J = (\sigma + jw\varepsilon)E \qquad (B.4)$$
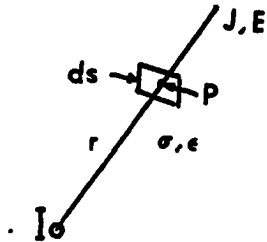
Fig. B.1.

Using Eqs. B.2 and B.4 to get

$$E = \frac{I}{4\pi r^2 (\sigma + jw\varepsilon)} a_r \qquad (B.5)$$

The electric potential can be found at any point p from

$$\Phi(p) = - \int_{\infty}^{r} E \, dr = \frac{I}{4\pi (\sigma + jw\varepsilon) r} \qquad (B.6)$$

If we let a point charge $q = q_0 \exp(jwt)$, then the current source I is related by the following equation

$$I = \frac{dq}{dt} = jwq \qquad (B.7)$$

Substituting Eq. B.7 into Eq. B.6, and letting $\sigma = 0$, we obtain

$$\Phi(p) = \frac{q}{4\pi\varepsilon r} \qquad (B.8)$$

Equation B.8 represents the electrostatic field due to a point charge q in a dielectric medium. Therefore, the electrostatic field due to a point charge can be considered

as a special case of a complex field due to an alternating current point source when $\sigma = 0$.

The above discussion shows that in this case, there exists dual relationships between the complex field and the electrostatic field, as shown in the table below.

Table B.1. Dual quantities' relationships between the complex field and the electrostatic field

Electrostatic	q	ε	$D = \varepsilon E$
Complex field	I	$\sigma + jw\varepsilon$	$J = (\sigma + jw\varepsilon)E$

B. A Current Point Source in Front of a Plane Boundary

Let an alternating current point source I be located at x=h, as shown in Fig. B.2. To solve this problem, we shall apply the image technique. The potential at point p_1 in the region of ε_1, σ_1 can be expressed as shown.

$$\Phi^{(1)}(p_1) = \frac{1}{4\pi(\sigma_1+jw\varepsilon_1)} \left(\frac{I}{R} + \frac{I'}{R'}\right) \tag{B.9}$$

and the potential in medium II at point p_2 can be expressed as

$$\Phi^{(2)}(p_2) = \frac{1}{4\pi(\sigma_2+jw\varepsilon_2)} \frac{I''}{R''} \tag{B.10}$$

At the boundary interface x=0, the following boundary conditions must hold:

$$\Phi^{(1)}(0,y) = \Phi^{(2)}(0,y) \tag{B.11}$$

and
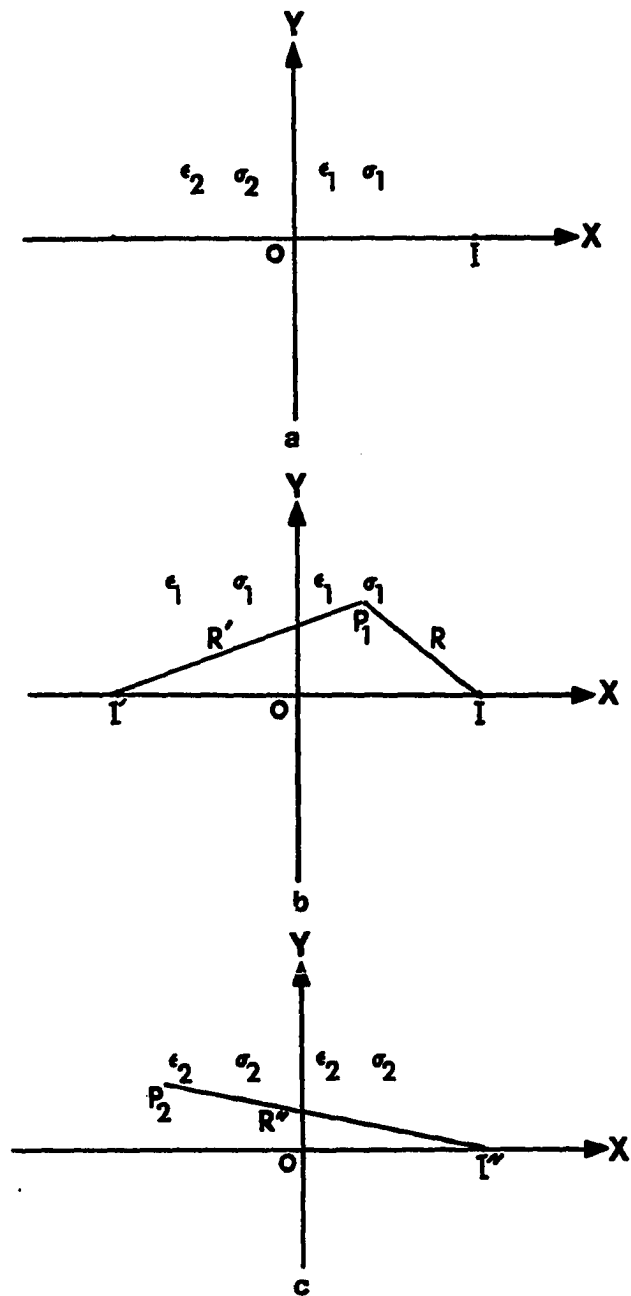
Fig. B.2. A current point source in front of a plane
          boundary

a) Original problem
b) Model for region I calculation
c) Model for region II calculation

$$J_x^{(1)} = J_x^{(2)} \tag{B.12}$$

where

$$J_x^{(1)} = -(\sigma_1+jw\epsilon_1) \frac{\partial\phi^{(1)}}{\partial x}(0,y) \tag{B.13}$$

$$J_x^{(2)} = -(\sigma_2+jw\epsilon_2) \frac{\partial\phi^{(2)}}{\partial x}(0,y) \tag{B.14}$$

Substituting Eqs. B.11-B.14 into Eqs. B.9 and B.10, we get the following:

$$I' = \frac{(\sigma_1+jw\epsilon_1) - (\sigma_2+jw\epsilon_2)}{(\sigma_1+jw\epsilon_1) + (\sigma_2+jw\epsilon_2)} I \tag{B.15}$$

and

$$I'' = \frac{2(\sigma_2+jw\epsilon_2)}{(\sigma_1+jw\epsilon_1) + (\sigma_2+jw\epsilon_2)} \tag{B.16}$$

Comparison of these results with the expressions of the electrostatic field due to point charge that has been discussed in this work again shows dual relationships. Equations B.15 and B.16 give the equivalent images of the source current I necessary to determine the field in both regions. By using this two media analysis as a background, extension to multilayers complex media can be done similarly.

XI. APPENDIX C: COMPUTER PROGRAMS

The computer programs used in this thesis are divided
into the following:

1. Point charge.

2. Three-phase transmission line.

Two programs are written for the point charge case. The
first one deals with the four dielectric media and the second
program is an extension to cover the five dielectric media
case. Each program is divided into two parts: the main
program, where all the parameters must be read such as the
magnitude of the charge, the location of the charge, the
thickness of each dielectric medium, and the different
permittivities characterizing the dielectric media. Once
these parameters are known, the magnitudes and the locations
of all the images are then determined. The potential and the
field equations of each medium that are written as subroutines
are then called by the main program in steps. The first two
subroutines to be called are medium I and medium II, followed
by medium II and medium III. In each case, the boundary
conditions were checked to determine how close they were.
Otherwise, more images were generated and the process was
repeated. The same idea applies to the five dielectric media
program.

The same idea applies to the five dielectric media program. In the three-phase transmission line case, four programs are written: two media, three media, four media and five media.

The two media program was developed to determine the line charges for the three-phase transmission line using the potential coefficients matrix. Each phase has a number of subconductors (NS) of the bundle type. The general method of charge computation was used as discussed in Chapter V, where each phase will be represented by a single line of charge located at the center of an equivalent conductor of radius (RE). This equivalent radius is a function of the bundle spacing (BS), the subconductor diameter (SD) and the number of subconductors. Once the potential coefficients matrix is determined (P), then the axial line charges can be determined from the relation [P] [q] = [v[, where [q] is a column vector that contains the three phase line charges and [V] is a column vector that contains the three-phase voltages. A subroutine CLINEQ installed on VAX B is called to solve for [q]. Once the line charges are determined, they will be assumed as a constant in the multilayer dielectric case.

The three, the four and the five dielectric media programs are constructed similarly to the idea of the point charge that was discussed earlier.

Table C.1.   The four dielectric media program

```
C        THIS IS THE FOUR DIELECTRIC MEDIA PROGRAM FOR THE POINT
C        CHARGE CASE.
C        THE IMAGES AND THEIR POSITIONS WILL BE DETERMINED IN ADVANCE.
C        THEN, THE MAIN PROGRAM WILL CALL THE DIFFERENT SUBROUTINES.
C        IF FLAG=1, THEN REGIONS (1) AND (2) BOUNDARY CONDITIONS
C        WILL BE CALCULATED.
C        IF FLAG=2, THEN REGIONS (2) AND (3) BOUNDARY CONDITIONS
C        WILL BE CALCULATED.
C
C        ......................................................
         common a,b,c,h,fk1,NP
         common Q1,L1,Q2,L2,Q3,L3,Q4,L4,Q5,L5,Q,NI,NII
         real q1(4001),I1(4001),q2(4001),I2(4001),q3(4001)
              REAL L3(4001),q4(2000),I4(2000),q5(2000),I5(2000)
         REAL DN1(10),EN1(10),ET1(10),EM1(10),V1(10)
         REAL DN2(10),EN2(10),ET2(10),EM2(10),V2(10)
         REAL DN3(10),EN3(10),ET3(10),EM3(10),V3(10)
C        ......................................................

         read(5,*)e0,e1,e2,e3,a,b,c,H,NP,NI,FLAG
         read(5,*)q
C        ......................................................
         alphi2=(e1-e2)/(e1+e2)
         alph23=(e2-e3)/(e2+e3)
         bet12=2.*e2/(e2+e1)
         bet21=2.*e1/(e1+e2)
         bet23=2.*e3/(e2+e3)
         bet32=2.*e2/(e2+e3)
C        ......................................................
         pi=3.14160
         NII=2*NI
         fk1=1.0/(4.*e0*pi)
         q1(1)=bet12*q
         I1(1)=a
         q0=alph12*q
         j=1
         i=1
41       CONTINUE
         k=j+1
         m=2*j
         q2(i)=alph23*q1(J)
         q3(i)=bet23*q1(J)
         q1(k)=-alph12*q2(J)
         q5(J)=bet21*q2(J)
         q4(J)=-q3(J)
         q3(m)=-alph23*q4(J)
         q2(m)=bet32*q4(J)
         I2(i)=I1(J)+b
         I3(i)=I1(J)+b
         I1(k)=I2(J)+b
         I5(J)=I2(J)+b
```

Table C.1.   Continued

```
        I4(J)=I3(J)+c
        I3(m)=I4(J)+c
        I2(m)=I4(J)+c
        IF(J.EQ.NI)GO TO 50
        J=J+1
        I=I+2
        GO TO 41
50      CONTINUE
C       .................................................................
        IF(FLAG.NE.1)GO TO 69
        call field1(e1,Q0,FLAG,DN1,ET1,EM1,V1)
        PRINT*,' '
        PRINT*,' '
        WRITE(6,53)
53      FORMAT('0',10X,'   DN1  ',5X,'    ET1',5X,'    EM1',5X,'    V1')
        DO 101 I=1,NP
        PRINT*,' '
        WRITE(6,55),DN1(I),ET1(I),EM1(I),V1(I)
55      FORMAT('0',10X,F8.4,5X,F8.4,5X,F8.4,5X,F8.4)
101     CONTINUE
        call field2(E2,FLAG,DN2,ET2,EM2,V2)
        PRINT*,' '
        PRINT*,' '
        WRITE(6,60)
60      FORMAT('0',10X,'   DN2  ',5X,'    ET2',5X,'    EM2',5X,'    V2')
        DO 102 I=1,NP
        PRINT*,' '
        WRITE(6,55)DN2(I),ET2(I),EM2(I),V2(I)
102     CONTINUE
        GO TO 999
69      CALL FIELD2(E2,FLAG,DN2,ET2,EM2,V2)
        PRINT*,' '
        PRINT*,' '
        WRITE(6,60)
        DO 110 I=1,NP
        PRINT*,' '
        WRITE(6,55)DN2(I),ET2(I),EM2(I),V2(I)
110     CONTINUE
        CALL FIELD3(E3,FLAG,DN3,ET3,EM3,V3)
        PRINT*,' '
        PRINT*,' '
        WRITE(6,77)
77      FORMAT('0',10X,'   DN3  ',5X,'    ET3',5X,'    EM3',5X,'    V3')
        DO 120 I=1,NP
        PRINT*,' '
        WRITE(6,55)DN3(I),ET3(I),EM3(I),V3(I)
120     CONTINUE
999     CONTINUE
        stop
        end
```

Table C.1. Continued

```
C      ........................................................
C          THIS IS REGION (1) SUBROUTINE
C
       subroutine field1(e1,Q0,FLAG,DN1,ET1,EM1,V1)
       common a,b,c,h,fk1,NP
       common q1,L1,Q2,L2,Q3,L3,Q4,L4,Q5,L5,Q,NI,NII
       real q5(2000),I5(2000),q1(4001),I1(4001),q2(4001)
            REAL L2(4001),q3(4001),I3(4001),q4(2000),I4(2000)
       REAL DN1(10),ET1(10),EN1(10),EM1(10),V1(10)
       IF(FLAG.EQ.1)X=B+C
       DNT1=0.0
       ETT1=0.0
       VT1=0.0
       DO 25 IP=1,NP
       Y=(IP-1)/100.0
       DO 27 J=1,NI
       if(j.ne.1)go to 10
       T1=((x-h)*(x-h)+y*y)
       A5=SQRT(T1)
       A55=1.0/A5
       A1=T1**(3/2.)
       a11=(x-h)/a1
       b11=y/a1
        T2=((x-h+2*a)*(x-h+2*a)+y*y)
       A6=SQRT(T2)
       A66=1.0/A6
       A2=T2**(3/2.)
       a22=(x-h+2*a)/a2
       b22=y/a2
       dnt1=dnt1+(a11*q+q0*a22)*fk1
       ett1=ett1+(b11*q+b22*q0)*fk1
       VT1=VT1+(A55*Q+Q0*A66)*FK1*100.0/E1
10         CONTINUE
       T3=((x+I5(j)-b-c)*(x+I5(j)-b-c)+y*y)
       A3=T3**(3/2.)
       a33=(x+I5(j)-b-c)/a3
       b33=y/a3
       A7=SQRT(T3)
       A77=1.0/A7
       dnt1=dnt1+q5(j)*fk1*a33
       ett1=ett1+q5(j)*fk1*b33/E1
       VT1=VT1+Q5(J)*A77*FK1*100.0/E1
27         CONTINUE
       DN1(IP)=DNT1
       EN1(IP)=DN1(IP)/E1
       ET1(IP)=ETT1
       V1(IP)=VT1
       EM1(IP)=SQRT(ET1(IP)*ET1(IP)+EN1(IP)*EN1(IP))
       DNT1=0.0
```

166

Table C.1. Continued

```
        ETT1=0.0
        VT1=0.0
25          CONTINUE
        return
        end
C   ......................................................
C      THIS IS REGION(2) SUBROUTINE
C
        subroutine field2(E2,FLAG,DN2,ET2,EM2,V2)
        common a,b,c,h,fk1,NP
        common q1,L1,Q2,L2,Q3,L3,Q4,L4,Q5,L5,Q,NI,NII
        real q1(4001),I1(4001),q2(4001),I2(4001),q3(4001)
            REAL L3(4001),q4(2000),I4(2000),q5(2000),I5(2000)
        REAL DN2(10),ET2(10),EM2(10),V2(10),EN2(10)
        X=B+C
        IF(FLAG.NE.1)X=C
        VT2=0.0
        ETT2=0.0
        DNT2=0.0
        DO 35 IP=1,NP
        Y=(IP-1)/100.0
        DO 36 J=1,NI
        D1=((X-L1(J)-B-C)*(X-L1(J)-B-C)+Y*Y)**(3/2.)
        D11=(X-L1(J)-B-C)/D1
        C11=Y/D1
        B8=SQRT((X-L1(J)-B-C)*(X-L1(J)-B-C)+Y*Y)
        B88=1.0/B8
        D3=((x+I2(J)-c)*(x+I2(J)-c)+y*y)**(3/2.)
        d33=(x+I2(J)-c)/d3
        c33=y/d3
        B10=SQRT((X+L2(J)-C)*(X+L2(J)-C)+Y*Y)
        B12=1.0/B10
        DNT2=DNT2+(Q1(J)*D11+Q2(J)*D33)*FK1
        ETT2=ETT2+(Q1(J)*C11+Q2(J)*C33)*FK1/E2
        VT2=VT2+(Q1(J)*B88+Q2(J)*B12)*FK1*100.0/E2
36          CONTINUE
        DN2(IP)=DNT2
        EN2(IP)=DN2(IP)/E2
        ET2(IP)=ETT2
        EM2(IP)=SQRT(EN2(IP)*EN2(IP)+ET2(IP)*ET2(IP))
        V2(IP)=VT2
        DNT2=0.0
        ETT2=0.0
        VT2=0.0
35          CONTINUE
        RETURN
        end
C   ......................................................
C      THIS IS REGION(3) SUBROUTINE
C
```

167

Table C.1. Continued

```
subroutine field3(e3,FLAG,DN3,ET3,EM3,V3)
common a,b,c,h,fk1,NP
common q1,I1,q2,I2,q3,I3,q4,I4,q5,I5,q,NI,NII
real Q5(2000),L5(2000),q1(4001),I1(4001),q2(4001)
     REAL L2(4001),q3(4001),I3(4001),Q4(2000),L4(2000)
REAL DN3(10),ET3(10),EM3(10),V3(10),EN3(10)
DNT3=0.0
DNT4=0.0
ETT3=0.0
ETT4=0.0
VT3=0.0
VT4=0.0
X=B+C
IF(FLAG.NE.1)X=C
DO 78 IP=1,NP
Y=(IP-1)/100.0
DO 79 J=1,NII
f1=((x-I3(J)-c)*(x-I3(J)-c)+y*y)
f10=f1**(3/2.)
g4=1.0/(Sqrt(f1))
f11=(x-I3(J)-c)/f10
f44=y/f10
DNT3=DNT3+Q3(J)*F11*FK1
ETT3=ETT3+Q3(J)*F44*FK1/E3
VT3=VT3+Q3(J)*G4*FK1*100.0/E3
79       CONTINUE
DO 80 J=1,NI
f3=((x+I4(j))*(x+I4(j))+y*y)
f30=f3**(3/2.)
f33=(x+I4(J))/f30
g6=1.0/(Sqrt(f3))
f55=y/f30
DNT4=DNT4+Q4(J)*F33*FK1
etT4=etT4+(Q4(J)*F55)*FK1/E3
vT4=vT4+Q4(J)*G6*FK1*100.0/E3
80       CONTINUE
DN3(IP)=DNT3+DNT4
ET3(IP)=ETT3+ETT4
EN3(IP)=DN3(IP)/E3
EM3(IP)=SQRT(EN3(IP)*EN3(IP)+ET3(IP)*ET3(IP))
V3(IP)=VT3+VT4
DNT3=0.0
DNT4=0.0
ETT3=0.0
ETT4=0.0
VT3=0.0
VT4=0.0
78       CONTINUE
RETURN
END
```

Table C.1.   Continued

```
C       THIS IS THE FIVE DIELECTRIC MEDIA PROGRAM FOR THE POINT
C       CHARGE CASE.THE IMAGES AND THEIR POSITIONS WILL BE DETERMINED
C       IN ADVANCE.THEN THE MAIN PROGRAM WILL CALL THE DIFFERENT SUBR.
C       IF FLAG=1,THEN REGIONS (1),(2) BOUNDARY CONDITIONS WILL BE
C       CALCULATED.IF FLAG=2,THEN REGIONS (2),(3) BOUNDARY CONDITIONS
C       WILL BE CALCULATED,AND FINALLY IF FLAG=3,THEN REGIONS (3),(4)
C       WILL BE CALCULATED
C       ..............................................................
        common a,b,c,d,h,fk1
        common q1,L1,Q2,L2,Q3,L3,Q4,L4,Q5,L5,Q6,L6,Q7,L7,Q
        COMMON NI,NI2,NI3,NP
        real Q1(2000),L1(2000),Q2(4000),L2(4000),q3(4000),L3(4000)
          REAL Q4(6000),L4(6000),Q5(6000),L5(6000),Q6(2000),L6(2000)
            REAL Q7(2000),L7(2000)
        REAL DN1(10),ET1(10),EN1(10),EM1(10),V1(10)
        REAL DN2(10),ET2(10),EN2(10),EM2(10),V2(10)
        REAL DN3(10),ET3(10),EN3(10),EM3(10),V3(10)
        REAL DN4(10),ET4(10),EN4(10),EM4(10),V4(10)
C       ..............................................................
        read(5,*)e0,e1,e2,e3,e4,a,b,c,d,H,NP,NI,FLAG
        read(5,*)q
C       ..............................................................
        alph12=(e1-e2)/(e1+e2)
        alph23=(e2-e3)/(e2+e3)
        alph34=(e3-e4)/(e3+e4)
        bet12=2.*e2/(e2+e1)
        bet21=2.*e1/(e1+e2)
        bet23=2.*e3/(e2+e3)
        bet32=2.*e2/(e2+e3)
        bet34=2.*e4/(e3+e4)
        bet43=2.*e3/(e3+e4)
C       ..............................................................
        pi=3.1416
        NI2=2*NI
        NI3=3*NI
        fk1=1.0/(4.*e0*pi)
        q1(1)=bet12*q
        l1(1)=a
        q0=alph12*q
        j=1
        i=1
        n=1
41         CONTINUE
        k=j+1
        m1=2*j
        m2=i+1
        n1=n+1
        n2=n+2
        q2(i)=alph23*q1(j)
        q3(i)=bet23*q1(j)
```

Table C.1. Continued

```
      q1(k)=-alph12*q2(J)
      q7(J)=bet21*q2(J)
      q4(n)=alph34*q3(i)
      q5(n)=bet34*q3(i)
      q3(m1)=-alph23*q4(J)
      q2(m2)=bet32*q4(J)
      q6(J)=-q5(J)
      q5(n1)=-alph34*q6(J)
      q4(n1)=bet43*q6(J)
      q4(n2)=alph34*q3(m1)
      q5(n2)=bet34*q3(m1)
      I2(i)=I1(J)+b
      I3(i)=I1(J)+b
      I1(k)=I2(J)+b
      I7(J)=I2(J)+b
      I4(n)=I3(i)+c
      I5(n)=I3(i)+c
      I3(m1)=I4(J)+c
      I2(m2)=I4(J)+c
      I6(J)=I5(J)+d
      I5(n1)=I6(J)+d
      I4(n1)=I6(J)+d
      I5(n2)=I3(m1)+c
      I4(n2)=I3(m1)+c
      IF(J.EQ.N)GO TO 72
      J=J+1
      I=I+2
      N=N+3
      GO TO 41
   72 CONTINUE
C
      ..................................................
      IF(FLAG.NE.1)GO TO 17
      call field1(e1,Q0,FLAG,DN1,ET1,EM1,V1)
      PRINT*,' '
      PRINT*,' '
      WRITE(6,19)
   19 FORMAT('0',10X,' DN1 ',5X,' ET1',5X,' EM1',5X,' V1')
      DO 121 I=1,NP
      PRINT*,' '
      WRITE(6,23)DN1(I),ET1(I),EM1(I),V1(I)
   23 FORMAT('0',10X,F8.4,5X,F8.4,5X,F8.4,5X,F8.4)
  121 CONTINUE
      call field2(e2,FLAG,DN2,ET2,EM2,V2)
      PRINT*,' '
      PRINT*,' '
      WRITE(6,60)
   60 FORMAT('0',10X,' DN2 ',5X,' ET2',5X,' EM2',5X,' V2')
      DO 123 I=1,NP
      PRINT*,' '
      WRITE(6,23)DN2(I),ET2(I),EM2(I),V2(I)
```

Table C.1.   Continued

```
123        CONTINUE
        GO TO 999
 17        CONTINUE
        IF(FLAG.NE.2)GO TO 25
        CALL FIELD2(E2,FLAG,DN2,ET2,EM2,V2)
        PRINT*,' '
        PRINT*,' '
        WRITE(6,60)
        DO 125 I=1,NP
        PRINT*,' '
        WRITE(6,23)DN2(I),ET2(I),EM2(I),V2(I)
125        CONTINUE
        CALL FIELD3(E3,FLAG,DN3,ET3,EM3,V3)
        PRINT*,' '
        PRINT*,' '
        WRITE(6,111)
111        FORMAT('0',10X,' DN3 ',5X,'   ET3','   EM3',5X,'   V3')
        DO 127 I=1,NP
        PRINT*,' '
        WRITE(6,23)DN3(I),ET3(I),EM3(I),V3(I)
127        CONTINUE
        GO TO 999
 25        CALL FIELD3(E3,FLAG,DN3,ET3,EM3,V3)
        PRINT*,' '
        PRINT*,' '
        WRITE(6,111)
        DO 134 I=1,NP
        PRINT*,' '
       .WRITE(6,23)DN3(I),ET3(I),EM3(I),V3(I)
134        CONTINUE
        CALL FIELD4(E4,FLAG,DN4,ET4,EM4,V4)
        PRINT*,' '
        PRINT*,' '
        WRITE(6,115)
115        FORMAT('0',10X,' DN4 ',5X,'   ET4',5X,'   EM4',5X,'   V4')
        DO 94 I=1,NP
        PRINT*,' '
        WRITE(6,23)DN4(I),ET4(I),EM4(I),V4(I)
 94        CONTINUE
999        CONTINUE
        STOP
        END
C        ...................................................................
C        THIS IS REGION (1) SUBROUTINE
C

        subroutine field1(e1,Q0,FLAG,DN1,ET1,EM1,V1)
        common a,b,c,d,h,fk1
        common q1,L1,Q2,L2,Q3,L3,Q4,L4,Q5,L5,Q6,L6,Q7,L7,Q
        COMMON NI,NI2,NI3,NP
        real Q1(2000),L1(2000),Q2(4000),L2(4000),Q3(4000),L3(4000)
```

Table C.1. Continued

```
          REAL Q4(6000),L4(6000),Q5(6000),L5(6000),Q6(2000),L6(2000)
       REAL Q7(2000),L7(2000)
       REAL DN1(10),ET1(10),EM1(10),EN1(10),V1(10)
       IF(FLAG.EQ.1)X=B+C+D
       DNT1=0.0
       ETT1=0.0
       VT1=0.0
       DO 20 IP=1,NP
       Y=(IP-1)/100.0
       DO 34 J=1,NI
       if(j.ne.1)go to 10
       T1=((x-h)*(x-h)+y*y)
       A1=T1**(3/2.)
       a11=(x-h)/a1
       b11=y/a1
       A5=SQRT(T1)
       A55=1.0/A5
        T2=((x-h+2*a)*(x-h+2*a)+y*y)
       A2=T2**(3/2.)
       a22=(x-h+2*a)/a2
       b22=y/a2
       A6=SQRT(T2)
       A66=1.0/A6
       dnt1=dnt1+(a11*q+q0*a22)*fk1
       ett1=ett1+(b11*q+b22*q0)*fk1/E1
       VT1=VT1+(A55*Q+A66*Q0)*FK1/E1
10        T3=((X+L7(J)-B-C-D)*(X+L7(J)-B-C-D)+Y*Y)
       A3=T3**(3/2.)
       a33=(x+l7(j)-b-c-d)/a3
       b33=y/a3
       A7=SQRT(T3)
       A77=1.0/A7
       dnt1=dnt1+q7(j)*A33*FK1
       ett1=ett1+q7(j)*B33*FK1/E1
       VT1=VT1+Q7(J)*A77*FK1/E1
34        CONTINUE
       DN1(IP)=DNT1
       ET1(IP)=ETT1
       EN1(IP)=DN1(IP)/E1
       V1(IP)=VT1*100.0
       EM1(IP)=SQRT(EN1(IP)*EN1(IP)+ET1(IP)*ET1(IP))
       DNT1=0.0
       ETT1=0.0
       VT1=0.0
20        CONTINUE
       RETURN
       end
C      .............................................................
C         THIS IS REGION (2) SUBROUTINE
C
```

Table C.1.   Continued

```
subroutine field2(e2,FLAG,DN2,ET2,EM2,V2)
common a,b,c,d,h,fk1
common q1,L1,Q2,L2,Q3,L3,Q4,L4,Q5,L5,Q6,L6,Q7,L7,Q
COMMON NI,NI2,NI3,NP
real Q1(2000),L1(2000),Q2(4000),L2(4000),Q3(4000),L3(4000)
REAL Q4(6000),L4(6000),Q5(6000),L5(6000),Q6(2000),L6(2000)
REAL Q7(2000),L7(2000)
REAL DN2(10),ET2(10),EN2(10),EM2(10),V2(10)
X=B+C+D
IF(FLAG.NE.1)X=C+D
DNT1=0.0
ETT1=0.0
VT1=0.0
DNT2=0.0
ETT2=0.0
VT2=0.0
DO 67 IP=1,NP
Y=(IP-1)/100.0
DO 43 J=1,NI
T1=((x-l1(J)-b-c-d)*(x-l1(J)-b-o-d)+y*y)
D1=T1**(3/2.)
d11=(x-l1(J)-b-c-d)/d1
c11=y/d1
B1=SQRT(T1)
B11=1.0/B1
DNT1=DNT1+Q1(J)*D11*FK1
ETT1=ETT1+Q1(J)*C11*FK1/E2
VT1=VT1+Q1(J)*B11*FK1/E2
43      CONTINUE
DO 53 J=1,NI2
T3=((x+l2(J)-c-d)*(x+l2(J)-c-d)+y*y)
D3=T3**(3/2.)
d33=(x+l2(J)-c-d)/d3
c33=y/d3
B2=SQRT(T3)
B22=1.0/B2
dnt2=dnt2+Q2(J)*D33*FK1
ett2=ett2+Q2(J)*C33*FK1/E2
VT2=VT2+Q2(J)*B22*FK1/E2
53      CONTINUE
DN2(IP)=DNT2+DNT1
ET2(IP)=ETT2+ETT1
V2(IP)=(VT2+VT1)*100.0
EN2(IP)=DN2(IP)/E2
EM2(IP)=SQRT(EN2(IP)*EN2(IP)+ET2(IP)*ET2(IP))
DNT2=0.0
ETT2=0.0
VT2=0.0
DNT1=0.0
ETT1=0.0
```

Table C.1.   Continued

```
                VT1=0.0
  67               CONTINUE
                RETURN
                end
C
C           THIS IS REGION (3) SUBROUTINE
C
                subroutine field3(e3,FLAG,DN3,ET3,EM3,V3)
                common a,b,c,d,h,fk1
                common q1,L1,Q2,L2,Q3,L3,Q4,L4,Q5,L5,Q6,L6,Q7,L7,Q
                COMMON NI,NI2,NI3,NP
                REAL Q1(2000),L1(2000),Q2(4000),L2(4000),Q3(4000),L3(4000)
                REAL Q4(6000),L4(6000),Q5(6000),L5(6000),Q6(2000),L6(2000)
                REAL Q7(2000),L7(2000)
                REAL DN3(10),ET3(10),EN3(10),EM3(10),V3(10)
                X=C+D
                IF(FLAG.NE.2)X=D
                DNT3=0.0
                ETT3=0.0
                VT3=0.0
                DNT4=0.0
                ETT4=0.0
                VT4=0.0
                DO 71 IP=1,NP
                Y=(IP-1)/100.0
                DO 72 J=1,NI2
                T1=((x-I3(J)-c-d)*(x-I3(J)-c-d)+y*y)
                F1=T1**(3/2.)
                f11=(x-I3(J)-c-d)/f1
                f44=y/f1
                C1=SQRT(T1)
                C11=1.0/C1
                DNT3=DNT3+Q3(J)*F11*FK1
                ETT3=ETT3+Q3(J)*F44*FK1/E3
                VT3=VT3+Q3(J)*C11*FK1/E3
  72               CONTINUE
                DO 75 J=1,NI3
                T3=((x+I4(J)-d)*(x+I4(J)-d)+y*y)
                F3=T3**(3/2.)
                f33=(x+I4(J)-d)/f3
                f55=y/f3
                B3=SQRT(T3)
                B33=1.0/B3
                DNT4=DNT4+Q4(J)*F33*FK1
                etT4=etT4+q4(J)*fk1*f55/e3
                VT4=VT4+Q4(J)*B33*FK1/E3
  75               CONTINUE
                DN3(IP)=DNT3+DNT4
                EN3(IP)=DN3(IP)/E3
                ET3(IP)=ETT3+ETT4
```

Table C.1. Continued

```
        V3(IP)=(VT3+VT4)*100.0
        eM3(IP)=SQRT(EN3(IP)*EN3(IP)+ET3(IP)*ET3(IP))
        DNT3=0.0
        ETT3=0.0
        VT3=0.0
        DNT4=0.0
        ETT4=0.0
        VT4=0.0
71         CONTINUE
        RETURN
        end
C  ..............................................................
C     THIS IS REGION (4) SUBROUTINE
C
        subroutine field4(E4,FLAG,dn4,ET4,EM4,V4)
        common a,b,c,d,h,fk1
        common q1,L1,Q2,L2,Q3,L3,Q4,L4,Q5,L5,Q6,L6,Q7,L7,Q
        COMMON NI,NI2,NI3,NP
        REAL Q1(2000),L1(2000),Q2(4000),L2(4000),Q3(4000),L3(4000)
        REAL Q4(6000),L4(6000),Q5(6000),L5(6000),Q6(2000),L6(2000)
        REAL Q7(2000),L7(2000)
        REAL DN4(10),ET4(10),EN4(10),EM4(10),V4(10)
        X=D
        DNT5=0.0
        ETT5=0.0
        VT5=0.0
        DNT6=0.0
        ETT6=0.0
        VT6=0.0
        DO 33 IP=1,NP
        Y=(IP-1)/100.0
        DO 43 J=1,NI3
        T1=((x-I5(J)-d)*(x-I5(J)-d)+y*y)
        D1=T1**(3/2.)
        d11=(x-I5(J)-d)/d1
        c11=y/d1
        B1=SQRT(T1)
        B11=1.0/B1
        dnT5=dnT5+(q5(J)*d11)*fk1
        etT5=etT5+(q5(J)*c11)*fk1/e4
        VT5=VT5+(Q5(J)*B11)*FK1/E4
43         CONTINUE
        DO 53 J=1,NI
        T2=((x+I6(J))*(x+I6(J))+y*y)
        D2=T2**(3/2.)
        d22=(x+I6(J))/d2
        c22=y/d2
        B2=SQRT(T2)
        B22=1.0/B2
        dnT6=dnT6+q6(J)*fk1*d22
```

Table C.1.   Continued

```
            etT6=etT6+q6(J)*fk1*c22/e4
            VT6=VT6+Q6(J)*B22*FK1/E4
     53         CONTINUE
            dN4(IP)=DNT5+DNT6
            EN4(IP)=DN4(IP)/E4
            ET4(IP)=ETT5+ETT6
            EM4(IP)=SQRT(EN4(IP)*EN4(IP)+ET4(IP)*ET4(IP))
            V4(IP)=(VT5+VT6)*100.0
            dnt5=0.0
            ett5=0.0
            VT5=0.0
            DNT6=0.0
            ETT6=0.0
            VT6=0.0
     33         CONTINUE
            RETURN
            END
     C      THIS IS THE TWO MEDIA PROGRAM WHERE THE FIRST MEDIA IS AIR
     C       AND THE SECOND MEDIA IS THE PERFECT CONDUCTOR GROUND
     C      COMPUTATION OF THE THREE PHASE LINE OF CHARGES USING THE
     C      GENERAL METHOD OF CHARGES COMPUTATION
     C      THE BUNDLE CONDUCTORS WILL BE REPRESENTED BY AN EQUIV.COND.
     C      SINGLE LINE OF CHARGE REPRESENTATION IS USED
     C      NOTICE THAT ALL THE INPUT DATA HAS TO BE IN METERS
     C      ......................................................
     C
            real H(3),BY(3),HI(3),BYI(3),P(3,3)
            real QR(3),QI(3),BR(3),BI(3),AR(3,3),AI(3,3)
            real QM(3),GAMA(3),XR(3),XI(3),EXM,EYM
            COMPLEX V(3),Q(3),EX,EY
     C
            READ(5,*)BS,NS,SD,N,NY,NX
            READ(5,*) (H(I),I=1,N)
            READ(5,*) (BY(I),I=1,N)
            READ(5,*) (V(I),I=1,N)
     C
     C      ......................................................
            PI=3.14159
            EO=8.85E-12
     C
            WRITE(6,10)BS,NS,SD,N,NY,NX
     10         FORMAT('1',//,10X,'BUNDLE SPACING        =',F10.2,//,10X,
            +       'NO.OF SUB COND.      =',I2,//,10X,'SUB COND.DIAM      ='
            +       ,F10.2,//10X,'NO.LIN CHARGES       =',I2,//,10X,
            +       'NO.OF POINTS ALONG Y =',I2,//,10X,'NO.OF POS.ABOVE GRD =',
            +       I2,//)
     C
     C      THIS GENERAL METHOD OF CHARGES COMPUTATION IS PRESENTED IN (11)
     C
            RE=(BS/2.)*((NS*SD/BS)**(1./NS))
```

Table C.1.   Continued

```
          FAC=1.0/(2.*PI*EO)
          RAD=180.0/PI
          DO 1 I=1,N
          BYI(I)=BY(I)
          HI(I)=-H(I)
   1         CONTINUE
C
C    COMPUTATION OF THE POT.COEFF.MATRIX
C
          DO 2 I=1,N
          DO 3 J=1,N
          IF(I.NE.J)GO TO 4
          HS=2.*H(I)
          P(I,J)=FAC*(ALOG(HS/RE))
          GO TO 5
   4     HS=SqRT((H(I)-HI(J))**2+(BY(I)-BYI(J))**2)
          DS=SqRT((H(I)-H(J))**2+(BY(I)-BY(J))**2)
          P(I,J)=FAC*(ALOG(HS/DS))
   5     CONTINUE
   3     CONTINUE
   2     CONTINUE
C
C
C    .............................................................
C    THE LINE OF CHARGES WILL BE DETERMINED USING THE SUBROUTINE
C    (CLINQ) INSTALLED ON VAX(B) UNDER THE EE.LIBRARY
C
          DO 6 I=1,N
          DO 6 J=1,N
          AR(I,J)=P(I,J)
          AI(I,J)=0.0
   6     CONTINUE
          DO 7 I=1,N
          BR(I)=ReAL(V(I))
          BI(I)=AImAG(V(I))
   7     CONTINUE
          NA=N
C
C
          WRITE(6,15)
  15     FORMAT('0',10X,'    REAL(Q) '5X,'    IMAG(Q)   ')
          CALL CIINQ(NA,AR,AI,BR,BI,1,XR,XI)
          DO 8 I=1,N
          QR(I)=XR(I)
          QI(I)=XI(I)
          Q(I)=cmplx(qr(I),qi(I))
          QM(I)=SqRT(QR(I)*QR(I)+QI(I)*QI(I))
          GAMA(I)=AtAN2(QI(I),QR(I))*RAD
          WRITE(6,20)QR(I),QI(I)
  20     FORMAT('0',10X,F12.8,5X,F12.8)
```

Table C.1. Continued

```
C
 8   CONTINUE
C
C    ..............................................................
C    THIS PART OF THE PROGRAM WILL COMPUTE THE ELEC.FIELD COMPON-
C    AT DIFFERENT POINTS ALONG THE TRANSVERSE PLANE OF THE TRAN.LINE
C
C
     FAC=FAC*1.0E-3
     DO 13 IX=1,NX
     X=IX-1
     WRITE(6,30)X
 30  FORMAT('1',10X,'HEIGHT ABOVE THE GROUND=',F7.2)
C
C
     WRITE(6,40)
 40  FORMAT('0',10X,'  ETM  ',5X,'  ENM  ',5X,'  EMAG ')
     ex=(0.0,0.0)
     ey=(0.0,0.0)
     do 12 IY=1,nY
     Y=IY-1
     do 11 i=1,n
     a1=x-H(i)
     b1=y-BY(i)
     A2=X+H(i)
     d1=a1*a1+b1*b1
     d2=A2*A2+B1*B1
     x1=a1/d1
     x2=A2/d2
     y1=b1/d1
     y2=B1/d2
     ex=ex+q(i)*fac*(x1-x2)
     ey=ey+q(i)*fac*(y1-y2)
 11  continue
C
C    THIS PART OF THE PROGRAM WILL COMPUTE THE MAXIMUM AMPLITUDE
C    OF AN ELLIPTICALLY POLORIZED ELEC.FIELD WHEN THE X AND THE Y
C    MAGNITUDES AND PHASES ARE GIVEN
C    EX IN THIS PROGRAM IS THE NORMAL COMPONENET IN (KV/M)
C    EY IN THIS PROGRAM IS THE TANGENTIAL COMPONENT IN (KV/M)
C
     IF(EY.EQ.0.0)GO TO 100
     eYr=(Real(eY))
     eYi=(Aimag(eY))
     eYm=Sqrt(eYr*eYr+eYi*eYi)
 100     CONTINUE
     EXR=(REAL(EX))
     EXI=(AIMAG(EX))
     eXm=Sqrt(eXr*eXr+eXi*eXi)
     IF(EXI.EQ.0.0.AND.EXR.EQ.0.0)EXP=0.0
     IF(EXP.EQ.0.0.AND.EXR.EQ.0.0)GO TO 110
```

Table C.1. Continued

```
          EXP=ATAN2(EXI,EXR)*RAD
110       IF(EYI.EQ.0.0.AND.EYR.EQ.0.0)EYP=0.0
          IF(EYP.EQ.0.0.AND.EYR.EQ.0.0)GO TO 120
          EYP=ATAN2(EYI,EYR)*RAD
120       CONTINUE
          IF(EXM.EQ.0.0)EMAG=EYM
          IF(EYM.EQ.0.0)EMAG=EXM
          IF(EXM.EQ.0.0.OR.EYM.EQ.0.0)GO TO 130
          alph=EYp*2./rad
          beta=EXp*2./rad
          com=(eXM*EXM)/(EYM*EYM)
          arg=-(sin(alph)+com*sin(beta))/(cos(alph)+com*cos(beta))
          angl=ATan(arg)
          test=cos(angl+alph)+com*cos(angl+beta)
          if(test.lt.0.0)angl=angl+3.1416
          emag=sqrt((1.0+com+cos(angl+alph)+com*cos(angl+beta))/2.)*EYM
130       continue
          WRITE(6,50)EYM,EXM,EMAG
C
C
 50   FORMAT('0',10X,(3(F7.4,5X)))
          ex=(0.0,0.0)
          ey=(0.0,0.0)
 12   continue
 13   CONTINUE

      stop
      end
C     THIS IS THE  FOUR DIELECTRIC PROGRAM FOR THE THREE PHASE LINE
C     CHARGES.THE LINE CHARGES WILL BE READ AS A DATA.
C     SIMALARLY TO THE POINT CHARGE CASE,AND AT THE SAME TIME THE
C     POSITION OF THE IMAGES WILL BE CALCULATED IN ADVANCE
C     THE MAIN PROGRAM WILL THEN CALL THE DIFFERENT SUBR.FOR B.C.
C     CALCULATION.
C     IF FLAG=1,THEN REGIONS (1),(2) B.C.VALUES WILL BE DETER.
C     IF FLAG=2,THEN REGIONS (2),(3) B.C.VALUES WILL BE DETER.
C     THE  B.C.VALUES ARE: NORMAL FLUX DENCITY,TANGETIAL ELE.FIELD
C     THE MAGNETUDE OF THE ELEC.FIELD WILL BE CALCULAED USING THE
C     THE BOUNDARY VALUES,AND THE SUBROUTIN (MAG)
C     NC=THE NO.LINE CHARGES (3)
C     NP=THE NO.OF POINTS ALONG THE Y AXIS (21)
C     NI=THE NO.OF IMAGES USED
C     IF THE NO.OF IMAGES TO BE USED>1000,THEN INCREASE THE DIM.SIZE
C     OF ALL THE CHARGES,AND THE CORRESPONDING POSITIONS
C     NOTE THIS PROGRAM CAN BE USED AS THREE DIEL.MEDIA BY LETTING
C     E2=E3
C
C     ...............................................................
      commON q,ax,by,h,c,b,NC,NP,q0,fk1,NI,NI2
      common q1,L1,Q2,L2,Q3,L3,Q4,L4,Q5,L5
      COMPLEX Q(3),FK1(3),DN1(21),EN1(21),ET1(21),V1(21)
```

Table C.1.   Continued

```
      COMPLEX DN2(21),EN2(21),ET2(21),V2(21),EN(21),ET(21)
      COMPLEX DN3(21),EN3(21),ET3(21),V3(21)
      COMPLEX DNT1,ETT1,VT1,DNT2,ETT2,VT2,DNT3,ETT3,VT3,XN,YT
      REAL Q1(3,2000),Q2(3,4000),Q3(3,4000),Q4(3,2000),Q5(3,2000)
      REAL Q0(3)
      REAL L1(3,2000),L2(3,4000),L3(3,4000),L4(3,2000),L5(3,2000)
      REAL ENM1(21),ETM1(21),EM1(21),DNM1(21),VM1(21),EMAG(21)
      REAL ENM2(21),ETM2(21),EM2(21),DNM2(21),VM2(21)
      REAL ENM3(21),ETM3(21),EM3(21),DNM3(21),VM3(21)
      REAL AX(3),BY(3),H(3),EMAG1(21)
C     ...............................................................
      read(5,*)e0,e1,E2,E3,B,C,NP,NI,FLAG,NC
      read(5,*) (q(i),i=1,NC)
      read(5,*) (ax(i),i=1,NC)
      read(5,*) (by(i),i=1,NC)
      read(5,*) (h(i),i=1,NC)
C     ...............................................................
      NI2=2*NI
      alph12=(e1-e2)/(e1+e2)
      alph23=(e2-e3)/(e2+e3)
      bet12=2*e2/(e2+e1)
      bet21=2*e1/(e2+e1)
      bet23=2*e3/(e2+e3)
      bet32=2*e2/(e2+e3)
C     ...............................................................
      pi=3.1416d0
      RAD=180.0/PI
      do 24 ip=1,nC
      q1(ip,1)=bet12
      l1(ip,1)=ax(ip)
      q0(ip)=alph12
      FK1(IP)=Q(IP)/(2.0*PI*E0)
 24   CONTINUE
      J=1
      i=1
 41      CONTINUE
      K=J+1
      m=2*j
      do 27 ip=1,nC
      q2(ip,i)=alph23*q1(ip,j)
      q3(ip,i)=bet23*q1(ip,j)
      q1(ip,k)=-alph12*q2(ip,j)
      q5(ip,j)=bet21*q2(ip,j)
      q4(ip,j)=-q3(ip,j)
      q3(ip,m)=-alph23*q4(ip,j)
      q2(ip,m)=bet32*q4(ip,j)
      l2(ip,i)=l1(ip,j)+b
      l3(ip,i)=l1(ip,j)+b
      l1(ip,k)=l2(ip,j)+b
      l5(ip,j)=l2(ip,j)+b
```

Table C.1. Continued

```
      I4(ip,J)=I3(ip,j)+c
      I3(ip,m)=I4(ip,j)+c
      I2(ip,m)=I4(ip,j)+c
   27 continue
      IF(J.EQ.NI)GO TO 50
      J=J+1
      I=I+2
      GO TO 41
   50 CONTINUE
C     ....................................................................
      IF(FLAG.NE.1)GO TO 69
      call FLD1(E1,FLAG,DNM1,ETM1,ENM1,EN1,ET1)
      PRINT*,' '
      WRITE(6,91)
   91 FORMAT('0',16X,'DNM1',13X,'ETM1',12X,'EMAG')
      DO 101 I=1,NP
      EN(I)=EN1(I)
      ET(I)=ET1(I)
  101      CONTINUE
      CALL MAG(EN,ET,NP,EMAG)
      DO 163 I=1,NP
      WRITE(6,92)DNM1(I),ETM1(I),EMAG(I)
      PRINT*,' '
   92 FORMAT(10X,F12.6,5X,F12.6,5X,F12.6,5X,F12.6)
  163      CONTINUE
      CALL FLD2(E2,FLAG,DNM2,ETM2,ENM2,EN2,ET2)
      PRINT*,' '
      WRITE(6,93)
   93 FORMAT('0',16X,'DNM2',13X,'ETM2',13X,'EMAG')
      DO 111 I=1,NP
      EN(I)=EN2(I)
      ET(I)=ET2(I)
  111      CONTINUE
      CALL MAG(EN,ET,NP,EMAG)
      DO 112 I=1,NP
      WRITE(6,92)DNM2(I),ETM2(I),EMAG(I)
      PRINT*,' '
  112      CONTINUE
      GO TO 999
   69 CALL FLO2(E2,FLAG,DNM2,ETM2,ENM2,EN2,ET2)
      PRINT*,' '
      WRITE(6,93)
      DO 110 I=1,NP
      EN(I)=EN2(I)
      ET(I)=ET2(I)
  110      CONTINUE
      CALL MAG(EN,ET,NP,EMAG)
      DO 119 I=1,NP
      WRITE(6,92)DNM2(I),ETM2(I),EMAG(I)
      PRINT*,' '
```

Table C.1. Continued

```
119       CONTINUE
      CALL FLD3(E3,FLAG,DNM3,ETM3,EN3,ET3)
      PRINT*,'
      WRITE(6,94)
 94   FORMAT('0',16X,'DNM3',13X,'ETM3',13X,'EMAG')
      DO 120 I=1,NP
      EN(I)=EN3(I)
      ET(I)=ET3(I)
 120      CONTINUE
      CALL MAG(EN,ET,NP,EMAG)
      DO 127 I=1,NP
      WRITE(6,92)DNM3(I),ETM3(I),EMAG(I)
      PRINT*,'
 127      CONTINUE
 999      CONTINUE
      STOP
      END
C  .........................................................
C  THIS IS REGION (1) SUBROUTINE
C
      subroutine FLD1(E1,FLAG,DNM1,ETM1,ENM1,EN1,ET1)
      commON q,ax,by,h,c,b,NC,NP,q0,fk1,NI,NI2
      common Q1,L1,Q2,L2,Q3,L3,Q4,L4,Q5,L5
      COMPLEX Q(3),FK1(3),DN1(21),EN1(21),ET1(21),V1(21)
      COMPLEX DNT1,ETT1,VT1
      REAL Q1(3,2000),Q2(3,4000),Q3(3,4000),Q4(3,2000),Q5(3,2000)
      REAL Q0(3),EMAG1(21)
      real L1(3,2000),L2(3,4000),L3(3,4000),L4(3,2000),L5(3,2000)
      REAL AX(3),BY(3),H(3),DNM1(21),ETM1(21),ENM1(21),VM1(21)
      IF(FLAG.EQ.1)X=B+C
      DNT1=(0.0,0.0)
      ETT1=(0.0,0.0)
      VT1=(0.0,0.0)
      do 25 IP=1,NP
      Y=IP-1
      DO 26 I=1,NC
      DO 27 J=1,NI
      If(J.ne.1)go to 10
      T1=(X-H(I))*(X-H(I))+(Y-BY(I))*(Y-BY(I))
      A1=(X-H(I))/T1
      B1=(Y-BY(I))/T1
      T2=(x-H(I)+2*AX(I))*(X-H(I)+2*AX(I))+(Y-BY(I))*(Y-BY(I))
      A2=(X-H(I)+2*AX(I))/T2
      B2=(Y-BY(I))/T2
      dnt1=dnt1+(a1+q0(I)*a2)*fk1(I)
      ETT1=ETT1+(B1+Q0(I)*B2)*FK1(I)/E1
 10 CONTINUE
      T3=(X+L5(I,J)-B-C)*(X+L5(I,J)-B-C)+(Y-BY(I))*(Y-BY(I))
      A3=(X+L5(I,J)-B-C)/T3
      B3=(Y-BY(I))/T3
```

Table C.1. Continued

```
      dnt1=dnt1+q5(I,J)*A3*FK1(I)
      ETT1=ETT1+Q5(I,J)*B3*FK1(I)/E1
27 continue
26 CONTINUE
      DN1(IP)=DNT1
      EN1(IP)=DN1(IP)/E1
      DNM1(IP)=cABS(DN1(IP))
      ENM1(IP)=DNM1(IP)/E1
      ET1(IP)=ETT1
      ETM1(IP)=cABS(ET1(IP))
      DNT1=(0.0,0.0)
      ETT1=(0.0,0.0)
25 CONTINUE
      return
      end
C    .............................................
C    THIS IS REGION (2) SUBROUTINE
C
      subroutine FLD2(e2,FLAG,DNM2,ETM2,ENM2,EN2,ET2)
      commON q,ax,by,h,c,b,NC,NP,q0,fk1,NI,NI2
      common q1,L1,Q2,L2,Q3,L3,Q4,L4,Q5,L5
      COMPLEX Q(3),FK1(3),DN2(21),ET2(21),V2(21),EN2(21)
      COMPLEX DNT2,ETT2,VT2,DNT1,ETT1
      REAL Q1(3,2000),Q2(3,4000),Q3(3,4000),Q4(3,2000),Q5(3,2000)
      REAL Q0(3)
      real L1(3,2000),L2(3,4000),L3(3,4000),L4(3,2000),L5(3,2000)
      REAL AX(3),BY(3),H(3),DNM2(21),ENM2(21),ETM2(21),EM2(21)
      X=B+C
      IF(FLAG.NE.1)X=C
      DNT1=(0.0,0.0)
      ETT1=(0.0,0.0)
      DNT2=(0.0,0.0)
      ETT2=(0.0,0.0)
      do 35 IP=1,NP
      Y=IP-1
      DO 33 I=1,NC
      DO 36 J=1,NI
      T1=(X-L1(I,J)-B-C)*(X-L1(I,J)-B-C)+(Y-BY(I))*(Y-BY(I))
      D1=(X-L1(I,J)-B-C)/T1
      C1=(Y-BY(I))/T1
      dnT1=dnT1+(q1(I,J)*d1)*fk1(I)
      ETT1=ETT1+Q1(I,J)*C1*FK1(I)/E2
36 CONTINUE
      DO 37 J=1,NI2
      T3=(x+l2(I,J)-C)*(X+L2(I,J)-C)+(Y-BY(I))*(Y-BY(I))
      D3=(X+L2(I,J)-C)/T3
      C3=(Y-BY(I))/T3
      dnt2=dnt2+(q2(I,J)*D3)*FK1(I)
      ETT2=ETT2+(Q2(I,J)*C3)*FK1(I)/E2
37 CONTINUE
```

Table C.1.   Continued

```
 33 CONTINUE
    DN2(IP)=DNT1+DNT2
    EN2(IP)=DN2(IP)/E2
    ET2(IP)=ETT1+ETT2
    DNM2(IP)=cABS(DN2(IP))
    ENM2(IP)=DNM2(IP)/E2
    ETM2(IP)=cABS(ET2(IP))
    DNT1=(0.0,0.0)
    ETT1=(0.0,0.0)
    DNT2=(0.0,0.0)
    ETT2=(0.0,0.0)
 35 CONTINUE
    return
    end
C   ...................................................
C   THIS IS REGION (3) SUBROUTINE
C
    subroutine FLD3(E3,FLAG,DNM3,ETM3,EN3,ET3)
    common q,ax,by,h,c,b,NC,NP,Q0,FK1,NI,NI2
    common q1,L1,Q2,L2,Q3,L3,Q4,L4,Q5,L5
    COMPLEX Q(3),FK1(3),DN3(21),EN3(21),ET3(21),V3(21)
    COMPLEX DNT3,ETT3,DNT4,ETT4
    REAL Q1(3,2000),Q2(3,4000),Q3(3,4000),Q4(3,2000),Q5(3,2000)
    REAL Q0(3)
    real L1(3,2000),L2(3,4000),L3(3,4000),L4(3,2000),L5(3,2000)
    REAL AX(3),BY(3),H(3)
    REAL DNM3(21),ETM3(21),ENM3(21),VM3(21)
    X=C
    DNT3=(0.0,0.0)
    ETT3=(0.0,0.0)
    DNT4=(0.0,0.0)
    ETT4=(0.0,0.0)
    DO 60 IP=1,NP
    Y=(IP-1)
    do 62 i=1,NC
    DO 63 J=1,NI2
    D1=(x-l3(I,J)-C)*(X-L3(I,J)-C)+(Y-BY(I))*(Y-BY(I))
    T1=(X-L3(I,J)-C)/D1
    T2=(Y-BY(I))/D1
    dnt3=dnt3+(q3(I,J)*t1)*FK1(I)
    ETT3=ETT3+(Q3(I,J)*T2)*FK1(I)/E3
 63 CONTINUE
    DO 64 J=1,NI
    D4=(X+L4(I,J))*(X+L4(I,J))+(Y-BY(I))*(Y-BY(I))
    T4=(X+L4(I,J))/D4
    T5=(Y-BY(I))/D4
    DNT4=DNT4+(Q4(I,J)*T4)*FK1(I)
    ETT4=ETT4+(Q4(I,J)*T5)*FK1(I)/E3
 64 CONTINUE
 62 CONTINUE
```

Table C.1. Continued

```
      DN3(IP)=DNT3+DNT4
      EN3(IP)=DN3(IP)/E3
      ET3(IP)=ETT3+ETT4
      DNM3(IP)=cABS(DN3(IP))
      ENM3(IP)=DNM3(IP)/E3
      ETM3(IP)=cABS(ET3(IP))
      DNT3=(0.0,0.0)
      ETT3=(0.0,0.0)
      DNT4=(0.0,0.0)
      ETT4=(0.0,0.0)
   60 CONTINUE
      RETURN
      END
C     ...............................................................
C     THIS SUB, ROUTINE WILL CALCULATE THE MAGNITUDE OF ELPTICALLY
C     POL.FIELD.THE MAGNITUDES AND THE PHASE ANGLES OF BOTH ELEC.
C     FIELD COMPONENTS HASE TO BE GIVEN
C
      SUBROUTINE MAG(EN,ET,NP,EMAG)
      COMPLEX EN(21),ET(21),XN,YT
      REAL EMAG(21)
      RAD=180./3.1416
      DO 1000 I=1,NP
      YT=ET(I)
      IF(YT.EQ.0.0)GO TO 1001
      YTR=REAL(YT)
      YTI=AIMAG(YT)
      YTM=SQRT(YTR*YTR+YTI*YTI)
 1001     CONTINUE
      XN=EN(I)
      XNR=REAL(XN)
      XNI=AIMAG(XN)
      XNM=SQRT(XNR*XNR+XNI*XNI)
      IF(XNI.EQ.0.0.AND.XNR.EQ.0.0)XNP=0.0
      IF(XNP.EQ.0.0.AND.XNR.EQ.0.0)GO TO 1002
      XNP=ATAN2(XNI,XNR)*RAD
 1002     IF(YTI.EQ.0.0.AND.YTR.EQ.0.0)YTP=0.0
      IF(YTP.EQ.0.0.AND.YTR.EQ.0.0)GO TO 1003
      YTP=ATAN2(YTI,YTR)*RAD
 1003     CONTINUE
      IF(XNM.EQ.0.0)EMAG(I)=YTM
      IF(YTM.EQ.0.0)EMAG(I)=XNM
      IF(XNM.EQ.0.0.OR.YTM.EQ.0.0)GO TO 1004
      ALPH=YTP*2./RAD
      BETA=XNP*2./RAD
      COM=(XNM*XNM)/(YTM*YTM)
      ARG=-(SIN(ALPH)+COM*SIN(BETA))/(COS(ALPH)+COM*COS(BETA))
      ANGL=ATAN(ARG)
      TEST=COS(ANGL+ALPH)+COM*COS(ANGL+BETA)
      IF(TEST.LT.0.0)ANGL=ANGL+3.1416
```

Table C.1. Continued

```
      EMAG(I)=SQRT((1.0+COM+COS(ANGL+ALPH)+COM*COS(ANGL+BETA))/2.)*YTM
1004      CONTINUE
1000      CONTINUE
      RETURN
      END
C     THIS IS HE FIVE DIELECTRIC MEDIA PROGRAM FOR THE THE THREE PHASE
C     LINE CHARGES.THE PROGRAM WORKS SIMALARLY TO THE FOUR MEDIA
C     CASE.THE BOUNDARY CONDITION WILL BE CALCULAED FIRST,THEN
C     THE MAGNITUDE OF THE ELEC.FIELD WILL BE CLCULATED BY THE
C     SUBR.(MAG).
C     ...................................................
      common q,ax,by,b,c,d,h,nc,q0,fk1,NI,NI2,NI3,NP
      common q1,l1,q2,l2,q3,l3,q4,l4,q5,l5,q6,l6,q7,l7
      complex q(3),FK1(3),DN1(21),EN1(21),ET1(21),V1(21)
      COMPLEX DN2(21),EN2(21),ET2(21),V2(21),EN(21),ET(21),XN,YT
      COMPLEX DN3(21),EN3(21),ET3(21),V3(21)
      COMPLEX DN4(21),EN4(21),ET4(21),V4(21)
      COMPLEX DNT1,ETT1,VT1,DNT2,ETT2,VT2
      COMPLEX DNT3,ETT3,VT3,DNT4,ETT4,VT4
      REAL Q1(3,6000),Q2(3,6000),Q3(3,6000),Q4(3,6000)
      REAL Q5(3,6000),Q6(3,6000),Q7(3,6000),Q0(3)
      real l1(3,6000),l2(3,6000),l3(3,6000),l4(3,6000)
      REAL L5(3,6000),L6(3,6000),L7(3,6000)
      REAL ENM1(21),DNM1(21),ETM1(21),EM1(21),VM1(21)
      REAL ENM2(21),DNM2(21),ETM2(21),EM2(21),VM2(21)
      REAL ENM3(21),DNM3(21),ETM3(21),EM3(21),VM3(21)
      REAL ENM4(21),DNM4(21),ETM4(21),EM4(21),VM4(21)
      REAL AX(3),BY(3),H(3),EMAG(21)
C     ...................................................
      read(5,*)e0,e1,e2,e3,e4,b,c,d,NP,NI,FLAG,NC
      read(5,*) (q(i),i=1,nc)
      read(5,*) (ax(i),i=1,nc)
      read(5,*) (by(i),i=1,nc)
      read(5,*) (h(i),i=1,nc)
      alph12=(e1-e2)/(e1+e2)
      alph23=(e2-e3)/(e2+e3)
      alph34=(e3-e4)/(e3+e4)
      bet12=2*e2/(e2+e1)
      bet21=2*e1/(e1+e2)
      bet23=2*e3/(e2+e3)
      bet32=2*e2/(e2+e3)
      bet34=2*e4/(e3+e4)
      bet43=2*e3/(e3+e4)
C     ...................................................
      pi=3.1416
      NI2=2*NI
      NI3=3*NI
      do 24 ip=1,nc
      q1(ip,1)=bet12
      l1(ip,1)=ax(ip)
```

Table C.1. Continued

```
      q0(ip)=alph12
      FK1(IP)=Q(IP)/(2*PI*EO)
   24 CONTINUE
      j=1
      i=1
      n=1
   41 CONTINUE
      k=j+1
      m1=2*j
      m2=i+1
      n1=n+1
      n2=n+2
      do 27 ip=1,nc
      q2(ip,i)=alph23*q1(ip,j)
      q3(ip,j)=bet23*q1(ip,j)
      q1(ip,k)=-alph12*q2(ip,j)
      q7(ip,j)=bet21*q2(ip,j)
      q4(ip,n)=alph34*q3(ip,i)
      q5(ip,n)=bet34*q3(ip,i)
      q3(ip,m1)=-alph23*q4(ip,j)
      q2(ip,m2)=bet32*q4(ip,j)
      q6(ip,j)=-q5(ip,j)
      q5(ip,n1)=-alph34*q6(ip,j)
      q4(ip,n1)=bet43*q6(ip,j)
      q4(ip,n2)=alph34*q3(ip,m1)
      q5(ip,n2)=bet34*q3(ip,m1)
      I2(ip,i)=I1(ip,j)+b
      I3(ip,i)=I1(ip,j)+b
      I1(ip,k)=I2(ip,j)+b
      I7(ip,j)=I2(ip,j)+b
      I4(ip,n)=I3(ip,i)+c
      I5(ip,n)=I3(ip,i)+c
      I3(ip,m1)=I4(ip,j)+c
      I2(ip,m2)=I4(ip,j)+c
      I6(ip,j)=I5(ip,j)+d
      I5(ip,n1)=I6(ip,j)+d
      I4(ip,n1)=I6(ip,j)+d
      I5(ip,n2)=I3(ip,m1)+c
      I4(ip,n2)=I3(ip,m1)+c
   27 continue
      IF(J.EQ.NI)GO TO 72
      J=J+1
      I=I+2
      N=N+3
      GO TO 41
   72 CONTINUE
      IF(FLAG.NE.1)GO TO 17
c ..............................................................
      call FLD1(E1,FLAG,dnM1,ETM1,EN1,ET1)
      PRINT*,'
```

Table C.1.   Continued

```
      WRITE(6,19)
  19  FORMAT('0',16X,'DNM1',14X,'ETM1',10X,'EMAG')
      DO 121 I=1,NP
      EN(I)=EN1(I)
      ET(I)=ET1(I)
  121      CONTINUE
      CALL MAG(EN,ET,NP,EMAG)
      DO 123 I=1,NP
      PRINT*,' '
      WRITE(6,23)DNM1(I),ETM1(I),EMAG(I)
  23  FORMAT('0',10X,F12.6,5X,F12.6,5X,F12.6)
  123      CONTINUE
      CALL FLD2(E2,FLAG,DNM2,ETM2,EN2,ET2)
      PRINT*,'
      WRITE(6,60)
  60  FORMAT('0',16X,'DNM2',14X,'ETM2',14X,'EMAG')
      DO 125 I=1,NP
      EN(I)=EN2(I)
      ET(I)=ET2(I)
  125      CONTINUE
      CALL MAG(EN,ET,NP,EMAG)
      DO 126 I=1,NP
      PRINT*,' '
      WRITE(6,23)DNM2(I),ETM2(I),EMAG(I)
  126      CONTINUE
      GO TO 999
  17  CONTINUE
      IF(FLAG.NE.2)GO TO 25
      CALL FLD2(E2,FLAG,DNM2,ETM2,EN2,ET2)
      PRINT*,'
      WRITE(6,60)
      DO 127 I=1,NP
      EN(I)=EN2(I)
      ET(I)=ET2(I)
  127      CONTINUE
      CALL MAG(EN,ET,NP,EMAG)
      DO 128 I=1,NP
      PRINT*,' '
      WRITE(6,23)DNM2(I),ETM2(I),EMAG(I)
  128      CONTINUE
      CALL FLD3(E3,FLAG,DNM3,ETM3,EN3,ET3)
      PRINT*,'
      DO 129 I=1,NP
      EN(I)=EN3(I)
      ET(I)=ET3(I)
  129      CONTINUE
      CALL MAG(EN,ET,NP,EMAG)
      WRITE(6,111)
  111      FORMAT('0',16X,'DNM3',14X,'ETM3',14X,'EMAG')
      DO 130 I=1,NP
```

Table C.1.   Continued

```
      PRINT*,' '
      WRITE(6,23)DNM3(I),ETM3(I),EMAG(I)
  130     CONTINUE
      GO TO 999
   25 CALL FLD3(E3,FLAG,DNM3,ETM3,EN3,ET3)
      PRINT*,' '
      DO 131 I=1,NP
      EN(I)=EN3(I)
      ET(I)=ET3(I)
  131     CONTINUE
      CALL MAG(EN,ET,NP,EMAG)
      WRITE(6,111)
      DO 135 I=1,NP
      PRINT*,' '
      WRITE(6,23)DNM3(I),ETM3(I),EMAG(I)
  135     CONTINUE
      CALL FLD4(E4,FLAG,DNM4,ETM4,EN4,ET4)
      PRINT*,' '
      DO 136 I=1,NP
      EN(I)=EN4(I)
      ET(I)=ET4(I)
  136     CONTINUE
      WRITE(6,115)
      CALL MAG(EN,ET,NP,EMAG)
  115     FORMAT('0',16X,'DNM4',14X,'ETM4',14X,'EMAG')
      DO 138 I=1,NP
      PRINT*,' '
      WRITE(6,23)DNM4(I),ETM4(I),EMAG(I)
  138     CONTINUE
  999     CONTINUE
      STOP
      END
C     ...................................................
      subroutine FLD1(E1,FLAG,DNM1,ETM1,EN1,ET1)
      common q,ax,by,b,c,d,h,nc,q0,fk1,NI,NI2,NI3,NP
      common q1,I1,q2,I2,q3,I3,q4,I4,q5,I5,q6,I6,q7,I7
      complex q(3),FK1(3),DN1(21),EN1(21),ET1(21),V1(21)
      COMPLEX DNT1,ETT1,VT1
      REAL Q1(3,6000),Q2(3,6000),Q3(3,6000),Q4(3,6000)
      REAL Q5(3,6000),Q6(3,6000),Q7(3,6000),Q0(3)
      REAL L1(3,6000),L2(3,6000),L3(3,6000),L4(3,6000)
      REAL L5(3,6000),L6(3,6000),L7(3,6000)
      REAL ENM1(21),ETM1(21),DNM1(21),EM1(21),VM1(21)
      REAL AX(3),BY(3),H(3)
      X=B+C+D
      DNT1=(0.0,0.0)
      ETT1=(0.0,0.0)
      VT1=(0.0,0.0)
      DO 20 IP=1,NP
      Y=IP-1
```

Table C.1.   Continued

```
      do 26 I=1,nc
      DO 34 J=1,NI
      if(j.ne.1)go to 10
      a1=(x-h(I))*(X-H(I))+(Y-BY(I))*(Y-BY(I))
      a11=(x-h(I))/a1
      b11=(y-by(I))/a1
      a2=(X-H(I)+2*AX(I))*(X-H(I)+2*AX(I))+(Y-BY(I))*(Y-BY(I))
      a22=(x-h(I)+2*ax(I))/a2
      b22=(y-by(I))/a2
      dnt1=dnt1+(a11+Q0(I)*A22)*FK1(I)
      ett1=ett1+(b11+Q0(I)*B22)*FK1(I)/E1
   10 CONTINUE
      a3=(x+l7(I,J)-b-c-d)*(X+L7(I,J)-B-C-D)+(Y-BY(I))*(Y-BY(I))

      a33=(x+l7(I,J)-b-c-d)/a3
      b33=(y-by(I))/a3
      dnt1=dnt1+q7(I,J)*A33*FK1(I)
      ett1=ett1+q7(I,J)*B33*FK1(I)/E1
   34 continue
   26 CONTINUE
      DN1(IP)=DNT1
      EN1(IP)=DN1(IP)/E1
      DNM1(IP)=CABS(DN1(IP))
      ENM1(IP)=DNM1(IP)/E1
      ET1(IP)=ETT1
      ETM1(IP)=CABS(ET1(IP))
      DNT1=(0.0,0.0)
      ETT1=(0.0,0.0)
      VT1=(0.0,0.0)
   20 CONTINUE
      RETURN
      end
C     ....................................................
      subroutine fLD2(E2,FLAG,DNM2,ETM2,EN2,ET2)
      common q,ax,by,b,c,d,h,nc,q0,fk1,NI,NI2,NI3,NP
      common q1,l1,q2,l2,q3,l3,q4,l4,q5,l5,q6,l6,q7,l7
      complex q(3),FK1(3),DN2(21),ET2(21),EN2(21)
      COMPLEX DNT21,ETT21,VT21,DNT22,ETT22,VT22
      REAL Q1(3,6000),Q2(3,6000),Q3(3,6000),Q4(3,6000)
      REAL DNM2(21),ETM2(21),VM2(21),ENM2(21)
      real Q5(3,6000),Q6(3,6000),Q7(3,6000),Q0(3)
      REAL L1(3,6000),L2(3,6000),L3(3,6000),L4(3,6000)
      REAL L5(3,6000),L6(3,6000),L7(3,6000)
      REAL AX(3),BY(3),H(3)
      DNT21=(0.0,0.0)
      ETT21=(0.0,0.0)
      VT21=(0.0,0.0)
      DNT22=(0.0,0.0)
      ETT22=(0.0,0.0)
      VT22=(0.0,0.0)
```

Table C.1. Continued

```
      X=B+C+D
      IF(FLAG.NE.1)X=C+D
      do 67 ip=1,NP
      Y=IP-1
      DO 30 I=1,NC
      DO 43 J=1,NI
      d1=(x-l1(I,J)-b-c-d)*(X-L1(I,J)-B-C-D)+(Y-BY(I))*(Y-BY(I))
      d11=(x-l1(I,J)-b-c-d)/d1
      c11=(y-by(I))/d1
      dnT21=dnT21+(q1(I,J)*d11)*fk1(I)
      etT21=etT21+(q1(I,J)*c11)*fk1(I)/E2
   43 CONTINUE
      DO 53 J=1,NI2
      d3=(x+l2(I,J)-c-d)*(X+L2(I,J)-C-D)+(Y-BY(I))*(Y-BY(I))
      d33=(x+l2(I,J)-c-d)/d3
      c33=(y-by(I))/d3
      dnT22=dnT22+(q2(I,J)*d33)*fk1(I)
      etT22=etT22+(q2(I,J)*c33)*fk1(I)/E2
   53 CONTINUE
   30 CONTINUE
      DN2(IP)=DNT21+DNT22
      EN2(IP)=DN2(IP)/E2
      ET2(IP)=ETT21+ETT22
      DNM2(IP)=CABS(DN2(IP))
      ENM2(IP)=DNM2(IP)/E2
      ETM2(IP)=CABS(ET2(IP))
      DNT21=(0.0,0.0)
      ETT21=(0.0,0.0)
      VT21=(0.0,0.0)
      DNT22=(0.0,0.0)
      ETT22=(0.0,0.0)
      VT22=(0.0,0.0)
   67 CONTINUE
      return
      end
C     ...................................................................
      subroutine fLD3(E3,FLAG,DNM3,ETM3,EN3,ET3)
      common q,ax,by,b,c,d,h,nc,q0,fk1,NI,NI2,NI3,NP
      common q1,l1,q2,l2,q3,l3,q4,l4,q5,l5,q6,l6,q7,l7
      complex q(3),FK1(3),DN3(21),ET3(3),EN3(3),V3(21)
      COMPLEX DNT31,ETT31,VT31,DNT32,ETT32,VT32
      REAL DNM3(21),ETM3(21),ENM3(21),VM3(21)
      REAL Q1(3,6000),Q2(3,6000),Q3(3,6000),Q4(3,6000)
      REAL Q5(3,6000),Q6(3,6000),Q7(3,6000),Q0(3)
      real l1(3,6000),l2(3,6000),l3(3,6000),l4(3,6000)
      REAL L5(3,6000),L6(3,6000),L7(3,6000)
      REAL AX(3),BY(3),H(3)
      X=C+D
      IF(FLAG.NE.2)X=D
      DNT31=(0.0,0.0)
```

Table C.1. Continued

```
      ETT31=(0.0,0.0)
      VT31=(0.0,0.0)
      DNT32=(0.0,0.0)
      ETT32=(0.0,0.0)
      VT32=(0.0,0.0)
      DO 71 IP=1,NP
      Y=IP-1
      do 72 I=1,nc
      DO 73 J=1,NI2
      f1=(x-I3(I,J)-c-d)*(X-L3(I,J)-C-D)+(Y-BY(I))*(Y-BY(I))
      f11=(x-I3(I,J)-c-d)/f1
      f44=(y-by(I))/f1
      dnT31=dnT31+q3(I,J)*f11*fk1(I)
      etT31=etT31+q3(I,J)*f44*fk1(I)/E3
   73 CONTINUE
      DO 74 J=1,NI3
      f3=(x+I4(I,J)-d)*(X+L4(I,J)-D)+(Y-BY(I))*(Y-BY(I))
      f33=(x+I4(I,J)-d)/f3
      f55=(y-by(I))/f3
      dnT32=dnT32+q4(I,J)*F33*FK1(I)
      etT32=etT32+q4(I,J)*f55*FK1(I)/E3
   74 CONTINUE
   72 CONTINUE
      DN3(IP)=DNT31+DNT32
      EN3(IP)=DN3(IP)/E3
      ET3(IP)=ETT31+ETT32
      DNM3(IP)=CABS(DN3(IP))
      ETM3(IP)=CABS(ET3(IP))
      ENM3(IP)=DNM3(IP)/E3
      DNT31=(0.0,0.0)
      ETT31=(0.0,0.0)
      VT31=(0.0,0.0)
      DNT32=(0.0,0.0)
      ETT32=(0.0,0.0)
      VT32=(0.0,0.0)
   71 CONTINUE
      RETURN
      END
C     ...................................................
      subroutine FLD4(E4,FLAG,DNM4,ETM4,EN4,ET4)
      common q,ax,by,b,c,d,h,nc,q0,fk1,NI,NI2,NI3,NP
      common q1,I1,q2,I2,q3,I3,q4,I4,q5,I5,q6,I6,q7,I7
      complex q(3),FK1(3),DN4(21),ET4(21),EN4(21),V4(21)
      COMPLEX DNT41,ETT41,VT41,DNT42,ETT42,VT42
      REAL DNM4(21),ETM4(21),ENM4(21),VM4(21)
      REAL Q1(3,6000),Q2(3,6000),Q3(3,6000),Q4(3,6000)
      REAL Q5(3,6000),Q6(3,6000),Q7(3,6000),Q0(3)
      real I1(3,6000),I2(3,6000),I3(3,6000),I4(3,6000)
      REAL L5(3,6000),L6(3,6000),L7(3,6000)
      REAL AX(3),BY(3),H(3)
```

Table C.1. Continued

```
      DNT41=(0.0,0.0)
      ETT41=(0.0,0.0)
      VT41=(0.0,0.0)
      DNT42=(0.0,0.0)
      ETT42=(0.0,0.0)
      VT42=(0.0,0.0)
      X=D
      do 33 ip=1,nP
      Y=IP-1
      DO 43 I=1,NC
      DO 53 J=1,NI3
      d1=(x-l5(i,j)-d)*(x-l5(i,j)-d)+(y-by(i))*(y-by(i))
      d11=(x-l5(i,j)-d)/d1
      c11=(y-by(i))/d1
      dnT41=dnT41+(q5(i,j)*d11)*fk1(i)
      etT41=etT41+(q5(i,j)*c11)*fk1(i)
53    CONTINUE
      DO 63 J=1,NI
      d2=(x+l6(i,j))*(x+l6(i,j))+(Y-BY(i))*(Y-BY(i))
      d22=(x+l6(i,j))/d2
      c22=(y-by(i))/d2
      dnT42=dnT42+q6(i,j)*D22*FK1(i)
      etT42=etT42+q6(i,j)*C22*FK1(i)
63    CONTINUE
43    CONTINUE
      DN4(IP)=DNT41+DNT42
      EN4(IP)=DN4(IP)/E4
      ET4(IP)=ETT41+ETT42
      DNM4(IP)=CABS(DN4(IP))
      ENM4(IP)=DNM4(IP)/E4
      ETM4(IP)=CABS(ET4(IP))
      DNT41=(0.0,0.0)
      ETT41=(0.0,0.0)
      DNT42=(0.0,0.0)
      ETT42=(0.0,0.0)
      VT41=(0.0,0.0)
      VT42=(0.0,0.0)
33    CONTINUE
      RETURN
      END
C     .................................................
      SUBROUTINE MAG(EN,ET,NP,EMAG)
      COMPLEX EN(21),ET(21),XN,YT
      REAL EMAG(21)
      RAD=180./3.1416
      DO 1000 I=1,NP
      YT=ET(I)
      IF(YT.EQ.0.0)GO TO 1001
```

Table C.1.   Continued

```
    YTR=REAL(YT)
    YTI=AIMAG(YT)
    YTM=SQRT(YTR*YTR+YTI*YTI)
1001    CONTINUE
    XN=EN(I)
    XNR=REAL(XN)
    XNI=AIMAG(XN)
    XNM=SQRT(XNR*XNR+XNI*XNI)
    IF(XNI.EQ.0.0.AND.XNR.EQ.0.0)XNP=0.0
    IF(XNP.EQ.0.0.AND.XNR.EQ.0.0)GO TO 1002
    XNP=ATAN2(XNI,XNR)*RAD
1002    IF(YTI.EQ.0.0.AND.YTR.EQ.0.0)YTP=0.0
    IF(YTP.EQ.0.0.AND.YTR.EQ.0.0)GO TO 1003
    YTP=ATAN2(YTI,YTR)*RAD
1003    CONTINUE
    IF(XNM.EQ.0.0)EMAG(I)=YTM
    IF(YTM.EQ.0.0)EMAG(I)=XNM
    IF(XNM.EQ.0.0.OR.YTM.EQ.0.0)GO TO 1004
    ALPH=YTP*2./RAD
    BETA=XNP*2./RAD
    COM=(XNM*XNM)/(YTM*YTM)
    ARG=-(SIN(ALPH)+COM*SIN(BETA))/(COS(ALPH)+COM*COS(BETA))
    ANGL=ATAN(ARG)
    TEST=COS(ANGL+ALPH)+COM*COS(ANGL+BETA)
    IF(TEST.LT.0.0)ANGL=ANGL+3.1416
    EMAG(I)=SQRT((1.0+COM+COS(ANGL+ALPH)+COM*COS(ANGL+BETA))/2.)*YTM
1004    CONTINUE
1000    CONTINUE
    RETURN
    END
```